INFORMATION TO USERS

UNIVERSITY OF CALIFORNIA

Los Angeles

An Integrated Geographic Information System and

Stormwater Management Modeling

A dissertation submitted in partial satisfaction of the

requirements for the degree Doctor of Philosophy

in Civil Engineering

by

Kenneth Mingchung Wong

1999

UMI Number: 9926330

UMI

300 North Zeeb Road
Ann Arbor, MI 48103
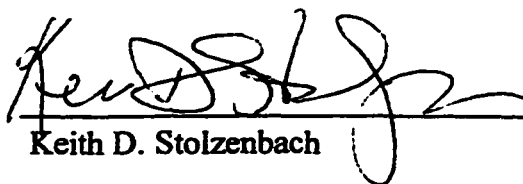
The dissertation of Kenneth Mingchung Wong is approved.

L. Donald Duke

Thomas C. Harmon

Keith D. Stolzenbach

Michael K. Stenstrom, Committee Chair

University of California, Los Angeles

1999

TABLE OF CONTENTS

LIST OF FIGURES

LIST OF TABLES

VITA

December 5, 1962	Born, Shanghai, China
1991	B.S., Electrical Engineering University of California, Los Angeles
1992	M.S., Civil Engineering University of California, Los Angeles
1991-1995	Graduate Student Researcher Department of Civil and Environmental Engineering University of California, Los Angeles
1994-1995	Teaching Assistant Department of Civil and Environmental Engineering University of California, Los Angeles
1995	Teaching Associate Department of Civil and Environmental Engineering University of California, Los Angeles
1995-present	Systems Analyst Noise Management Bureau Los Angeles World Airports City of Los Angeles

PUBLICATIONS AND PRESENTATIONS

Wong, K.M., Strecker, E., and Stenstrom, M.K., A GIS to Estimate Storm-water Pollutant Mass Loadings. Journal of Environmental Engineering–ASCE, 1997 August, Vol. 123, No. 8, pp. 737-745.

Wong, K.M., Stenstrom, M.K. (1996) An Integrated Geographic Information Systems and Watershed Modeling, Proceedings of 69th Annual Conference & Exposition, Water Environment Federation (WEF), October 5-9, Dallas, TX.

Wong, K.M., Strecker, E., and Stenstrom, M.K. (1997) A Picture Worth More than 1,000 Words, Geographic information system provides fine detail for nonpoint source model. Water Environmental & Technology. Vol. 9, No. 1, pp. 41–46.

ABSTRACT OF THE DISSERTATION

An Integrated Geographic Information System and

Stormwater Management Modeling

By

Kenneth Mingchung Wong

Doctor of Philosophy in Civil Engineering

University of California, Los Angeles, 1999

Professor Michael K. Stenstrom, Chair

An integrated stormwater management model with GIS for the urban

stormwater process was developed and validated through the calibration procedure and

model simulations. The integrated GIS/Model developed included a steady and a

deterministic model.

An integrated GIS and empirical urban runoff model was developed to estimate

the annual pollutant loadings in the Santa Monica Bay Watershed. The runoff equation

derived from the rational method was successfully embedded in the GIS. Within the

GIS, all the physical characteristics (data coverages) of the watershed were

successfully linked and related with the runoff model. A combination of a GIS and an

empirical urban runoff model can be used as a tool to test the potential nonpoint source control strategies.

A GIS provides a stable and an efficient platform to store and manipulate an substantial amount of data required by stormwater modeling. Since a GIS stores the data in reference to the spatial features of the physical world, it can be used to identify the spatial relationships between map features. The model's prediction of the annual pollutant loadings in the watershed can easily be identified in a GIS from the largest unit of the whole watershed to the smallest unit of land use polygons. This feature provides an efficient way to pinpoint the heavily polluting areas in a watershed.

An integrated form of GIS and a deterministic stormwater model were developed. The original Storm Water Management Model (SWMM) was modified and adapted on the Ballona Creek Watershed. A GIS was integrated with the modified SWMM to process the data management part of GIS/SWMM model. An procedure to generate mean areal precipitation data using the raster-based GIS was developed. The method was found to be feasible in estimating mean areal precipitation data in watershed that has a limited number of rain gauges.

A model calibration algorithm was developed and evaluated for the urban stormwater process. A total of ten storm events were used for calibration. The calibrated parameters were able to predict the model outputs with reasonable accuracy.

1. INTRODUCTION

1.1 Dissertation Organization

This dissertation is divided into five chapters. The first two chapters include an overview of the problems in urban stormwater pollution and modeling. The second chapter contains a paper that was published in the Journal of Environmental Engineering, ASCE in 1997. This paper demonstrates a successful integration of GIS and an empirical stormwater model to predict annual pollutant loadings. The subsequent chapters, Chapters 4 and 5, contain an extension of work from Chapter 3. These two chapters investigate the integration of a deterministic stormwater model, calibration algorithm, and use of the GIS as the preprocessor/postprocessor.

1.2 Overview of the Problem

The quantity and the quality of urban runoff constitutes problems of both a historical and current nature. In earlier times, wastewater treatment was provided only for point sources (e.g., municipal sewage and industrial wastewater) in urbanized areas. Stormwater was not treated, although flood control facilities were constructed. The potential of urban runoff pollution on the surrounding surface water (coastal water, river, and stream, etc.,) and within the watershed has been gradually recognized

for the past two decades as equal or greater in importance than point sources (NOAA, 1991).

By definition, an urbanized area is an area of concentrated human activity. The direct consequence of this activity is the accumulation of waste materials on the urbanized areas which are mostly covered with impervious materials (concrete, asphalt, etc.); subsequently, during storm events, the accumulated pollutants are likely to be transported by runoff as it moves through the urbanized storm drain systems, streams, and eventually to receiving waters. This transport process is relatively fast due to the efficient urbanized drainage systems. Therefore, the buffering ability of urban watershed to pollutant discharges during storm events is much less than natural streams.

Many studies have shown that nonpoint sources, such as stormwater runoff, may contain harmful toxic contaminants (Lau *et al.*, 1993). Other previous studies have also shown nonpoint sources as the major cause of surface water quality degradation in many areas of the United States, surpassing pollutant loadings to receiving waters from point sources such as treated sewage and industrial discharges (Gilliland, 1987; US EPA, 1983).

Nonpoint source pollution processes, such as stormwater runoff, are inherently

difficult to model due to their stochastic nature in both time and space domains

(Corbitt, 1989). Both the quantity and the quality responses from nonpoint source

pollution are influenced by an enormously complex hydrologic and hydraulic system,

such as meteorology, geological conditions, drainage systems, and land use practices.

Furthermore, nonpoint source pollution modeling generally requires organizing and

processing large amounts of data, that is either not feasible or difficult to implement,

without the aid of computer automation.

The idea of Geographic Information System (GIS) technology was first

conceived to a number of geographers almost 3 decades ago (ESRI, 1992). In its

infancy stage, GIS was merely known as a computer system for storing and organizing

spatial information. Its usage to a wider audience was restricted by the relatively high

cost of computer hardware and the limited power of the computer technology. But

during the last decade, the rapid decline in computer hardware costs and the great

advancement in computer technology enable many organizations to apply GIS

technology to a variety of applications. GIS technologies have been used for high-

quality cartography, land use planning, natural resource management, environmental

assessment and planning, tax mapping, ecological research, emergency vehicle

dispatch, demographic research, utilities, remote sensing, business applications and

other smaller application. It has the potential to be one of the most popular computer applications ever to emerge.

Applications of GIS technology within the modeling community have gained widespread acceptance as a valuable tool because of their ability to carry out complex spatial operations and to link spatial and descriptive information. They enable us to organize data from different problems and sources to understand their spatial relationships. Integrating GIS technology with computer models can help us understand and address some of the most pressing problems human beings face today.

1.3 Objectives

The purpose of this investigation is to develop a stormwater management system to evaluate and control of stormwater pollution and to demonstrate the potential improvement of data management in stormwater modeling using GIS as the preprocessor. The specific objectives are as follows,

1. Develop an integrated GIS and Stormwater Management Model to simulate a large watershed.

2. Develop a spatial-enabled database to replace paper/map type information to facilitate data management and maintenance.

3. Define accuracy and uncertainty of watershed's parameters by incorporating a calibration algorithm within the stormwater model.

4. Provide a method of evaluating the potential impact of Best Management Practices (BMPs).

A framework of an integrated GIS and stormwater management is developed in the study. The integrated system consists of 4 major components: GIS preprocessor/postprocessor, GIS databases with over a half gigabytes of watershed information, stormwater process simulation model and calibration algorithm. The system was implemented using FORTRAN, ARC/INFO and ArcView GIS (ESRI, 1998). ARCINFO and ArcView GIS are based on the Relational Database Management System (RDBMS) technology which can manage both vector and raster spatial database. All watershed related information (both spatial and attribute) are stored within the GIS which manages and interfaces with the stormwater process model. A optimization routine was implemented into FORTRAN codes and incorporated within the stormwater process model to calibrate the watershed's parameters. Originally the system was developed to model the hydrologic, hydraulic, and water quality parts of stormwater processes. Because of the unavailability of water quality data and quantity of the work involved, only the hydrologic and hydraulic processes were simulated and calibrated. However, with the availability of water

quality data, the methodology developed in this study can easily be applied on water

quality modeling.

2. LITERATURE REVIEW

2.1 Storm Water

Rainfall is the basic controlling factor in stormwater runoff processes. As rain falls from the sky, a portion is intercepted on the surface either by vegetation or other objects (natural or man made). The remaining portion reaches the soil surface (pervious surface) and seeps into the ground. This process is called infiltration. Collection in small holes or dips is called depression storage. If the rainfall rate exceeds the infiltration rate or exceeds the depression storage capacity, surface runoff will occur. This surface runoff moves downslope as an irregular sheet of overland flow in variable velocities, depending on the land slope and friction. Along the flow path of the surface runoff, pollutants have accumulated on the surface in dry weather, from either point or nonpoint sources. They can be entrained in the storm flow, transported and emptied out to receiving water bodies. The detrimental effects on the receiving water bodies and its ecology by the stormwater process is significant and sometimes staggering.

2.1.1 Point and Nonpoint sources

There are two types of pollution sources that attribute to the worsening of water quality problems in the nation's water bodies, such as in lakes, estuaries, rivers, and

coastal regions. They are generally called point and nonpoint sources. Point sources include discharges from wastewater treatment plants, and are relatively easy to identify, appearing as a "point" on a map. Nonpoint sources are many and are spread out on a map, which makes them difficult or impossible to locate. Nonpoint sources include atmospheric fallout, construction, mining, agriculture, irrigation return flows, streambank erosion, and individual disposal. Furthermore, the amount of pollutants produced from nonpoint sources can be very large. Nonpoint sources contribute significant percentages of the total loadings to the receiving waters, such as biochemical oxygen demand (BOD_5) (57%), nitrogen (88%), phosphorous (87%), and total suspend solids (98%) (Gilliland and Baxter-Potter, 1987). Overall, they are generally categorized into two types: rural and urban nonpoint sources.

2.1.2   Rural Nonpoint Sources

The major portion of rural nonpoint sources affect large areas, which are mostly devoted to agricultural activities. The pollutants discharged are typically related to farming practices, such as animal wastes, fertilizers, pesticides, herbicides, fungicides, and other related agricultural chemicals. Other typical water quality parameters, such as BOD_5, COD, total suspend solids, nitrogen, and phosphorus, are also found in the runoff. Several studies have shown the resulting water quality are

affected by the following factors: soil types; climate; land uses; cover crops;

management practices; topography of the area (Wanielista and Yousef, 1992).

2.1.3 Urban Nonpoint Sources

Urban watersheds are typically characterized by impervious surfaces and

efficient drainage systems, as compared with rural watersheds. Urban runoff also has

the potential to contain many more pollutants as a result of increased human activities.

The diversity of its sources is impressive; pollutants can consist of vehicle pollutants,

heavy metals, pesticides, fertilizers, and toxins. Surface runoff under these conditions

is significantly different from rural runoff. On impervious surfaces, nearly all rainfall

becomes surface runoff and thereby, less pollutants infiltrate into the soil. This

drastically reduces the buffering capability of a watershed to mitigate water pollution.

Urban drainage systems designed to prevent flooding generally increase stormwater

pollution because the accumulated pollutants are quickly washed into channels and

streams, to the eventual receiving water bodies.

The potential effects on the ecology of the water bodies are enormous because

unlike the rural watershed, the urban watershed can not be used as a buffering zone to

reduce the pollutant loadings. The occurrence of this harmful process is not limited to

the storm water events. During dry weather, low flows from various discharges are

carried by storm drains to the receiving waters were they may have harmfull effects. In summary, urban runoff can cause problems in the receiving waters that are as varied as the sources and nature of the stormwater itself.

2.1.4   Stormwater Modeling

In light of the complexity of the stormwater process in an urban watershed, an urban stormwater model is needed to study the behavior of the system. The system here refers to the urban watershed. An urban stormwater model uses mathematical relationships to simulate the movement of stormwater and the transported pollutants through an urban watershed in response to rainfall and watershed conditions. An urban model plays an important role in understanding the behavior of the system or evaluating strategies for the operation of the system. This understanding could not be obtained by other means. By integrating an urban model with a geographic information system (GIS), it further enhances the capability of studying the complex behavior of the urban watershed.

An urban stormwater model can generally be divided into two types: deterministic and stochastic. Any model falling between these two types is called a parametric model, which has both the deterministic and stochastic natures. Urban runoff models are generally parametric models because the system is too complicately

to be fully described by physical laws. Inevitably, some randomness and

unpredictability exist and a parametric model must be used to supplement the

capability of a pure deterministic model. As described by Karplus (1976), an urban

watershed system may fall between the mechanical and biological systems in the realm

of Karplus' Rainbow, which is depicted in Figure 2.1.
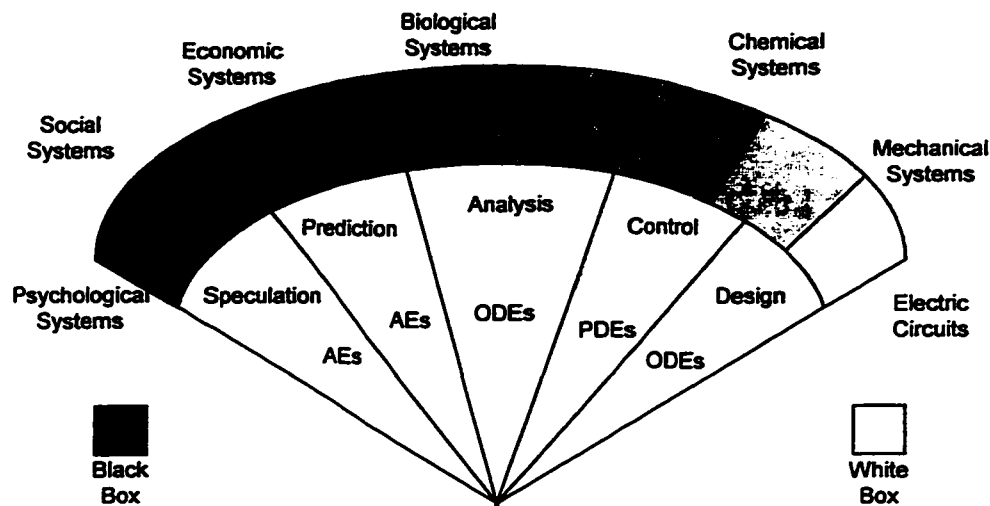
Figure 2.1 Karplus' Rainbow

2.1.4.1 Deterministic Model

A deterministic model, in essence, is an exact representation of a system based

on a certain set of physical laws. A deterministic model should be able to predict

precisely the outcome of every physical process in a system. For a deterministic urban

watershed model, all model parameters are based on the laws of mass, momentum, and

continuity conservation. Many existing models are based on this set of physical laws; however, many physical processes describing fluid mechanics are too complicated to describe with deterministic analytical methods, which produce inaccurate solutions. Therefore, empirical methods are often used.

For example, the commonly used rational method for rainfall runoff is derived from the empirical approach. The rational method is used in this study to predict the pollutant loadings in conjunction with a GIS, and that will be the topic for the next section. Another example, Huber and Dickinson (1988) derived a nonlinear reservoir equation to describe the evaporation, rainfall, and infiltration processes in an urban watershed (SWMM, 1988). These three processes are not well understood and the only viable solution to this type of problem is an empirical approach, which is quite often the most commonly used method in an urban watershed modeling.

2.1.4.2 Stochastic Model

A stochastic model is not based on any physical principle. A stochastic model may produce different outputs from the same inputs under the same physical conditions. Although the output may be different, the distribution of outputs will likely have a similar distribution or pattern. Since stochastic methods are not investigated in this study, no further literature review will be done in this section.

2.1.5 Geographic Information System

2.1.5.1 Classification

An accurate interpretation of land use coverage and the physiography of drainage basins is directly related to the stormwater modeling process, because each characteristic may contribute to the pollutant loading and surface runoff. An effective means of quantifying drainage basin characteristics is needed to understand the stormwater runoff.

2.1.5.1.1 Land Use

Geographic information systems (GIS) can improve the process of land use classification by facilitating the integration of remotely sensed imagery and ancillary data, hence improving the accuracy of land use classification. Rado et al. (1991) used a GIS to overlay a vector coverage of land use on raster satellite imagery to better delineate land use classes. Treitz et al. (1992) used a similiar technique called the GIS matrix overlay to obtain a 78% average interpretation accuracy of land use and land cover. Kim (1993) further refined the process of urban land use classification by using the technique of remote sensing and a geographic information system. The process was named Feature-oriented Urban Classification. It involves the process object generation, texture parameters extraction from the objects, and classification based on enhanced

texture parameters. The combined process showed 100% accuracy for the medium

density residential region and 94% overall classification accuracy.

2.1.5.1.2   Drainage

Quantification of drainage basin characteristics is a laborious and time

consuming process. It usually requires the gathering and processing of a huge amount

of data in order to quantify only a few selected characteristics for a drainage basin.

With GIS technology, the whole process can be greatly simplified and improved. Eash

(1994) developed a GIS automated system named the Basin Characteristics System

(BCS). It consists of four processing steps: creation of four GIS digital maps;

assignment of attribute information to digital maps; quantification of 24 morphometric

basin characteristics from digital maps and quantification of two climatic basin

characteristics from precipitation data sources. The author concluded that the BCS

method produces a comparable result with the manual topographic map method, but

takes significantly less time to quantify an equivalent number of basin characteristics

for a drainage basin.

Jenson and Domingue (1988) demonstrated the extraction of topographic

structure, delineation of watersheds and overland flow paths from digital elevation

models (DEM) using GIS. Smith and Brilly (1992) and Treitz et al (1992) extracted drainage characteristics using GIS in a similar fashion.

2.1.5.2 Integrating with Model

2.1.5.2.1   Runoff Estimation

Stuebe and Johnston (1990) stated that problems may arise with traditional manual runoff estimation methods when watersheds lack relatively flat terrain. The alternative method used in their study was a combination of the Soil Conservation Service (SCS) runoff curve number model and a raster based GIS. Three digitalized coverage layers (elevation, soils, and landcover) were input into a raster based GIS. Three additional layers were obtained by using the map algebra arithmetic. The first layer was the crossproduct of the hydrologic soil and landcover layers, with each calculated unit of the new layer assigned a runoff curve number. The second and third layers for each cell contained a runoff depth. The runoff volume was then obtained based on the value of previous layer. The final results showed the difference between methods ranged from 0.9 to 32.8 percent, with a mean difference of 16.5 percent. The author concluded the GIS-generated runoff estimates were similar with the manually generated estimates, and tended to be advantageous if watershed areas are large or numerous. The manual method was preferred for flatter watersheds because of GIS's difficulty in flat watershed delineation.

A similar study by Vieux (1990) demonstrated the spatial data handling

capabilities of a GIS by integrating it with a distributed process, hydrologic model.

Their approach was divided into two steps: a GIS was first used to generate a

triangular irregular network to provide land surface slope; next, the kinematics wave

equation was linked with a GIS to produce a finite element solution of overland flow.

The author concluded that the GIS was an ideal platform to handle a large amount of

parameters or data required by the distributed process model.

2.1.5.2.2   Water Quality Estimation

Stormwater process modeling is a problem associated with extensive

geographic areas. It requires the integration and display of numerous types of

geographic information, a task for which GIS's are particularly well suited. The role of

GIS in nonpoint source process, especially in urban stormwater runoff, will be

reviewed here.

In urban areas, stormwater runoff is a significant nonpoint source. Pollutants

carried in stormwater runoff include some of the same pollutants associated with point

source runoff, such as sediment, nutrients, oxygen demanding organic materials,

bacteria, and toxic pollutants, such as heavy metals and volatile organic compounds

(Nix, 1994). Urban nonpoint source pollution is a function of land uses but other

physical characteristics such as slope, soil types, hydrology, and meteorology of an area, also affect the extend of pollution. For urban stormwater modeling, empirical models that primarily dependent on land use data are commonly used to estimate pollutant loading.

Ventura and Kim (1993) used an urban water quality model, SLAMM (Source Loading and Management Model) and coupled it with a vector based GIS to estimate the pollutant loadings of each land use polygon in their studied sewershed. In their study, the GIS was programmed to generate and manage digital data layers, conduct overlay and spatial analysis, and data transfer to SLAMM to estimate total pollutant loadings for each sewer junction. Their results showed the estimated event mean runoff volume and suspended solids loadings were within 15 and 20 percent of observed values, respectively.

Gilliland and Baxter-Potter (1987) used a raster based GIS named the Raster Geographic Information System for Mapping (RGISM) and three separate equations: the Soil Conservation Service Curve Number technique (SCSCN) for the prediction of potential runoff; the Universal Soil Loss Equation of the prediction of potential erosion; and an empirical loading function for the prediction of bacterial densities in runoff. These three equations were input to each grid-cell of RGISM and coupled with other coverage layers, such as soil type, topography, and land use to produce the three

dimensional maps of runoff potential, sediment pollution potential, and bacterial pollution potential to the studied watershed.

Heidtke and Auer (1993) used a similar approach to derive the phosphorous export coefficient for the studied drainage system to estimate the phosphorus loadings to the local receiving water body. Xu et al (1993), He et al (1993), and others have all used similar land use driven empirical nonpoint models with a GIS to estimate pollutant loadings in either rural or urban watersheds.

2.2 Geographic Information System

Originally geographic information systems (GIS) were limited only in use to geographers. Presently, GIS is commonly applied to many different applications by business, government, and academia. Its definition has also changed and can be stated as follows (ESRI, 1992):

An organized collection of computer hardware, software, geographic data, and personnel designed to efficiently capture, store, update, manipulate, analyze, and display all forms of geographically referenced information.

2.2.1 Spatial Operation

The ability to perform spatial operations on the data or coverages differentiate GIS from many computer programs, such as spreadsheets, statistics packages, or drafting packages. The spatial operation can be divided into two types: aspatial queries, which do not require latitude and longitude information, such as the query asking for the average number of people working with GIS in each location; spatial queries, which require the precise location or characteristic of the geographic information, such as latitude, longitude, and the elevation. GIS typically answer both aspatial and spatial queries by linking data from different sets of coverage or database. The ability of data linkage is essential in the overall design of GIS applications; it greatly enhances the type of questions a GIS can answer by matching information from different databases. From Figure 2.2, data linkage can be divided into two types: exact and nonexact matching, where nonexact matching can be further divided into hierarchical and fuzzy matching.

Data Linkage

Exact Matching

Nonexact Matching

Hierarchical
Matching

Fuzzy
Matching
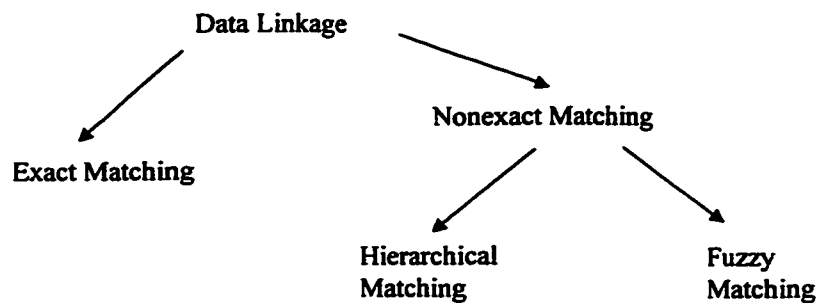
Figure 2.2 Data Linkage of a GIS

2.2.2 Exact and Nonexact Matching

Data linkage using exact matching is achieved by joining two or more databases (files or coverages) through a common key to extract additional information in other databases about the same set of features. The process is straight forward, as compared to the nonexact process of hierarchical and fuzzy matching. Hierarchical matching is needed when certain types of information are collected in more detail or more frequently than other types of information and from smaller areas. The process will first group the less frequent observations together until they cover the same area as the larger group, then total the observations, and then perform the exact matching. The last matching process is the fuzzy matching, which is especially useful when dealing many sets of coverage. On many occasions, the boundaries of the smaller areas do not match those of the larger ones. The process joins the overlayed coverages which do not match with their data boundaries. The desired data and areas of the resultant new layer containing the characteristics of all coverages are then computed. Fuzzy matching enables a GIS to analyze over a million possible combinations if numerous datasets are required. A GIS can perform all these operations because it uses geography, or space, as the common key between the coverages. Data are linked only if they relate to the same geographic area.

2.2.3 GIS Functional Elements

There are five essential elements that a GIS must contain which are data

acquisition, preprocessing, data management, manipulation and analysis, and product

generation. Each of these five elements can be viewed as a continuing process which

will be described briefly in this section.

2.2.3.1 Data Acquisition

Data acquisition is the process of identifying and gathering the data required

for a GIS application. The number of procedures involved greatly depends on the

nature of a specific GIS application. It might require gathering data by preparing maps

from field observations, contracting for aerial photography and satellite imagery, and

surveying available databases and documents. A GIS application is of little value until

this initial phase of data acquisition locates and identifies all the relevant data.

Furthermore, an acceptable level of results derived through the spatial analysis of a

GIS database needs to be made in this initial stage because the accuracy of the results

depends on the the accuracy and precision of the underlying datasets.

2.2.3.2 Preprocessing

Preprocessing involves manipulating the data obtained from the initial phase in

order to read it into the GIS. This process generally includes the following two sub-

processes: data format conversion and objects identification. The original data usually need to be processed before they can be utilized in the GIS. The conversion process typically involves extracting information from maps, aerial photographs, satellite imagery, and printed records and then converting these information into a GIS database. The second sub-process is object identification, which is basically a set of rules to catalog the locations of objects in the datasets in a consistent manner. Objects might consist of streets, railways, streams, and rivers.

2.2.3.3 Data Management

The data management process is the central part of a GIS which provides for data entry, update, deletion, and retrieval. Optimum GIS performance is highly depend on this process. A well designed database can greatly increase the performance of a GIS, whereas a poorly designed database can even disrupt the operation a GIS.

2.2.3.4 Manipulation and Analysis

Manipulation and analysis are the central theme of a GIS. In this process the analytical operations occur and the new information can be derived. A GIS provides a complete range of analytical capabilities for analysis, but for certain specific tasks, it can also be linked with external analytical modules to increase its capability. These modules are sometimes written in FORTRAN, C, and C++.

2.2.3.5 Product Generation

The final functional element of a GIS is the product generation, where final outputs from the GIS are created. The outputs might include statistics or figures, graphical displays, and images of map. It is very important to know now these outputs or products are directly related to the databases within the GIS. The capability of generating the output from an analytic process, and placing it back into the geographic database for other types of analysis, uniquely separates the GIS from other programs.

2.2.4 Data Structures

There are two basic types of map information that are used to describe data within the GIS. The first type of information is spatial information, which describes the location and shape of geographic features and their spatial relationships to other features. The second type is descriptive information, which describes the spatial features. These two types of map information are generally organized into two types of data structures: vector and raster data structures. The choice of data structure depends highly on the nature the specific GIS application, because each data structure offers uniquely different advantages and disadvantages. This will be reviewed and discussed in a later section.

2.2.4.1 Vector

Vector data structures are based on elemental points whose locations are known to an arbitrary level precision. They have three major geographic feature types: points, lines, and polygons. All feature types are stored using a Cartesian (x,y) coordinate system to reference desired features on the Earth's surface. Point feature type is simply a discrete location identified by a single set of x,y coordinate, which may represent a location that has no area, such as the well location. Line feature type (or arc) is recorded as a series of ordered coordinates, which are connected by a series of point feature types. It represents linear shape objects on the earth's surface that have no width or area, such as highways and streams. The last feature type is a polygon (or area) which is also recorded as a series of ordered coordinates, but with an enclosed figure. Polygon feature types might have different shapes or sizes, but all have area. Examples are land use areas and water bodies. Fig 2.3 depicts the three feature types in a typical vecter based GIS.

For a vector data structure based GIS, the spatial relationships between points, lines, and polygons are depicted using topology, which is defined as an mathematical procedure for explicitly defining spatial relationships. The ability to use topological relationships enables a GIS to process and store data more efficiently, even with very large databases. It also allows GIS to perform analysis between different data feature

types, such as modeling the flow through connecting lines in a stream and overlaying geographic features.

Points

Lines (Arcs)

Polygons
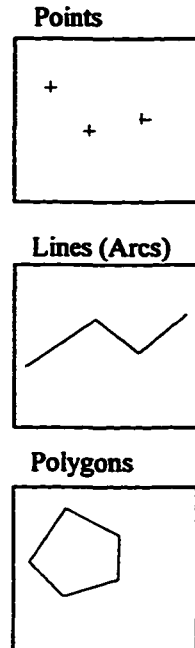
Figure 2.3 The Three Basic Components of a Vector GIS

2.2.4.2 Raster

Another commonly used data structure is a raster or cell based organization of spatial data. A geographic feature on Earth's surface is divided into many evenly sized rectangular shaped cells, with each cell surrounded by eight neighborhood cells. The distances between cells in the raster are constant in both the row and column directions; in other words, the cells in the raster are square. In contrast to a vector data structure, raster structure has limited geographic specificity. This results because the

ability to specify a location in space is limited by the size of the cells. Since certain geographic features may fall within a cell element, it is not possible to exactly locate them. However, a raster data structure excels in the areas of modeling applications, such as hydrological and groundwater modeling.

2.2.4.3 Others

There are more data structure types that are occasionally used in a GIS, which include pyramidal, quadtree, dime, arc-node, relational, and digital line. In most cases, all the above data structures can be converted either to a vector type or a raster type and will not be reviewed in this chapter.

3. A STEADY MODEL: A GIS TO ESTIMATE STORMWATER

POLLUTANT MASS LOADINGS

ABSTRACT: In order to develop a monitoring program for the Santa Monica Bay watershed, a land-use runoff model was developed using a geographic information system (GIS) coupled to an empirical runoff model. The GIS/model has simple data requirements, as compared to more complex models that require routing information, and is useful for predicting receiving water loading on an annual basis or for single storm events. This approach can also be used to graphically present model results in simple and intuitive ways that provide better insight to managers and planners in evaluating pollution sources and control strategies. The GIS/model was used to locate monitoring stations in the most economical way. The model predictions can be used to improve the evaluation of Best Management Practices to control pollutant discharges. Receiving water pollutant contributions from point and nonpoint sources can be compared to develop more economical strategies for overall pollutant minimization.

3.1 Introduction

In many locations, nonpoint sources of water pollution have been recognized as equal or greater in importance than point sources. This is due in part to the continuing efforts to reduce pollution from point sources (e.g., increasing treatment requirements for both municipal and industrial wastewaters) over the past two decades (NOAA 1991), as well as recognition that nonpoint sources, such as stormwater, may contain harmful toxic contaminants (Lau *et al*. 1993, Bay *et al*. 1993). Other studies have also

shown nonpoint sources as the major cause of surface water quality degradation in many areas of the United States, surpassing pollutant loadings to receiving waters from point sources, such as treated municipal and industrial wastewaters (Gilliland and Baxter-Potter 1987; Driscoll *et al*. 1990).

Pollution from treated wastewater discharges through the two major outfalls from Los Angeles City's Hyperion and Los Angeles County's Joint Water Pollution Control Plants has decreased by more than an order of magnitude during the past twenty years. As a result, nonpoint sources now contribute an increased fraction of the total pollutant mass to the Santa Monica Bay (SMB). Treatment plant expansion is currently underway to provide full secondary treatment for the foreseeable future. In addition, with the estimated 1993 population of over nine million in Los Angeles County, there will be greater probability for pollutants to be discharged to the receiving water through spills, illicit discharges, atmospheric fallout, stormwater runoff from increased paving, stormwater conveyance and activities such as automobile use and maintenance.

Nonpoint pollution processes, such as stormwater runoff, are inherently difficult to model due to their stochastic nature in both time and space domains (Corbitt 1989). Furthermore, nonpoint source pollution modeling generally requires

organizing and processing of large amounts of spatially referenced data, that is either

not feasible or difficult to implement, without the aid of computer automation.

Geographic Information System (GIS) technology has matured over the last ten

years and has gained widespread acceptance as a valuable tool because of its ability to

carry out complex spatial operations and to link spatial and descriptive information.

Ventura and Kim (1993) used an urban water quality model, SLAMM (Source

Loading and Management Model) and coupled it with a vector based GIS to estimate

the pollutant loadings of each land use polygon in their studied sewershed. Gilliland

and Baxter-Potter (1987) demonstrated the application of a GIS to predict nonpoint

source pollution potential from agricultural sources. Other studies have also shown the

application of GIS to either predict or estimate the pollutant loads from agricultural

sources (Engel *et al.* 1993; Heidtke and Auer 1993; Xu *et al.* 1993). The GIS

facilitates the handling of voluminous quantities of data that impedes traditional

modeling approaches and allows the fine discritization of watershed data that is

required for detailed analysis. The example presented herein is for a greater and more

complex site with a more parameters than previously used.

The goal of this study is to estimate the annual pollutants emission to Santa

Monica Bay, so that catchments with the largest contribution of each pollutant can be

identified and prioritized for developing a monitoring program and applying best

management practices (BMPs). An empirical model generally does not require an extensive data gathering effort to model the annual events; in addition, the relatively large area of Santa Monica Bay watershed makes a vector based GIS particularly well suited as a back-end database management tool to handle both the spatial and attribute database. Therefore, an empirical model coupled with a vector GIS was used in this investigation. A physical process model could also be used in this study, but the data and time requirements are prohibitive and are not required to achieve the stated goals. There are certain advantages of using a raster-based GIS, but they are not significant at the limited detail and precision of this work.

An empirical urban runoff model is described in this paper. After briefly discussing the model structure, the implementation of a GIS with the model and its application to the Santa Monica Bay watershed are discussed in detail. The mass emission rates from different size sub-basins in the Santa Monica Bay watershed are presented. This information was used to develop a monitoring program to estimate mass emissions to Santa Monica Bay (Stenstrom and Strecker 1993b). Two hypothetical scenarios are shown to illustrate the utility of the GIS/model in predicting the impact of BMPs. Finally, a summary and conclusion are presented based on the model's predictions, along with their implications for future management of the Santa Monica Bay Watershed.

3.2 Methodology

The modeling procedure is divided into two parts: The first part is an empirical runoff model, described previously (Stenstrom *et al.* 1984; Stenstrom and Strecker 1993a), which uses local rainfall data, land use data, drainage data, and local and national water quality data to estimate pollutant loadings to the receiving waters. The second part involves the implementation of a vector GIS, which is utilized for back-end database management tool and spatially interfacing the empirical urban runoff model. Fig. 1 is an overview of the modeling process.
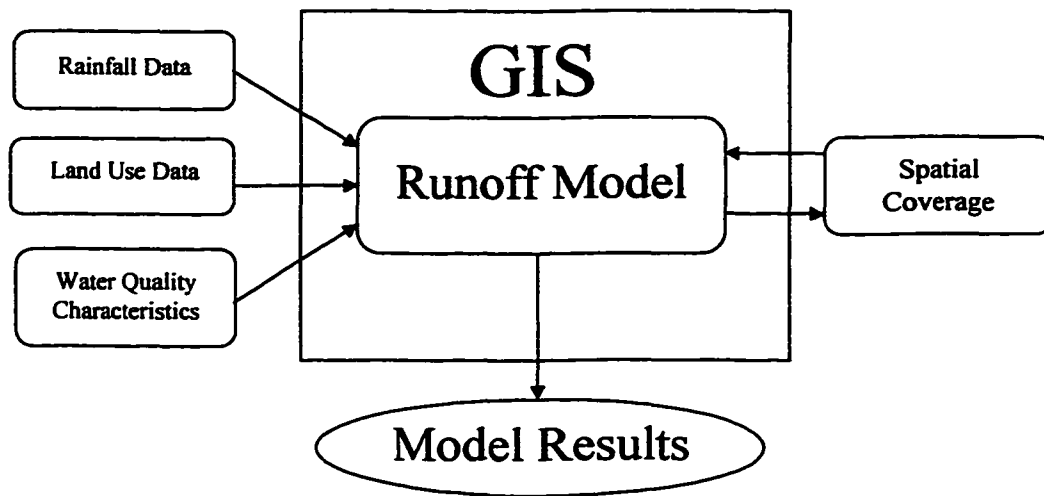
Figure 3.1 Overview of Modeling Process

3.2.1 Watershed Description

Santa Monica Bay (SMB), shown in Figure 2, is a major receiving water for one of the largest population centers in the United States. It is bounded on the north by Point Dume and on the southeast by Palos Verdes Point, a linear distance of about 60 km. The Bay extends from the shoreline of Los Angeles and the adjacent cities of Santa Monica, El Segundo, Redondo Beach, and Malibu westward to water depths greater than 500 m. The total area of the SMB watershed as defined by Figure 2 is 1072 km^2, of which 464 km^2 are urban areas and the remainder are either classified as non-urban (open, parks, etc.) or unknown areas (less than 0.2%). Santa Monica Bay serves approximately nine million people as a major recreational resource, providing fishing, boating, and swimming activities. The watershed contains the largest commercial center on the west coast for manufacturing, aerospace, and petrochemical industries (NOAA 1991). In addition, Los Angeles International Airport (LAX) in the city of El Segundo is one of the busiest airports in the nation, with numerous flights directly over Santa Monica Bay watershed. The opportunities for pollutants to be discharged to the local drainage systems either from land or aerial fallout and eventually to Santa Monica Bay are great.
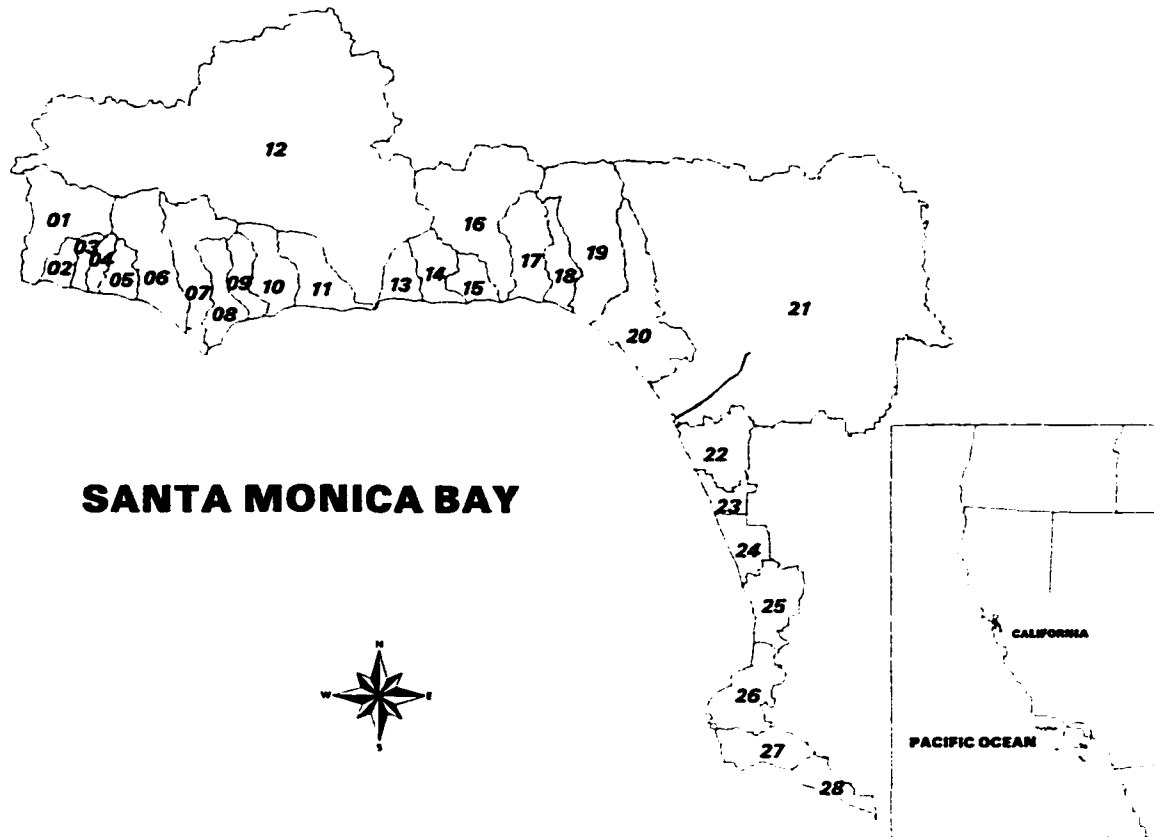
Figure 3.2 Santa Monica Bay Watershed and Subbasin Boundaries

3.2.2 Land Use

Three sets of land use data from Southern California Association of

Governments (SCAG) were used in this study. They were interpreted and derived from

aerial photographs taken in 1987, 1990, and 1993. The original goal of using these

three data sets was to compare the pollutant loading results due to the effect of

urbanization. Due to limited growth over the six year period, and the improved

interpretation from the aerial photography, very few changes in the data sets due to

growth were found. Therefore, only the most recent 1993 land use data were utilized.

The land use definitions and descriptions in this study are a slightly modified version

of Anderson Land use Classification (Anderson *et al.* 1976), where level II

classification (Level II classification represents land use categories by two digits code)

is used to describe the predominant geographic attributes of the watershed. The eight

land use categories utilized in this study are shown in Table 1. The minimum level of

accuracy in identifying land use and land-cover categories from remote sensing data

should be at least 85 percent, as stated by Anderson and others (1976). Therefore, a

minimum of 85 percent accuracy of the above two land use data sets were assumed in

this study.

An important characteristic of land use is the expected stormwater runoff rate.

Previous investigators, through analysis of a large set of rainfall-runoff data from many

studies on urban areas, and highways, have shown that the runoff coefficient (RV,

defined as the overall average ratio of runoff to rainfall) are highly correlated to

impervious surface area (IMP) (US EPA 1983; Driscoll *et al.* 1990). This assumption

was adopted in this study and is shown in Eq. (1).

$$RV = 0.007\ IMP + 0.1 \hspace{3cm} (1)$$

where RV = runoff coefficient; IMP = impervious area (expressed as a percentage). In this study, impervious surface area percentage for a given land use category area was based upon the Santa Monica Bay (SMB) Drainage Area Characteristics (Los Angeles County Department of Public Works, Alhambra, CA). Driscoll's *et al.* (1990) relationship between the IMP and RV (Eq. (1)) was used to determine the value of runoff coefficient for each land use type. The values of IMP and RV utilized for the eight land use categories modeled in this study are shown in Table 1. The GIS is used to implement the above procedures and will be discussed in more detail in the later sections. Subsequently after the determination of runoff coefficients for each catchment, annual average storm runoff volume can then be estimated for the whole watershed using the equations discussed in the next paragraph.

Table 3.1 Land-Use Characteristics

Land Use Category	Impervious Surface Area[a] [%]	Runoff Coefficient[b]
Single-family	42	0.39
Multi-family	68	0.58
Commercial	92	0.74
Public	80	0.66
Light Industrial	91	0.74
Other Urban	80	0.66
Open	0	0.10
Unknown	65	0.56

[a]Based on Los Angeles County Department of Public Works, NPDES Permit No. CA0061654, Attachment 1, Santa Monica Bay Drainage Basin, Drainage Area Characterization.
[b]Estimates based on percent imperviousness and runoff coefficient relationship given in FHWA (1990).

3.2.3 Rainfall

Rainfall data were collected from 10 gages in the watershed, including the Los Angeles Airport (LAX) gage station, over a 42 year period. Synoptic Rainfall Analysis Program (SYNOP, Woodward Clyde Consultants, Inc. 1989) was used to compute the mean, standard deviation, and the coefficient of variation for all of the rainfall event statistics. To facilitate the modeling process, rainfall correction factors (CF) were derived from both the 50-year, 24-hour rainfall and the 1990-91 seasonal total isohyetal map. These were used in conjunction with the average storm rainfall (ASRF) at the LAX rain gage station to scale the rainfall for each catchment to reflect spatial variations within the watershed. Based on the Rational Method (Viessman *et al.* 1989), annual average storm runoff volumes (ASV) for each catchment were then calculated by multiplying the CF, the ASRF at LAX, the area, and the runoff coefficient (RV) as shown in Eq. (2). The annual average storm runoff (AASV) of each catchment was calculated by multiplying ASV from Eq. (2) and the average number of storms per year (NSTORM) as shown in Eq. (3). Since this study was only concerned in rainfall events which produce runoff, all rainfall events with a volume of less than 2.5 mm were discarded from the statistical analysis. For the Santa Monica Bay watershed, the average time between storms varies from 198 to 258 hours (8 to 11 days) during the wet season. The coefficient of variation of the time between storms ranges from 1.10 to 1.36 from rainfall records of 10 selected rain gages in the SMB watershed (Stenstrom and Strecker 1993a). Therefore, NSTORM is approximately

equal to 16 storm events in each wet season. The average storm rainfall and the annual average storm runoff were calculated as follows:

$$ASV_i \quad = \quad RV \cdot AREA \cdot CF \cdot ASRF_{LAX} \qquad (2)$$

$$AASV_i \quad = \quad ASV_i \cdot NSTORM \qquad (3)$$

where $ASRF$ = average storm rainfall[m]; $AASV$ = annual average storm runoff[m³/year]; ASV = annual average storm runoff volume[m³]; CF = rainfall correction factor; $NSTORM$ = average number of storms per year[year⁻¹]; $AREA$ = area of catchment i[m²]. The GIS/model can be used for different periods or for single events.

3.2.4 Water Quality

The eleven water quality parameters are of concern to urban nonpoint source runoff and were modeled in this study. They are: total suspend solids (TSS), biochemical oxygen demand (BOD), chemical oxygen demand (COD), nitrite and nitrate (NO23), total Keldahl nitrogen (TKN), total phosphorus (TP), soluble phosphorous (SP), total copper (Cu), total lead (Pb), total zinc (Zn), and total oil and grease (O&G).

These parameters were chosen for their general tendency to be indicators of problems in urban runoff, and because sufficient data were available from national and/or local data to estimate land use contributions.

To use the empirical model, it is necessary to know the site median event mean concentration (EMC) of each pollutant for each land use type. To determine the EMCs for different land uses, all agencies who monitor stormwater discharge to SMB were surveyed. No one agency has this responsibility and fifteen sources of data were found that were collected from 47 monitoring locations for a variety of water quality parameters. A total of 43,015 data points were collected. Unfortunately, much of the data were not particularly useful, since they were collected by different agencies using different methodologies for varying purposes.

Most of the water quality data were grab samples which represent instantaneous values of pollutant concentrations. In most cases, a single instantaneous value cannot be used to represent average conditions; furthermore, it does not describe the variability of the pollutant concentrations (Wanielista and Yousef 1993). In addition, much of the data were collected during dry weather conditions, and are not useful for assessing stormwater pollutant discharges. To improve estimates of site median EMCs, the SMB data were compared to US EPA's Nationwide Urban Runoff Program (NURP) database, which were composite samples collected from known land

uses (Driscoll *et al.* 1990). A comparison of the appropriate subset of the water quality

data collected in the SMB watershed to the corresponding NURP data showed that the

SMB watershed concentrations are generally much higher, and median SMB

concentrations approximate 90th percentile NURP concentrations (Stenstrom and

Strecker 1993a). The higher concentrations may occur because of the reduced rainfall

of the SMB watershed, as compared to NURP sites, as well as from potentially larger

urbanization in the Los Angeles area. No oil and grease (O&G) data were collected in

the NURP study, and O&G concentrations were estimated from previous findings by

Stenstrom et al. (1984) and Fam et al. (1987).

Previous researchers have shown the variable EMCs in stormwater runoff from

urban areas can be adequately described by a lognormal distribution (Driscoll *et al.*

1990). If the EMCs are log-normally distributed, site median EMCs can be

transformed to the mean runoff event concentrations (*ME*), using Eq. (4).

$$ME \quad = \quad SM\sqrt{1+CV^2} \tag{4}$$

Where: SM = site median EMC[mg/L]; ME = event mean concentration[mg/L]; CV =

coefficient variation. A typical value for the coefficient variation (CV) of pollutant

concentrations is 0.71 for urban areas (Driscoll *et al.* 1990). Therefore, event mean

concentration is approximately 23 percent greater than the site median EMC (SM). The

estimated annual loading for individual pollutants (APL) is expressed as:

$$APL_i = AASV \cdot ME_i \cdot CF \qquad (5)$$

Where APL = annual pollutant loadings[kg/year]; ME = event mean

concentration[mg/L]; CF = conversion factor for runoff volume to liters; i = pollutant i

3.3 GIS Implementation

A UNIX-based GIS, ARC-INFO 7.0.4 (ARC/INFO 1992) was used for the GIS

on an IBM RISC/6000 POWERstation Model 550E. The database for this GIS/model

consists of three spatial coverages: a land use coverage, a sub-basin coverage, and a

catchment coverage. All three coverages were available in ARC-INFO native format,

and were originally developed by scanning USGS maps with drainage data provided

by the Los Angeles County Department of Public Works. The land use, sub-basin, and

catchment coverages are related with rainfall and runoff attribute data to form an

integrated GIS/model to estimate the pollutant loadings from the watershed. Land use

polygons are adopted as the smallest unit for analysis. These three spatial coverages

have the following general characteristics: Sub-basin coverage (BA) contains 28

polygons; Catchment coverage (CA) contains 500 polygons within the 28 polygons

above; 1993 land use coverage (**LU93**) contains 6498 polygons within the 500

polygons of **CA**.

Fig. 3 shows the distribution of land use pattern in the Santa Monica Bay

watershed in 1993. Table 2 and 3 illustrate the land use pattern of **LU93** land use

coverage and the land use by sub-basins, respectively. Open, single and multiple

family are the predominated land uses, where they account for close to 85 percent of

the total land use in the SMB watershed. The majority of the open and single/multiple

family land uses are located in sub-basin 12 (Malibu drainage) and sub-basin 21

(Ballona Creek drainage), respectively.

Table 3.2 Areal Distribution of Land-Use Coverage

Land use coverage (1)	Land use area [Hectares (% of total)]								
	Unknown (2)	Single Family (3)	Multi-Family (4)	Commercial (5)	Public (6)	Light Industrial (7)	Other Urban (8)	Open (9)	Total (10)
LU93	9 (0.01)	26102 (24.4)	8070 (7.5)	4902 (4.6)	2526 (2.4)	2213 (2.1)	2845 (2.7)	60509 (56.5)	107178

Table 3.3 Land-Use Distribution in 28 Subbasins (Based on LU93)

Sub-basin(1)	Percentage of Land Use Area								Total Area [hectares] (10)
	Single-family(2)	Multi-family(3)	Commer-cial(4)	Public(5)	Light Industrial(6)	Other Urban(7)	Open(8)	Unknown(9)	
1	1	0	0	0	0	0	98	0	2915
2	3	0	0	0	0	0	97	0	578
3	11	1	0	0	0	0	88	0	449
4	8	0	0	0	0	0	92	0	477
5	9	0	0	0	0	0	91	0	815
6	9	0	0	1	0	0	89	0	2777
7	9	1	0	0	0	0	88	0	2469
8	21	2	0	0	0	0	76	0	1371
9	10	0	0	0	0	1	88	0	902
10	5	1	0	0	0	0	94	0	1525
11	4	1	1	4	0	0	90	0	1741
12	9	2	1	1	0	2	85	0	28444
13	11	1	1	0	0	0	86	0	912
14	12	2	0	0	0	0	86	0	1281
15	3	0	0	0	0	0	96	1	837
16	10	0	0	0	0	0	90	0	5102
17	12	2	0	1	0	2	83	0	2016
18	23	3	1	2	0	2	69	0	1149
19	21	1	0	1	0	0	77	0	4266
20	41	22	11	4	4	3	16	0	3622
21	42	17	11	5	4	3	18	0	33692
22	26	6	3	5	1	41	19	0	2037
23	6	5	7	0	62	13	7	0	665
24	64	12	9	6	1	1	7	0	1103
25	52	21	8	9	1	2	7	0	1750
26	67	5	2	3	0	1	22	0	1993
27	37	3	2	2	1	3	53	0	1521
28	45	4	1	5	0	0	45	0	948

Santa Monica Bay

- ☐ Single Family
- ■ Multi-Family
- ☐ Other Urban
- ■ Open
- ■ Unknown
- ▤ Commercial
- ▨ Public
- ■ Light Industrial
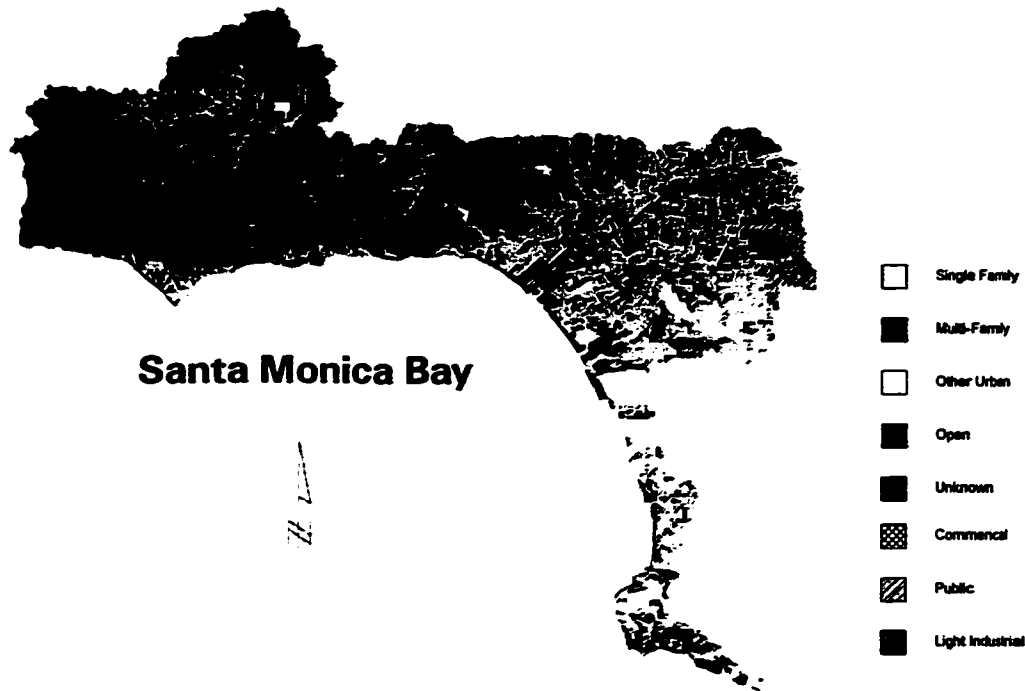
Figure 3.3 Land-Use Pattern in SMB Watershed (Based on 1993 Land-Use Data)

Figure 2 shows the distribution of 28 sub-basins in the SMB watershed. The sub-basins are lumped into three major regions and they are categorized in the following way: Sub-basins 1-19 make up the North Bay; Sub-basins 20-22 make up the West Los Angeles; Sub-basins 23-28 make up the South Bay.

The GIS modeling work can be divided into three main steps: The first step is to link the land use coverage with rainfall and runoff coefficient information (Eq. (1) to Eq. (3)), and also to link the catchment coverage (CA) with the corresponding rainfall correction factor (CF) which is used to reflect the spatial variation of rainfall pattern.

The second step is to the overlay the sub-basin coverage (**BA**) with the two new

coverages created in the first step, to form the final coverage, which will be used to

estimate the pollutant loadings. The last step is to link the eleven water quality

characteristics (Eq. (4)) with the final coverage.

There are two basic ways of linking an attribute table to a table of geographic

records. A relational join command is used to perform the relational join operation,

which expands the geographic file to permanently include the attribute file. A relate

operation temporarily links the attribute file with the geographic file in which the two

links are separately stored. There are advantages to each method that depend on the

data storage requirements, the speed of the computer, and other miscellaneous factors

(ARC/INFO 1992). Since there are only four equations (variables) needed to link with

LU93 and **CA** spatial coverages, and also because join operations are generally faster

to manipulate than relate operations, the relational join is used in step (1). The first

"join" operation is a "one to many" relationship (one land use or runoff coefficient is

related to many different polygons) between the land use coverage and the runoff

coefficient attribute table (Equation 1). The second "join" operation is a "one to one"

relationship between the catchment coverage and the rainfall correction factor attribute

table.

Land use Polygons

Overlay

Catchment Polygons

Overlay
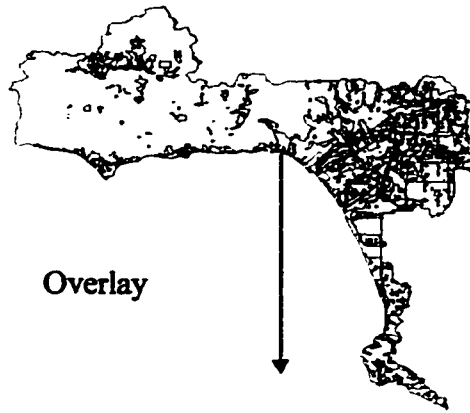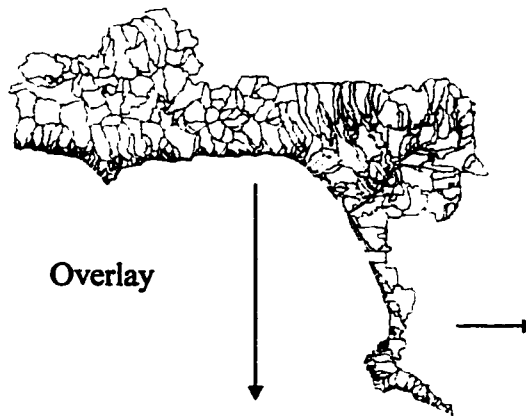
$$C_i = \sum_{k=1}^{8} \sum_{n=1}^{N} AASV_{n,k,j} \cdot ME_{n,k,j} \cdot G$$

Basin Polygons

$$B_j = \sum_{i=1}^{M} C_i$$
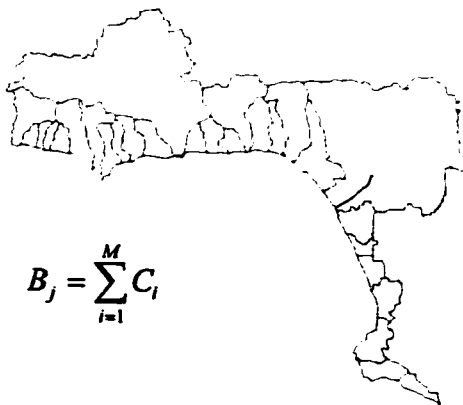
Figure 3.4 Spatial Union Operation Using GIS and Nonpoint Source Modeling: (a) Land-Use Polygons; (b) Catchment Polygons; (c) Basin Polygons

After the superimposing the land use, the catchment, and the sub-basin coverages, Eq. (2) through Eq. (5), can then be implemented in the GIS/model. This process is a union, which creates an output coverage by overlaying the three spatial coverages. All polygons and attributes from these three spatial coverages are combined and preserved at the output coverage. The order of the union operation is important because all duplicate parameters except the one in the first input coverage are deleted. Therefore, the spatial union operation between the land use coverage and the catchment coverage must precede the operation between the output coverage and the sub-basin coverage, in order to preserve the variable "AREA" of the land use coverage. The variable "AREA" of LU93 represents the "AREA" term in Eqs. (2) and (3). Fig. 4 depicts the overall spatial union operations of second step.

The estimated pollutant loading formula from Eq. (5) is then linked with the resultant output coverage (or table) to calculate the eleven pollutant loadings from each catchment polygon and also from each sub-basin polygon. This process is facilitated if the GIS has built-in statistics commands. Eq. (6) and (7) are used to estimate the pollutant loadings from catchment i (C_i) in sub-basin j, and sub-basin j (B_j), respectively.

$$C_i = \sum_{k=1}^{8} \sum_{n=1}^{N} AASV_{n,k,i} \cdot ME_{n,k,i} \cdot G \qquad (6)$$

$$B_j = \sum_{i=1}^{M} C_i \qquad\qquad (7)$$

where $AASV$ = average annual storm volume [m³/yr]; ME = event mean

concentration[mg/L]; G = conversion factor (m³·mg/L to kg) [10^{-3}];C_i = estimated

annual pollutant loading of catchment i [kg/yr]; B_j = estimated annual pollutant

loading of sub-basin j [kg/yr]; N = total number of land use polygons with land use

type k within catchment i; M = total number of catchment polygons within sub-basin j;

k = land use type; n = land use polygon n within the catchment i.

3.4 Results

The GIS/model was used to determine the areas (Basins) and land uses

producing the most polluted runoff. The annual pollutant loadings and the annual unit

pollutant loadings from each land use category are shown in Tables 4 and 5,

respectively. In Table 4, the annual pollutant loadings for each land use are in metric

ton per year (MT/yr), whereas in Table 5, the annual unit pollutant loadings for each

land use are in metric ton per hectare per year (MT/hectare/yr), which are calculated by

normalizing for the different land use areas. As shown in Table 4, the single-family

land use produces the highest loading of all pollutants among all land uses except for

Open, which has a higher TSS load. This results because the Single-family and Open

land uses together account for more than 80% of the total area (see Table 2). Table 4

shows the oil and grease contributions from Commercial, Public, and Light Industrial

areas, which are approximately 46% of the total oil and grease emissions, even though

the overall area size accounts for only 9% (see Table 2) of the total area in SMB

watershed. The normalized land use loadings in Table 5 show commercial, public, and

light industrial areas have the highest per unit area contributions. High loadings can be

produced from relatively small areas within the watershed. This results oil and grease

runoff is strongly correlated with land use, resulting in a large variation in emission

rates (Fam *et al.* 1987).

Table 3.4 Annual Pollutant Loadings for Each Land Use (Based on LU93)

Land Use	Annual Pollutant Loadings (MT per year)										
	TSS	BOD5	COD	Total P	Solube P	TKN	NO2+NO3	Total Cu	Total Pb	Total Zn	Oil&Grease
(1)	(2)	(3)	(4)	(5)	(6)	(7)	(8)	(9)	(10)	(11)	(12)
Single-family	12316	722	5946	36	11	183	79	4	15	15	127
Multi-family	3985	285	2467	12	2	46	19	2	8	7	417
Commercial	2683	209	1342	6	3	30	18	1	3	10	328
Public	1215	94	607	3	1	13	8	0	2	5	148
Light Industrial	1127	88	564	3	1	13	8	0	1	4	138
Other Urban	1603	114	992	5	1	18	8	1	3	3	168
Open	14383	59	2789	15	4	82	43	2	4	13	0
Unknown	0	0	0	0	0	0	0	0	0	0	0

It is not possible to calibrate the GIS/model, because data are not available (one

of the purposes of this project was to develop the GIS/model in order to develop a

monitoring program). The only estimates for discharge to the Bay were performed by

SCAG (1988), and only for sub-basins 12 and 21. A detailed comparison was presented by Stenstrom and Strecker (1993a), and is too lengthy to repeat here; however, the comparisons were generally good, considering the challenging nature of monitoring wet weather pollutant flow. For sub-basin 21, which is highly developed, the model generally predicted higher emissions for 6 contaminants and flow rate than estimated by SCAG; the model averaged 83% higher. For sub-basin 12, which contains a large fraction of open or undeveloped land, the models predictions were 32% lower than SCAG's estimates for the same pollutants. Emissions or lead were quite different between the model and SCAG's estimates, which may be due to total versus dissolved measurement differences. The authors consider this is good agreement. One possible source of the differences is that the model is calibrated using water quality data collected over the 1972-91 period, as opposed to a single year.

Table 3.5 Unit Pollutant Loadings for Each Land Use (Based on LU93)

Land Use	Annual Unit Pollutant Loadings (MT per hectare per year)										
	TSS	BOD5	COD	Total P	Soluble P	TKN	NO2+NO3	Total Cu	Total Pb	Total Zn	Oil&Grease
(1)	(2)	(3)	(4)	(5)	(6)	(7)	(8)	(9)	(10)	(11)	(12)
Single-family	5.E-01	3.E-02	2.E-01	1.E-03	4.E-04	7.E-03	3.E-03	2.E-04	6.E-04	6.E-04	5.E-03
Multi-family	5.E-01	4.E-02	3.E-01	1.E-03	3.E-04	6.E-03	2.E-03	2.E-04	1.E-03	9.E-04	5.E-02
Commercial	5.E-01	4.E-02	3.E-01	1.E-03	5.E-04	6.E-03	4.E-03	2.E-04	7.E-04	2.E-03	7.E-02
Public	5.E-01	4.E-02	2.E-01	1.E-03	5.E-04	5.E-03	3.E-03	2.E-04	6.E-04	2.E-03	6.E-02
Light Industrial	5.E-01	4.E-02	3.E-01	1.E-03	5.E-04	6.E-03	3.E-03	2.E-04	6.E-04	2.E-03	6.E-02
Other Urban	6.E-01	4.E-02	3.E-01	2.E-03	3.E-04	6.E-03	3.E-03	3.E-04	1.E-03	1.E-03	6.E-02
Open	2.E-01	1.E-03	5.E-02	3.E-04	7.E-05	1.E-03	7.E-04	3.E-05	7.E-05	2.E-04	0.E+00
Unknown	9.E+00	7.E-01	6.E+00	3.E-02	6.E-03	1.E-01	5.E-02	5.E-03	2.E-02	2.E-02	1.E+00

Annual Pollutant Loadings
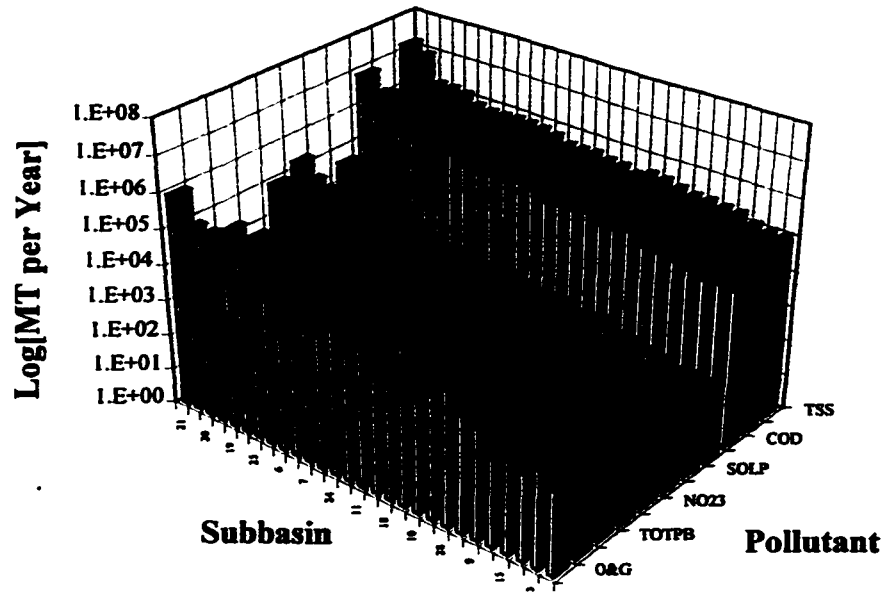
Unit Pollutant Loadings
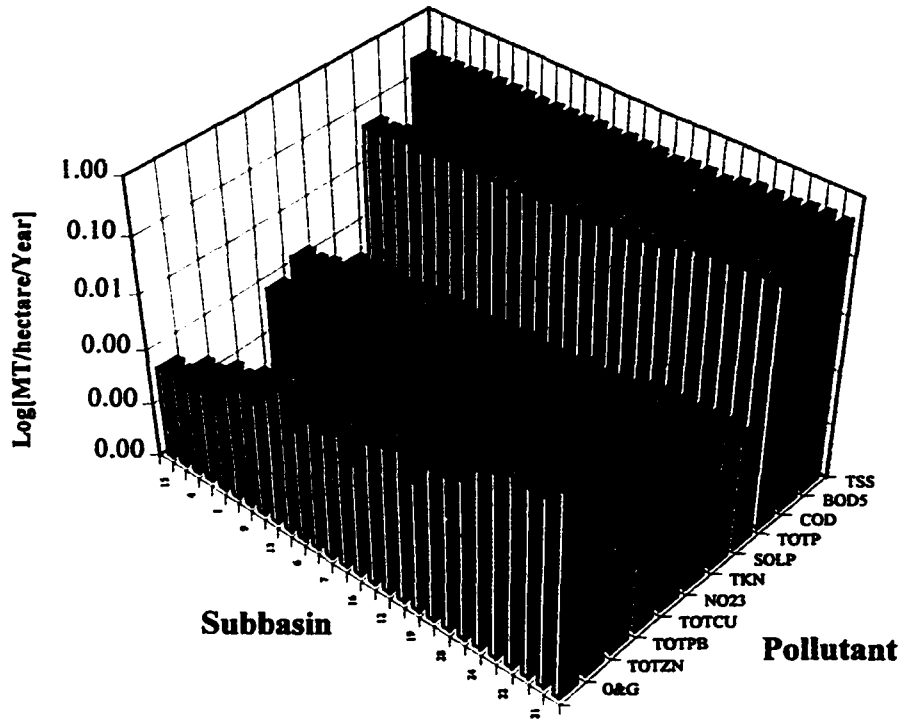
Figure 3.5 Pollutant Loadings for 28 Subbasins (Based on 1993 Land-Use Coverage):
(a) Annual Pollutant Loadings; (b) Unit Pollutant Loadings

Fig. 3-5 shows the annual and unit pollutant loadings from the 28 sub-basin in the watershed. For all eleven pollutants, the Ballona Creek drainage (sub-basin 21), which drains the greater part of Los Angeles Metropolitan area, shows the highest loadings, followed by the Malibu drainage (sub-basin 12). The remaining 26 sub-basin watersheds only contribute 35% of the total loading. Sub-basin 21 shows the largest percentage loadings of oil and grease. These observations are explained by the land use and the total areas in sub-basin 21, as shown in Table 3-3. This sub-basin includes four major interstate freeways (Freeways and major roads are lumped into the Other Urban land use category), networks of complicated transportation systems, heavy concentration of multi-family residential area, and other miscellaneous urban structures. The unit pollutant loadings were highest for sub-basin 23, followed closely by sub-basins 21, 20, and 22. This is expected because of their high proportions of industrial areas, utility facilities, and other urbanized areas. These sub-basins also have the highest loadings and unit loadings of oil and grease. The ability to rank pollutant emissions will be useful if problems associated with specific pollutants are identified in the Bay; the GIS/model results are a starting point to look for ways of reducing emissions.

The GIS/model results were used to design a monitoring program (Stenstrom and Strecker 1993b), which has become the structure for the Los Angeles County Department of Public Works monitoring program for the drainages area into Santa

Monica Bay. Using the GIS/model, it is easy to position monitoring stations at locations that will sample a minimum fraction of the runoff. For example, selecting sub-basins 12 and 21 will sample approximately 65% of the total runoff, based upon flow rate. It is also possible to select monitoring locations based upon other criteria, such as the anticipated mass loadings of some particular pollutant. Another possibility is to use the GIS/model to select small land parcels that are predominately composed of single land uses. In this way stations are selected to be used to collect data for additional model calibration and validation. For the Santa Monica Bay monitoring program, the five sub-basins with the greatest emissions were initially selected as mass emission stations. These included sub-basins 12 and 21. A similarly sized group was selected as land use stations. The results of this monitoring program will eventually become available for model verification and additional model development.

To illustrate the potential uses of the GIS/model for stormwater management, the following two hypothetical scenarios are used as examples. Scenario one, uses sub-basin 12 (Thousand Oaks drainage) to illustrate the impact of land use changes on the pollutant annual discharges. Sub-basin 12, as shown in Table 3-3, has nearly 90% open land use. By transforming 20% of the Open land use to other land use categories, such as Single-Family and Multi-Family, the increase in annual pollutant emissions can be calculated, and the results are shown in Table 3-6. These are potential changes that might occur with increasing population. From Table 3-6, the pollutant O&G shows a

larger increase in the annual loading and a wider range of the percent annual loading increases among the six hypothetical land use transformations. The smallest and largest increases in the annual loadings impacted from the hypothetical land use transformation are the single-family and other urban land uses, respectively. The commercial and light industrial land uses also receive significant increases in the annual loadings.

Table 3.6 Scenario One: Annual Pollutant Loadings in Subbasin 12

Pollutant	Annual Loadings of Subbasin 12 (MT per year)						
	Open	20% of Open land use are transformed to the following land uses					
		Single-family	Multi-family	Commercial	Public	Light Industrial	Other Urban
(1)	(2)	(3)	(4)	(5)	(6)	(7)	(8)
TSS	8,520	10,038	10,195	10,499	10,145	10,469	10,609
BOD5	191	340	356	427	400	425	415
COD	2,497	3,532	3,994	3,809	3,631	3,794	4,250
TP	14	20	21	20	19	20	22
SP	4	6	5	7	6	7	6
TKN	68	102	95	97	93	97	99
NO23	33	2	3	3	3	3	3
Total Cu	2	8	11	9	8	9	12
Total Pb	5	12	14	21	20	21	15
Total Zn	10	47	13	51	48	51	45
O&G	138	145	415	501	458	498	458

In scenario two, we use the GIS and model to illustrate the impact of BMPs on the annual discharge to Santa Monica Bay. The GIS/model can be programmed to predict the impact of BMPs, and two hypothetical BMPs are tested: a campaign to reduce the amount of fertilizer used on lawns of single and multiple family housing, and a control program to reduce the oil and grease discharge into the storm drains on

commercial and industrial land uses. Both BMPs assume that a 50% reduction in site mean concentration occurs because of the best management practice. For simplicity, we assume that 100% of the nitrate in the urban runoff from these land uses is from fertilizer use. Table 3-7 shows that a 50% reduction in residential fertilizer use (or a 50% reduction in event mean concentration of nitrite and nitrate) reduces annual NO23 emission by approximately 28%. As for the second BMP, a 50% reduction in the amount of oil and grease discharge (or a 50% reduction in event mean concentration of oil and grease) results in close to 14% reduction in the annual O&G discharge. Table 3-7 also shows the most significant and the least significant sub-basin impacted from the two given hypothetical BMPs. Sub-basin 21 (Ballona Greek drainage) shows the largest reduction in both the annual NO23 and O&G discharge. Sub-basin 1 and 4 (Malibu drainage) show no significant reduction in the annual O&G and NO23 emission, respectively.

Table 3.7 Scenario Two: Annual NO23 and O&G Loadings (MT/yr)

Pollutant (1)	SMB		Most Significant Sub-basin		Least Significant Sub-basin	
	Before (2)	After (3)	Before (4)	After (5)	Before (6)	After (7)
NO23[a]	182	133	87[b]	59	0.41[c]	0.38
O&G[a]	1336	1103	869[b]	699	0[d]	0

[a]Assumption: 50% reduction in mean event concentration of NO23 and O&G
[b]Subbasin 21;
[c]Subbasin 2;
[d]Subbasin 1,3,4,5,9,15

The technique shown in these two hypothetical cases may be valuable for city planners and others to mitigate the growth in nonpoint pollution due to the land use changes. It should also be useful for government agencies to determine the impact and cost/benefit of different proposed BMPs. Such analysis will help in the development of an optimum stormwater pollution control strategy.

Table 3.8 Comparison of Model Predictions with Annual Emissions from Hyperion Treatment Plant

Parameter (1)	Model[a] (93) (2)	Hyperion[b] (92) (3)	Total Load[c] (4)	D_NPS[d][%] (5)
TSS	37,000	19,000	56,000	66
BOD	1,600	41,000	42,600	4
TP	80	2,500	2,580	3
NO2+NO3	180	132[e]	312	58
Cu	10	16	26	39
Pb	37	1	38	97
Zn	57	35	92	62
O&G	1,300	5,900	7,200	18

Units are all in MT/year.
[a]Based on 1993 land use data.
[b]Using 1992 annual average data.
[c]Total Load = Total Annual emission of the Model and the Hperion Treatment Plant.
[d]D_NPS = Model emission (nonpoint source) as a percentage of Total Load.
[e]Using the Nitrate Nitrogen (NO_3-N) only.

To illustrate the significance of nonpoint source pollution, annual emission data from the Hyperion Wastewater Treatment Plant (HTP) of City of Los Angeles (Santa Monica Bay Restoration Project 1993) are compared with the model results. The Hyperion Plant and a petroleum oil refinery are the only facilities which have NPDES permits to discharge into Santa Monica Bay. Hyperion has more than 100 times the flow rate of the refinery, which has a activated sludge plant for effluent treatment. For the purpose of this example, we assume that Hyperion represents 100% of the point source pollution to Santa Monica Bay. Both Hyperion and nonpoint sources are presented in Table 9, which shows the range of differences of the annual emissions. The nonpoint source contribution (column 5) for some pollutants, such as total phosphorus, is quite low (3%). For other pollutants, such as lead, the nonpoint sources are the major sources (97%). In 1993, the Hyperion Wastewater Treatment Plant was only capable of treating approximately 50% of the flow to full secondary standards. When construction of the new facilities are completed, and 100% secondary treatment is possible, the relative point source contribution will be much less. This suggests that if further reductions in pollution to Santa Monica Bay are required, nonpoint sources should be evaluated first. Also the Hyperion Plant discharges through a long outfall, and the dilution further reduces its impact The storm drains discharge at the beach or surf, in close human contact, which probably increases their impact.

3.5 Conclusions

In this study we have shown the feasibility of imbedding an urban runoff model into a Geographic Information System (GIS) to estimate the annual pollutant loadings to the Santa Monica Bay Watershed. The overall framework takes advantage of the built-in relational database management technology of the GIS to construct an accurate and detailed database. This database depicts the watershed geographic attributes and relates them using the urban runoff model. Critical and sensitive areas of varying sizes within the watershed can be accurately located by using the built-in graphical display capability of the GIS. This integration of a nonpoint source model and a GIS offers a powerful tool to assist watershed managers in developing control strategies to improve water quality within local drainage systems. It also allows the managers to evaluate impacts of various BMPs with given hypothetical conditions.

Many factors need to be considered in evaluating stormwater management alternatives, and cost-effectiveness is a paramount factor. Cost-effectiveness is generally measured by either reduction in specific pollutants or mass removal at least cost. For stormwater measures, costs are generally site specific, which may depend on land cost, availability of funds, and many other factors. The methodology presented in this paper can be further extended by integrating nonpoint source computer models and optimization techniques into the GIS. Within this framework, alternative stormwater

management methods can be simulated for specific critical areas in determining the least cost combination of water quality control alternatives.

3.6 Acknowledgments

3.7 References

Anderson, J.R., Hardy, E.T., Roach, J.T., and Witmer, R.E. (1976). "A land use and land cover classification system for use with remote sensor data," U.S. Geological Survey Professional Paper 964.

ARC/INFO User Guide. (1992). Environmental Systems Research Institute, Inc. Version 6.1.1, Redlands, CA.

Bay, S.M., D.J. Greenstein, S.L. Lau, M.K. Stenstrom, and C.G. Kelley, "Toxicity of Dry Weather Flow from the Santa Monica Bay Watershed," *Bulletin of Southern California Academy of Sciences*, Vol. 95, pp. 33-45, 1996.

Cline, T.J., Molinas, A., and Julien, P.Y. (1989). "An Auto-Cad-Based Watershed Information System for the Hydrologic Model HEC-1," *Water Resources Bulletin*. Vol. 25, No. 3, pp. 641-652.

Corbitt, R.A. (1989). *Standard Handbook of Environmental Engineering*. McGraw Hill, Inc., New York, NY.

Driscoll, E.D., Shelley, P.E., and E.W. Strecker (1990). *Pollutant Loadings and Impacts from Stormwater Runoff, Volume III*: Analytical Investigation and Research Report. FHWA-RD-88-008, Federal Highway Administration, Washington, DC.

Duckson, Jr., D.W. (1989). "Land-Use and Water-Quality Relationships in the Georges Creek Basin, Maryland," *Water Resources Bulletin*. Vol. 25, No. 4, pp. 801-807.

Elmasri, R., and Navathe, S.B. (1989). *Fundamentals of Database Systems*. The Benjamin/Cummings Publishing Company, Inc., Redwood City, CA.

Engel, B.A., Srinivasan, R., Arnold, J., and Rewerts, C. (1993). "Nonpoint Source (NPS) Pollution Modeling Using Models Integrated with Geographic Information Systems (GIS)," *Wat. Sci. Tech*. Vol. 28, No. 3-5, pp. 685-690.

Fam, S., Stenstrom, M.K., and Silverman, G. (1987). "Hydrocarbons in Urban Runoff," *Journal of Environmental Engineering*, ASCE. Vol. 113, No. 5, pp. 1032-1046.

Gilliland, M.W., and Baxter-Potter, W. (1987). "A Geographic Information System to Predict Non-Point Source Pollution Potential," *Water Resources Bulletin*. Vol. 23, No. 2, pp. 281-291.

Heidtke, T.M., and Auer, M.T. (1993). "Application of a GIS-Based Nonpoint Source Nutrient Loading Model for Assessment of Land Development Scenarios and Water Quality in Owasco Lake, New York," *Wat. Sci. Tech.* Vol. 28, No. 28, pp. 595-604.

Joint Water Pollution Control Plant Annual Monitoring Report (1993). County Sanitation Districts of Los Angeles County. NPDES No. CA0053813. RWQCB Order No. 91-112. Monitoring and Reporting Program No. 1758, Whittier, CA.

Kim, K. (1993). *Feature-Oriented Urban Classification Using Remote Sensing and a Geographical Information System.* Ph.D. Diss., The University of Wisconsin, Madison. Madison, WI.

Lau, S.L., Bay, S., and Stenstrom, M.K. (1993). "Contaminants in Urban Runoff and their Impact on Receiving Waters," Presented at: Asian WaterQual '93: Fourth IAWQ Asian Regional Conference on Water Conservation and Pollution Control, Oct. 5-9, 1993, Jakarta, Indonesia.

Marsalek, J. (1991). "Pollutant Loads in Urban Stormwater: Review of Methods for Planning-Level Estimates". *Water Resources Bulletin.* Vol. 27, No. 2, pp. 283-291.

National Oceanic and Atmospheric Administration (1991). *Contaminant Trends in the Southern California Bight: Inventory and Assessment.* NOAA Technical Memorandum NOS ORCA 62, Seattle, Washington.

National Research Council (1990). *Monitoring Southern California's Coastal Waters.* National Academy Press, Washington, DC.

Sabins, Jr., F. F. (1987). *Remote Sensing, Principles and Interpretation.* 2nd Edition. W. H. Freeman and Company, New York, NY.

Southern California Association of Governments (SCAG) (1988). "State of the Bay," Southern California Association of Governments, Los Angeles, CA.

Silverman, G.S., Stenstrom, M.K., and Fam, S. (1988). "Land Use Considerations in Reducing Oil and Grease in Urban Stormwater Runoff," *Journal of Environmental Systems.* Vol. 18, No. 1, pp. 31-47.

Stenstrom, M.K. and Strecker, E.W. (1993a). *Annual Pollutants Loadings to Santa Monica Bay from Stormwater Runoff,* Assessment of Storm Drain Sources of Contaminants to Santa Monica Bay, Vol. 1. Report No. UCLA ENGR 93-62, University of California, Los Angeles, Los Angeles, CA.

Stenstrom, M.K and Strecker, E.W. (1993b). *Surface Drainage Water Quality Monitoring Program Plan,* Assessment of Storm Drain Sources of Contaminants to Santa Monica Bay, Vol. III, Report No. UCLA-ENG-93-64, University of California, Los Angeles, Los Angeles, CA.

Stenstrom, M.K., Silverman, G.S., and Bursztynsky, T.A. (1984). "Oil and Grease in Urban Stormwaters," *Journal of Environmental Engineering,* ASCE. Vol. 110, No. 1, pp. 58-72.

Santa Monica Bay Restoration Project (1993). *Characterization Study of the Santa Monica Bay Restoration Plan*, Santa Monica Bay Restoration Project, Monterey Park, CA.

Tim, U.S., Mostaghimi, S., and Shanholtz, V.O. (1992). "Identification of Critical Nonpoint Pollution Source Areas Using Geographic Information Systems and Water Quality Modeling," *Water Resources Bulletin*. Vol. 28, No. 5, pp. 877-887.

US Environmental Protection Agency (1983). Final Report on the National Urban Runoff Program. Water Planning Division, US EPA, Prepared by Woodward-Clyde Consultants, Oakland, CA.

Ventura, S.J., and Kim, K. (1993). "Modeling Urban Nonpoint Source Pollution with a Geographic Information System," *Water Resources Bulletin*. Vol. 29, No. 2, pp. 189-198.

Viessman, Jr., Lewis, G.L., and Knapp, J.W. (1989). *Introduction to Hydrology*. Harper & Row Publishers, New York, NY.

Walker, J.F., Pickard, S.A., and Sonzogni, W.C. (1989). "Spreadsheet Watershed Modeling for Nonpoint-Source Pollution Management in a Wisconsin Basin," *Water Resources Bulletin*. Vol. 25, No. 1, pp. 139-147.

Wanielista, M.P., and Yousef, Y.A. (1993). *Stormwater Management*. John Wiley & Son, Inc., New Work, NY.

Woodward-Clyde Consults, Inc. (1989). "Analysis of Storm Event Characteristics for

Selected Rainfall Gauges throughout the United States," Report to the US EPA,

Office of Water, Nonpoint Source Program. Oakland, CA.

Xu, F., Prato, T., and Fulcher, C. (1993). "Broiler Litter Application to Land in an

Agricultural Watershed: A GIS Approach," *Wat. Sci. Tech.* Vol. 28, No. 3-5,

pp. 111-118.

3.8 Notation

The following symbols are used in this paper:

$AASV$ = Average Annual Storm Volume [m^3/yr]

APL = Annual Pollutant Loadings

$AREA_i$ = Area of Catchment i within sub-basin j [Hectare]

$ASRF$ = Average storm rainfall

ASV = Average storm runoff volumes

B_j = Estimated Annual Pollutant Loading of sub-basin j [kg/yr]

C_i = Estimated Annual Pollutant Loading of catchment i [kg/yr]

CF = Conversion Factor for runoff volume to liters

CV = Coefficient Variation

EMC = Event Mean Concentration

G = Conversion Factor (m^3 mg/L to kg) [10^{-3}]

IMP	=	impervious area (expressed as a percentage)
k	=	Land use type.
M	=	Total number of catchment polygons within sub-basin *j*.
ME	=	Event Mean Concentration[mg/L]
N	=	Total number of land use polygons with land use type *k* within catchment *i*.
n	=	Land use polygon *n* within the catchment *i*.
RV	=	runoff coefficient; and
SM	=	Site Median EMC[mg/L]

4. A DETERMINISTIC MODEL: MODEL DEVELOPMENT

4.1 Introduction

The watershed chosen for this research is Ballona Creek Watershed. The reasons for choosing this watershed are two fold: a) no attempt had been made by previous investigators to model such a large watershed because of the complexity of the data management required; b) The availability of hourly stream flow data which are necessary to calibrate the model's parameters.

A deterministic model based on a well-respected urban stormwater model is developed in this chapter, and the second half of this chapter discusses a portion of GIS work which is used as a preprocessor/postprocesser to the urban stormwater model.

4.2 Deterministic Urban Stormwater Model

In the previous chapter, an empirical steady state urban runoff model integrated with GIS was developed and applied on to estimate annual pollutant loadings. In this chapter, a deterministic model is developed which is used to simulate single stormwater events. While many researchers have developed urban runoff models to simulate single stormwater events in watersheds from a range of few acres to tens of

acres in total area. None of the previous studies, however, had developed a deterministic single event urban stormwater model to study a watershed with over 50,000 acres in total area. Furthermore, an optimization method is used in this study to find the best possible parameters instead of a more traditional way of trial-and-error "eyeballing" best fit procedures. The next section will focus on the formulation of a well-respected stormwater model. The optimization method will be discussed in the next chapter.

4.2.1 Modification of Storm Water Management Model Version 4.3

The Environmental Protection Agency (EPA) Storm Water Management Model (SWMM) has been used by numerous investigators and applied on numerous watersheds both in the U.S. and other parts of the world. It has been thoroughly investigated under the scrutiny by many users over the years. Therefore, it will be used as the basis to simulate the stormwater process in this research. The latest SWMM version 4.3 was modified for the urban stormwater process.

The SWMM was developed as single-event model specifically for the analysis of combined sewer overflows (Metcalf and Eddy Inc. 1971). Through continuous maintenance and support, the model has been applied to all types of storm water

management from urban drainage to flood routing and floodplain analysis. Figure 4.1 illustrates a general operational schematic of SWMM.

SWMM version 4.3 was originally designed for small watersheds and with limited capabilities. It has an upper limit of handling 500 subcatchments and channels/pipes. In order to adapt the model to this investigation, a number of modifications have been made and they are listed as follows: Seven processes (or blocks) were removed from the original SWMM version 4.3. They are process 2 – statistics, process 3 – graph, process 4 – combine, process 5 – rain, process 6 – temp, process 9 – extran, process 10 – storage/treatment. A new process was added which uses optimization technique to calibrate the SWMM. The executive block (process 1) is replaced by a new main block to accommodate the addition of calibration process. Process 7 – runoff and 8 – transport, were heavily modified to be able to handle larger watersheds, a greater number of subcatchments and channels/pipes.
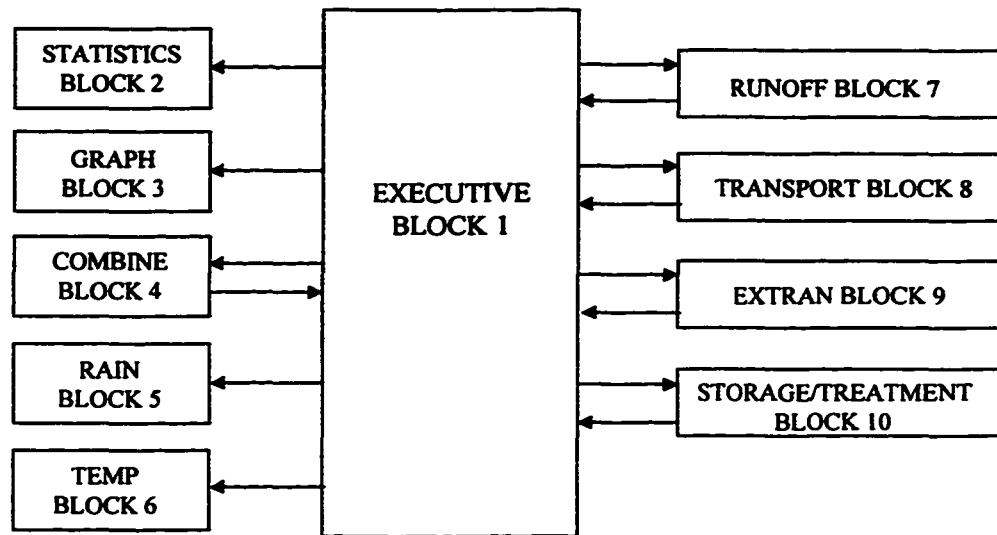
Figure 4.1 A General Operational Schematic of SWMM. (Adopted from Huber and Dickinson, 1988)

The original SWMM version 4.3 has 10 processes and is able to simulate 500

subcatchments and 500 channels/pipes. The modified SWMM has 3 processes and the

number of subcatchments and channels/pipes was increased to 1580 and 4300,

respectively. The removed processes from the original SWMM are replaced by the

GIS, which acts as a preprocessor/postprocessor for the modified SWMM. The

modified version GIS/SWMM is illustrated in Figure 4.2.
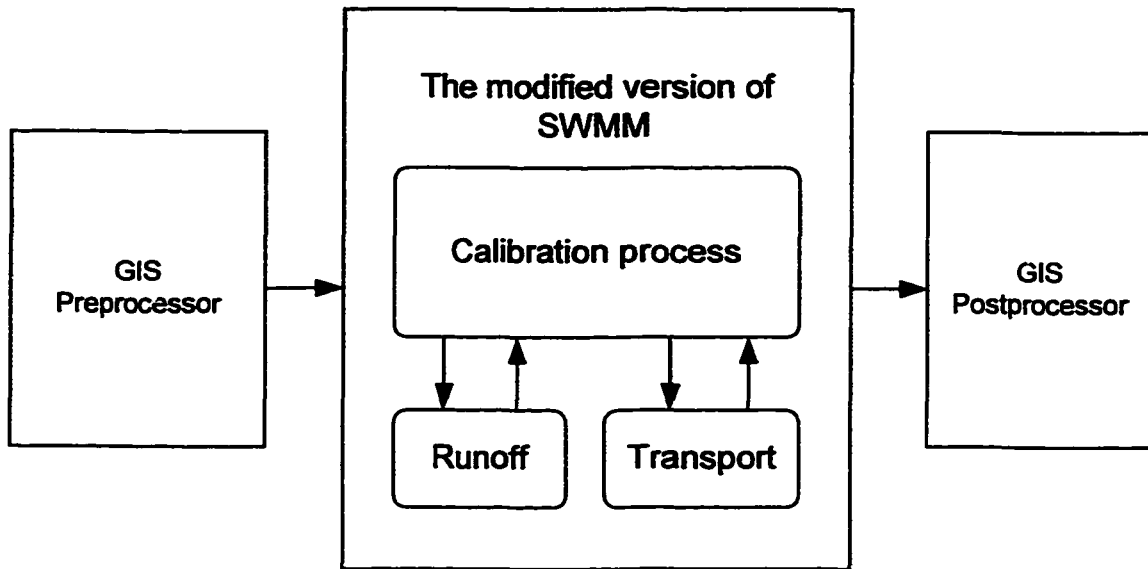
Figure 4.2 Modified GIS/SWMM for the Urban Stormwater Process

4.2.2 Formulation of SWMM

This section describes the development of the runoff and transport processes of

the modified version of SWMM depicted in Figure 4.2. The GIS

preprocessor/postprocessor modules and the calibration process will be discussed in

the following section and the next chapter, respectively.

4.2.2.1 Runoff Process

The RUNOFF process is the heart of SWMM. It simulates surface runoff and

pollutant loads in response to precipitation and surface pollutant accumulations

(Roesner and Aldrich, 1988). The runoff process is modeled by two governing equations, which are the continuity and Manning's equations. Eq. (4.1) is the continuity equation used to simulate the volume of water on the surface of the watershed. The term on the left hand side of Eq. (4.1) is the change of stored water volume of the watershed (or subcatchment). The first term on the right hand side of Eq. (4.1) is the rainfall excess or net inflow to the subcatchment and the second term is the runoff or outflow from the subcatchment

$$\frac{dV}{dt} = \frac{d(A.d)}{dt} = A.i_e - Q$$ (4.1)

Where V = $A.d$ =   volume of water on the subbasin. [ft^3]

A =   area of the subbasin. [ft^2]

d =   depth of water on the subbasin. [ft]

i_e =   rainfall excess (the rainfall intensity less the

evaporation per infiltration rate. [ft/sec]

Q =   runoff flow rate from the subbasin. [ft^3/sec]

To model the surface runoff on the subcatchment, Manning's equation is used and it can be expressed as follows,

$$Q = A_c \left(\frac{\beta}{n}\right) R^{2/3} S_o^{1/2}$$ (4.2)

Where A_c =   cross-sectional area of flow over the subwatershed. [ft^2]

    n =   Manning's roughness coefficient.

    R =   Hydraulic radius of flow over the subcatchment, [ft]

    S_O =   slope of the subwatershed. [feet per foot]

    β =   1.49

The cross sectional area of flow is defined as

$$A_c = W(d - d_p)$$ (4.21)

Where W =   width of flow over the subcatchment

    d_p =   depth of maximum depression storage, [ft]

By assuming the depth of flow is very small and knowing the hydraulic radius is the cross sectional area of flow divided by the wetted perimeter. Therefore, Eq. 4.21 can be rewritten as

$$R = \frac{W(d - d_p)}{W} = d - d_p$$ (4.22)

and Eq. 4.2 can be rewritten as

$$Q = \frac{W\beta}{n}(d - d_p)^{5/3} S_o^{1/2}$$ (4.23)

Plugging Eq. 4.21, 4.22, and 4.2 into Eq. 4.1 and then divided by A gives

$$\frac{dd}{dt} = i_e - \left[\frac{\beta . W}{A_c . n}\right](d - d_p)^{5/3} . S_o^{1/2}$$ (4.3)

Eq 4.3 and 4.23 are the two governing equations used in Runoff process. Eq. 4.1 can be approximated by a finite difference approximation of the derivative as follows,

$$\frac{d_{n+1} - d_n}{\Delta t} = \overline{i_e} - \frac{\overline{Q}}{A}$$ (4.4)

Where Δt = time step size. [seconds]

$n+1, n$ = subscripts indicating conditions at the end of time step $n+1$ and the end of time step n.

$\overline{i_e}$ = average precipitation intensity during time step $n+1$. [m/sec]

$\overline{Q}$ = average runoff flow rate during time step $n+1$. [m³/sec]

By calculating the average runoff flow rate as a function of the average depth of flow, Eq. 4.4 becomes:

72

$$\frac{d_{n+1} - d_n}{\Delta t} = \overline{i_e} - \left[\frac{\beta.W}{A.n}\right](\overline{d} - d_p)^{\frac{5}{3}}.S_o^{\frac{1}{2}} \qquad (4.5)$$

Where $\overline{d} = \dfrac{d_n + d_{n+1}}{2}$, average depth of flow during time step $n+1$.

Both Eq. 4.23 and 4.5 are used to solve for d_{n+1} and Q at each time step $n+1$ using the numerical technique of Newton-Raphson algorithm.

The pollutant process simulation is based on the relationship between the accumulation and washoff of pollutants on the subcatchment surface. Equation 4.5 is the governing equation used to model the pollutant washoff rate.

$$P_{off} = \frac{-dP_p}{dt} = R_c.r^n.P_p \qquad (4.5)$$

Where P_{off} = pollutant washoff rate at time t. [quantity/s]

P_p = amount of pollutant p on the subbasin surface at time t.

[quantity]

R_c = washoff coefficient. [mm^{-1}]

r = runoff rate over the subbasin at time t. [mm/s]

n = exponent for the runoff rate.

4.2.2.2 Transport Process

The TRANSPORT process is used to route both the surface flows and pollutant loads through a sewer system, where the sewer system refers to any form of pipe and/or channel system in a watershed. The flow routing can be represented by the following two partial differential equations, which are commonly called the Saint-Venant Equations: Eq. 4.6 and Eq. 4.7. Eq. 4.6 and Eq. 4.7 are the momentum and continuity equations. The three terms on the left hand side of Eq. 4.6 are pressure force, convective, and local acceleration. The other two terms on the right hand side are gravity force and friction. The first term in Eq. 4.7 represents the inflows and outflows to a control volume, and the second is the change in amount of water in control volume.

$$\frac{\partial h}{\partial x} + \frac{v}{g} \cdot \frac{\partial v}{\partial x} + \frac{1}{g} \cdot \frac{\partial v}{\partial t} = S_o - S_f \tag{4.6}$$

$$\frac{\partial Q}{\partial x} + \frac{\partial A}{\partial t} = 0 \tag{4.7}$$

Where h = water depth. [ft]

v = average flow velocity. [ft/sec]

x = distance along the conduit. [ft]

t = time. [sec]

g =   gravity acceleration. [32.2ft/sec]

S_O =   Invert slope of the conduit. [feet per foot]

S_f =   friction slope. [feet per foot]

Q =   flow rate. [ft^3/sec]

A =   cross-sectional area of flow. [ft^2]

Assuming the flow propagates in only the downstream direction and with negligible surcharge conditions, all three terms on the left hand side of Eq. 4.6 can be neglected. By using Manning's equation, the simplified version of Eq. 4.6 is obtained and shown in Eq. 4.8.

$$Q = \frac{k}{n} . A . R^{\frac{2}{3}} . S_o^{\frac{1}{2}} \qquad (4.8)$$

Where Q =   Manning's roughness coefficient.

R =   hydraulic radius. [m]

β =   1.49

The Continuity equation, Eq. 4.7, is approximated by a finite difference equation as follows,

$$\frac{(1-w_t)(A_{j,n+1} - A_{j,n}) + w_t(A_{j+1,n+1} - A_{j+1,n})}{\Delta t} +$$

$$\frac{(1-w_t)(Q_{j+1,n} - Q_{j,n}) + w_x(Q_{j+1,n+1} - Q_{j,n+1})}{\Delta x} = 0$$

(4.9)

Where Δt = $t_{n+1} - t_n$, time step size, seconds

Δx = $x_{j+1} - x_j$, distance interval length (the conduit length)

$j, j+1$ = subscripts indicating conditions at the upstream end and the

downstream end of conduit M, respectively

$n, n+1$ = subscripts indicating conditions at the end of time step n (which

is also the beginning of time step $n+1$) and the end of time step

$n+1$, respectively

w_t, w_x = weights

Eq. 4.8 and 4.9 are solved together to find the two unknowns $Q_{j+1,n+1}$ and $A_{j+1,n+1}$ at the downstream end of conduit M at time step $n+1$. Figure 4.3 contains two snap shots of conduit M at time step $n\Delta t$ and $(n + 1) \Delta t$, respectively.
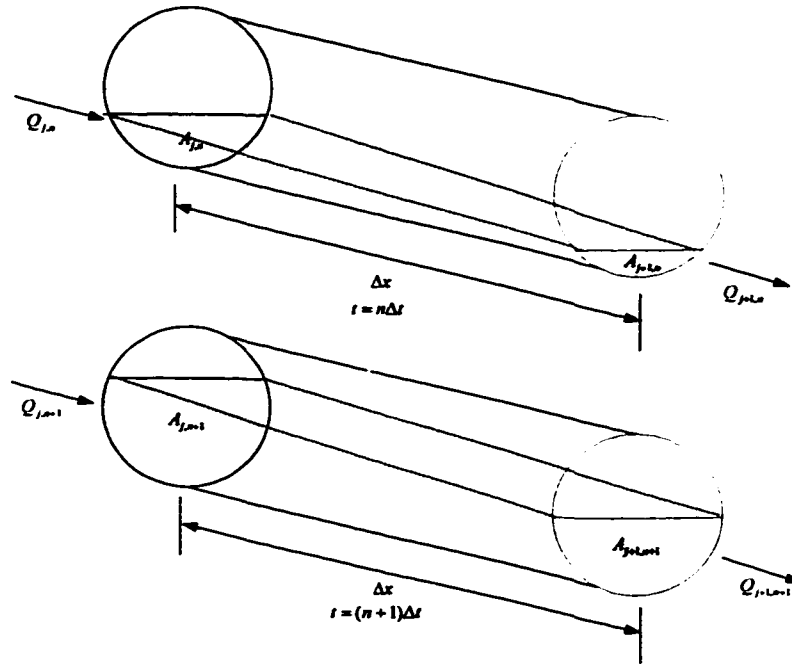
Figure 4.3 The Two Unknowns Q and A of Conduit M at time step $n\Delta t$ and $(n+1)$ Δt

The governing equation to route pollutants through the sewer system are:

$$\frac{dVC}{dt} = \frac{V.dC}{dt} + \frac{C.dV}{dt} = \left(Q_i.C_i\right) - \left(Q.C\right) - K.C.V \pm L \qquad (4.10)$$

Where C =   pollutant concentration in conduit. [quantity/unit volume]

   V =   volume of water in conduit. [m^3]

   Q_i =   inflow rate. [m^3/sec]

$$C_i \quad = \quad \text{inflow pollutant concentration. [quantity/unit volume]}$$

$$Q \quad = \quad \text{outflow rate. [m}^3\text{/sec]}$$

$$K \quad = \quad \text{first-order decay coefficient. [sec}^{-1}\text{]}$$

$$L \quad = \quad \text{source (or sink) term. [quantity/sec]}$$

By assuming the following parameters Q, Q_i, C_i, V, L, and $\dfrac{dV}{dt}$ to be constant over the

solution time interval, t to $t + \Delta t$. Eq. 4.10 is then readily integrated over the time

interval t to $t + \Delta t$ with

$$C(0) = C(t) \tag{4.11}$$

to yield

$$C(t + \Delta t) = \left(\frac{\dfrac{Q_i C_i + L}{V}}{\dfrac{Q}{V} + K + \dfrac{1}{V}\dfrac{dV}{dt}} \right)\left(1 - e^{-\left(\frac{Q}{V} + K + \frac{1}{V}\frac{dV}{dt}\right)\Delta t} \right) + C(t) e^{-\left(\frac{Q}{V} + K + \frac{1}{V}\frac{dV}{dt}\right)\Delta t}$$

Thus, the concentration at the end of the time step is predicted as the sum of a

weighted inflow concentration and a decaying concentration from the previous time

step.

4.3 GIS – Preprocessor

The GIS used in this study was Environmental System Research Institute

(ESRI) ARC/INFO version 7.0.3 running in AIX 3.2.5 on an IBM RISC/6000 Model

550E, ARC/INFO version 7.1.2 and ArcView version 3.1 running in Microsoft NT

version 4.0. The GIS work can be divided into four parts: rainfall data estimation,

drainage data generation, channels/pipes generation, and slope data estimation.

One of the complexities of urban stormwater modeling is data management. As

described in the Chapter One, urban stormwater modeling generally requires a

substantial amount of information or data, which are fed into the model. The output

data are equally large and as complicated and difficult to manage as the input data. In

addition, the ability of a model to simulate urban runoff process is highly dependent on

the accurate estimation of spatial parameters in the watershed. The ability of GIS to

store and link spatial and attribute data efficiently makes it an ideal platform for urban

stormwater modeling. This section describes the development of GIS as the

preprocessor for the GIS/SWMM process. The preprocessing part includes rainfall,

drainage, channels/pipes, and slope estimations.

4.3.1 Rainfall Estimation

Precipitation data are the most important component in urban stormwater modeling. Because rainfall data drive the model and produce runoff, an accurate estimation of rainfall data often determines the success of many modeling efforts. An ideal way of collecting rainfall data is to have sufficient number of rain gauges placed at every possible location. In this way, the spatial distribution of rainfall falling on a watershed can be fully represented. However, it is often necessary to compute estimates of mean areal precipitation for a catchment from limited number of rain gauges.

Singh and Chowdhury (1986) reviewed thirteen different methods for computing mean areal rainfall in three different hydrologic environments. The result of their investigation showed all thirteen methods yielded comparable estimates, and there was no particular basis to claim that one method is significantly better than the other. Therefore, of the thirteen methods investigated, the inverse distance-squared method (IDSM) was chosen for rainfall estimation. IDSM is convenient to implement using a raster GIS, but the accuracy is highly dependent on the size of raster cell. Raster cells can easily be adjusted to obtain the desired accuracy. However, one of the drawbacks for this method is the requirement of computing resources and time.

4.3.1.1 Inverse Distance-Squared Method

Most of the methods that are used for estimating mean areal precipitation can be expressed as linear combinations of the observations. If n gauges, with values P_1, P_2, ..., P_n, are available for estimating precipitation in a catchment, then the estimate of mean areal precipitation can be represented by Eq. 4.10,

$$\overline{P} = \sum_{i=1}^{n} a_i P_i \tag{4.10}$$

Where the station weights a_1, a_2, a_3, ..., a_n are nonnegative constants that sum to 1.

For the inverse distance-squared method, the mean areal precipitation is estimated by first interpolating rainfall at gauge sites onto a rectangular grid and then estimating areal precipitation by summing estimates from grid boxes within the catchment. The estimate for the jth grid box is

$$\overline{P}_j = a \sum_{j=1}^{n} d_{ij}^{-2} P_i \tag{4.11}$$

Where d_{ij} =   Distance from gauge i to the center of grid box j

n =   Total number of rain gauge

P_i =   Precipitation at gauge i

In Eq. 4.11, a is the inverse of the sum of the inverse distance-squared method values for all gauges and it can be represent as follows,

$$a = \left(\sum_{i=1}^{n} d_{ij}^{-1} \right)^{-1}$$

(4.12)

If m grid boxes are used to estimate the total area of catchment, then the mean areal precipitation is the arithmetic mean of the m estimates obtained from Eq. 4.11. The station weights in Eq. 4.10 for the IDSM can be expressed as follows,

$$a_i = \frac{1}{m} \sum_{j=1}^{m} \frac{a}{d_{ij}^2}$$

(4.13)

Eq. 4.11 to 4.13 can be written in an equivalent form in cell-based GIS and their GIS representation can be found in Appendix A.

4.3.2   GIS - Drainage Characteristics

The total area of the Ballona Watershed is 53,694 acres and there are 1579 subcatchments within the watershed. Each subcatchment was manually digitized and converted into GIS databases (coverages) based on the information provided by the drainage maps from the Los Angeles County of Public Works and the Bureau of Engineering, City of Los Angeles. Each subcatchment is delineated based on the location of inlets (catch basins) and the flow direction of each street provided by the drainage maps. A 1993 land use database from Southern California of Association

Government (SCAG) was used to determine the imperviousness of the watershed. A detail description of drainage GIS databases and their development work are included in Appendix B.

4.3.3 GIS - Channels/Pipes Characteristics

The total length of channels/pipes in the Ballona Creek Watershed is over 176 miles long, and there are 2648 channels/pipes. There are 1579 catchbasins (inlets) (same as the number of subcatchments). All channels/pipes are also manually digitized and converted to GIS database based on the information from the drainage maps. The attribute information of channels/pipes, catchbasins, and the spatial information (locations) of catchbasins are related back to the spatial GIS database using the dynamic segmentation procedure. The development work and procedures are included in Appendix C.

4.3.4 GIS - Slope Estimation

USGS 7.5 Minute Digital Elevation Model (DEM) Spatial Data Transfer System (SDTS) data combing with GRID module of ARCINFO GIS were used to compute the subcatchment and channels/pipes slope values. The slope values were then used to compute the depression storage and other parameters of each subcatchment. The developmental portion of this work are included in Appendix B.

5. MODEL IMPLEMENTATION AND CALIBRATION

The implementation and calibration of the modified GIS/SWMM are presented in this chapter. The physical model developed in Chapter 4 consists of partial differential equations (PDEs) as well as algebraic equations and they are solved numerically using finite difference and other numerical methods. The GIS acts as a preprocessor for the model inputs. It is mainly responsible for the management of the following databases: drainage, land use, channels/pipes and other attribute related databases. The total size of the databases managed by the GIS is approximately one-half GigaByte. After the databases are processed by GIS, the data are then written to a text file according to the format and structure required by the model. An optimization procedure using the Complex Method of Box (Box, 1965) was incorporated into the modified GIS/SWMM model to calibrate the model's four parameters based on the model predictions and data collected from the watershed outlet.

5.1 Model Implementation

The governing equations developed in Chapter 4 were implemented into FORTRAN 77 codes. A Microsoft FORTRAN PowerStation Version 4.0 running on Microsoft NT Version 4.0 was used as the main compiler to implement the model. The following machines have been used successfully to run the model: 1) Compaq

Professional Workstation AP200 Dual Pentium II 400 MHz with 512 MB RAM and

54 GB storage; 2) Dell Dimension XPS Pentium II 233 MHz with 384 MB RAM and

4.5 GB storage; 3) IBM PC compatible AMD K6 233 MHz with 192 MB RAM and 11

GB storage. The codes have also successfully compiled by IBM AIX XL FORTRAN

Version 2.3 running on an IBM RISC 6000 POWERstation machine (Model 550)

using IBM AIX operating system.

The are one finite and one algebraic equations per subcatchment for the surface

runoff process. As for the flow routing process, there are also one finite and one

algebraic equations per channel/pipe. The total number of equations for the model is

listed in Table 5.1.

Table 5.1 Number of Equations in Each Process

Equation Type	Runoff Process	Transport Process
PDE	1579	2648
AE	1579	2648
PDE – Partial Differential Equation AE – Algebraic Equation		

The modified SWMM is written in a modular form and the code uses 102

subprograms and a total of 37250 lines of source code and comments. The original

limitation of the SWMM have been removed and the number of subcatchments or

channels/pipes it models can be adjusted in the dimension declaration section. Only the

capacity and speed of the computer limit the number of subcatchment and

channels/pipes that can be included in the model.

5.1.1   Watershed Description

The Ballona Creek Watershed is a highly urbanized area where it has over 65

percent of the area is residential land use and over 19 percent are either commercial or

public/industrial land uses. Because of its high urbanization, the effect of urban runoff

to the receiving water – Santa Monica Bay during storm events is significant. The land

use distribution of Ballona Creek Watershed is tabulated in Table 5.2.

Table 5.2 Land Use Distribution of Ballona Creek Watershed

Land Use	Area (Acres)	Area in Percent
Single Family	23839	44.68
Multiple Family	10749	20.15
Commercial	6813	12.77
Public	2252	4.22
Light Industrial	2208	4.14
Other	1150	2.16
Open	6339	11.88

Information based on 1993 SCAG Land Use Data

The total area of Ballona Creek Watershed is 53,694 acres and 1579 subcatchments are delineated within the watershed. Rainfall falling on each subcatchment turns into overland surface runoff and flows are collected into a single inlet (catchbasin). Surface runoff flow entering into the inlet is then routed through the connected channel or pipe (open and closed). Finally, all surface flow is summed up at the watershed outlet after routing through 2648 channels/pipes. Figure 5.1 shows the scale down version of the watershed with overland surface runoff flowing into the catchbasins and Figure 5.2 illustrates the Ballona Creek Watershed with subcatchments, channels/pipes, and the flow gauge at the watershed outlet.
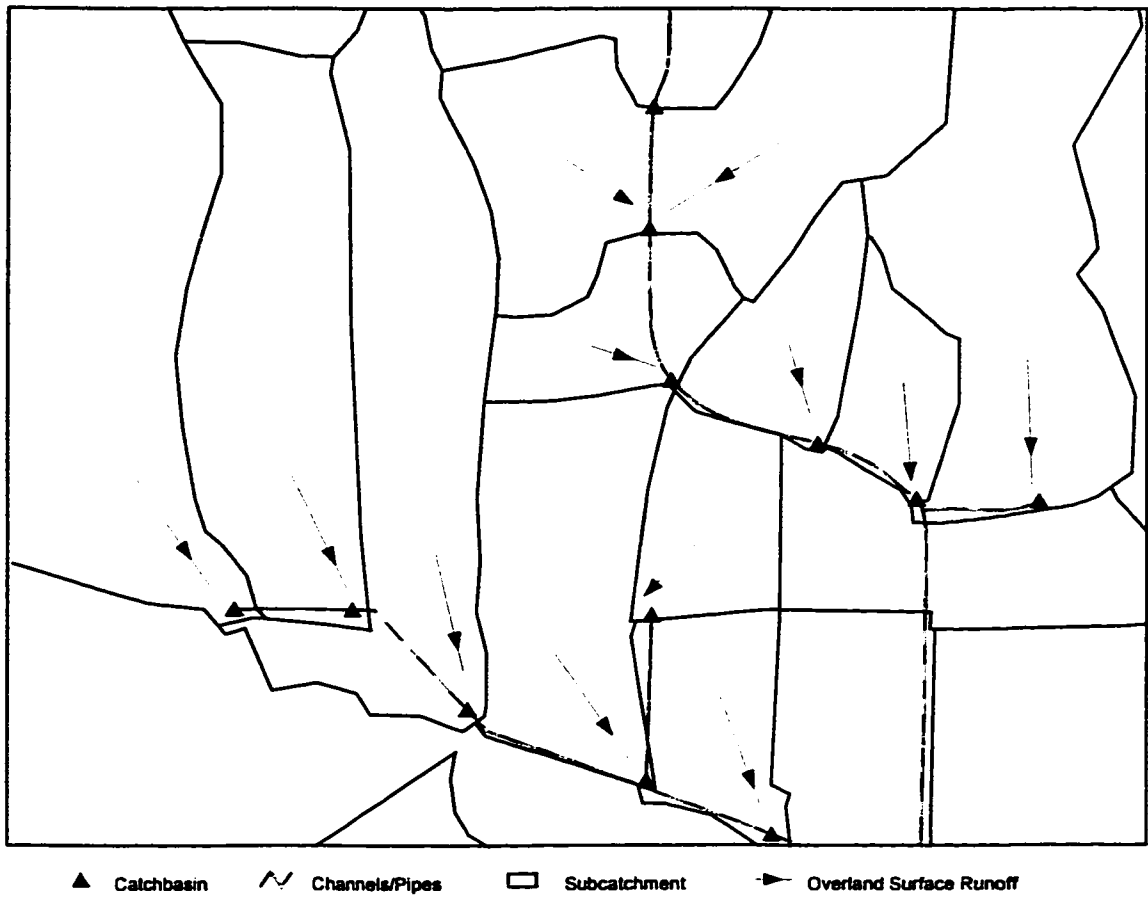
Figure 5.1 Overland Surface Runoff flowing within subcatchments and Channels/Pipes
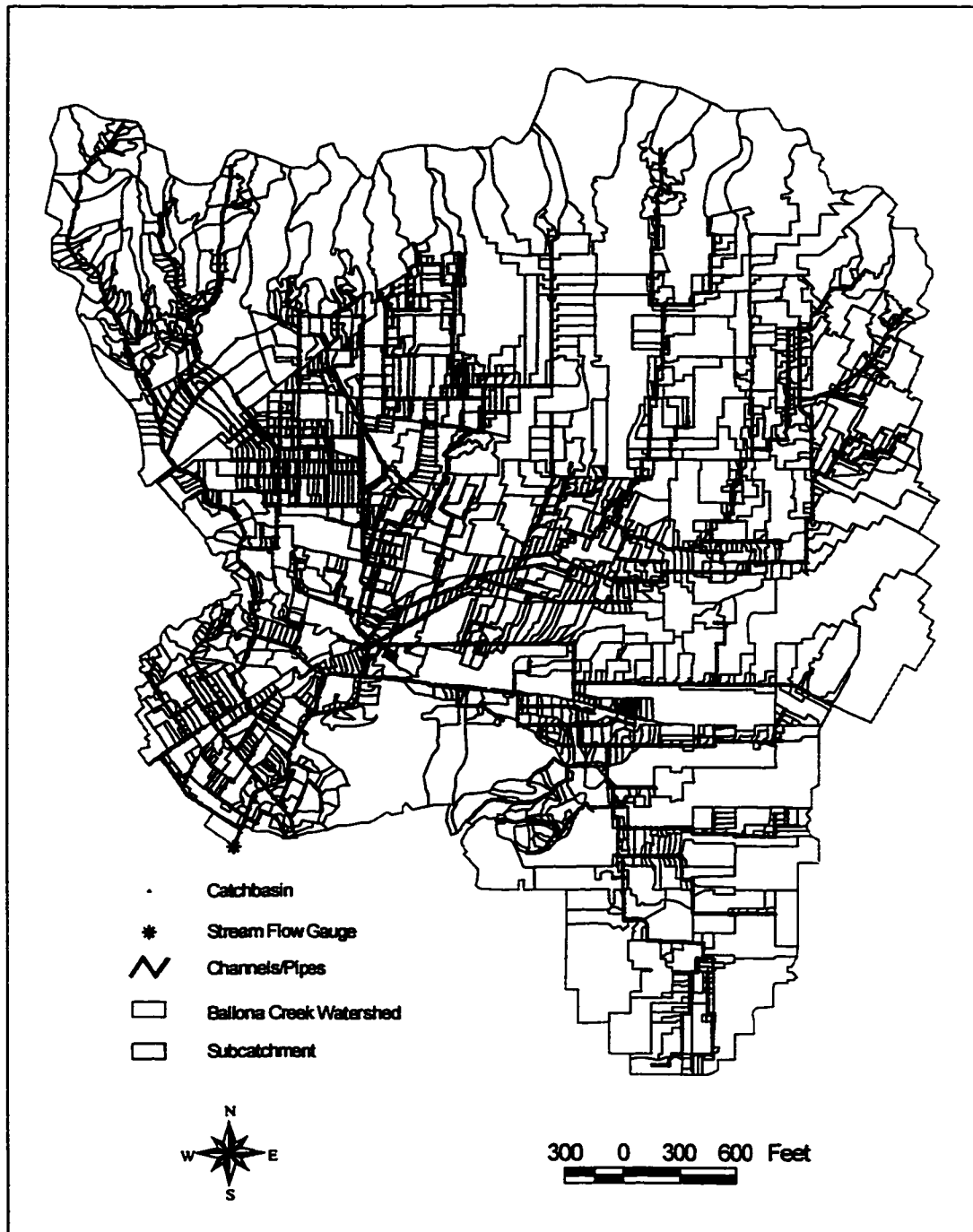
Figure 5.2 The Study Area: The Ballona Creek Watershed

5.1.2 Model Inputs

There are three input files for the modified GIS/SWMM model. The first and second input files: INPUTA.DAT and OHYDRO.DAT are for the calibration process and they will be discussed in the later section. The third input file (INPUT.DAT) input file is for the runoff and transport processes. Table 5.3 summarizes the input data description of INPUT.DAT and the parameter values either computed from the GIS processes (see Appendixes) or cited from the literatures. Table 5.4 shows a portion of INPUT.DAT file.

Table 5.3 Summary of Data Structure in INPUT.DAT

Data Type	Description	Values
Rainfall	Rainfall Intensity	From NOAA 1996
	Time of Storm Event	Hourly Rainfall Data
Subcatchment	Catchment Number	From GIS Processes
	Inlet(or Catchbasin) Number	From GIS Processes
	Catchment Width	From GIS Processes
	Area	From GIS Processes
	Average Imperviousness	From GIS Processes
	Slope	From GIS Processes
	Impervious Manning's Coefficient	0.012 - 0.013
	Pervious Manning's Coefficient	0.035
	Impervious Depression Storage Coefficient	0 - 4.985
	Pervious Depression Storage Coefficient	0.15
Infiltration	Average Capillary Suction	9 [in]
	Saturated Hydraulic Conductivity	0.118 [in/hr]
	Initial Moisture Deficit	0.26 [ft/ft]
Channels/Pipes	Channel/Pipe Number	From GIS Processes
	Upstream Connection Channels/Pipes (up to 3)	From GIS Processes
	Channel/Pipe Type (e.g. Trapezoidal, box,...)	From GIS Processes
	Geometry (e.g. length, width, ...)	From GIS Processes
	Slope	From GIS Processes
	Manning's Roughness Coefficient	0.013 - 0.027
Output Options		

Table 5.4 INPUT.DAT

```
*
*    Ballona Watershed Rainfall-Runoff Simulation
*
* rainfall data occurred on 11/26/1994 starting at 04:00 with 46 time steps
*  metric isnow nrgag infilm kwalty ivap nhr nmn nday month iyrstr
b1 0     0    1     1      0      0    4   0   26   11    94
*
* rainfall on 11/26/1994
*  ktype kinc kprint kthis ktime kprep nhisto thisto tzrain
e1 0 4 0 0 1 1 4 1.0 5
e3 0.016 0.044 0.042 0.01
*
* subcatchment parameters
* jk namew ngto   width   area    imp  wslope  i_n   p_n  wstore1 wstore2 suct hydcon
smdmax
h1 1    2 5789   1355.1  998.947 27.18 0.11339 0.013 0.350 0.08804 0.15000 9.00 0.12
0.26
h1 1    3 6154    773.4  746.304 52.08 0.10274 0.012 0.350 0.09240 0.15000 9.00 0.12
0.26
h1 1    4 6258   1086.1  195.450  4.17 0.17672 0.013 0.350 0.07084 0.15000 9.00 0.12
0.26

   .    .   .      .       .      .     .       .     .     .       .      .    .
   .    .   .      .       .      .     .       .     .     .       .      .    .
   .    .   .      .       .      .     .       .     .     .       .      .    .
   .    .   .      .       .      .     .       .     .     .       .      .    .

h1 1 1578 6496   1303.9    2.563 85.37 0.05644 0.012 0.350 0.12392 0.15000 9.00 0.12
0.26
h1 1 1579 6499   1995.4    4.259 76.78 0.05644 0.012 0.350 0.12392 0.15000 9.00 0.12
0.26
h1 1 1580 5635   1930.8    5.080 47.19 0.01152 0.013 0.350 0.27000 0.15000 9.00 0.12
0.26
*
* Channels/Pipes parameters
*
*  noe nue(1) nue(2) nue(3)  ntype   dist  geoml pslope  rough geom2 barrel geom3
e1 5001    1     0     0     19      0      0     0       0     0     0      0
e1 5002    8     0     0     19      0      0     0       0     0     0      0
e1 5003    5     0     0     19      0      0     0       0     0     0      0
e1 5004    4     0     0     19      0      0     0       0     0     0      0
e1 5005    9     0     0     19      0      0     0       0     0     0      0

   .    .   .     .     .     .      .      .     .       .     .     .      .
   .    .   .     .     .     .      .      .     .       .     .     .      .
   .    .   .     .     .     .      .      .     .       .     .     .      .
   .    .   .     .     .     .      .      .     .       .     .     .      .

e1 2641 6373    0     0      2    617.007 11.00  1.431  0.013  9.00  0     0.00
e1 2642 2641  1877    0      2     88.000 11.00  1.431  0.013  9.00  0     0.00
e1 2643 6578    0     0      2     70.625 12.00  1.408  0.013 10.00  0     0.00
e1 2644 2643  2036    0      2    673.376 12.00  1.408  0.013 10.00  0     0.00
e1 2645 5899    0     0      1    758.964  8.50  1.039  0.013  0.00  0     0.00
e1 2646 6561    0     0      1    380.566  3.75  0.063  0.013  0.00  0     0.00
e1 2647    0    0     0      1    316.021  2.00  1.116  0.013  0.00  0     0.00
e1 2648 5348    0     0      1     79.506  2.00  1.116  0.013  0.00  0     0.00
*
* print nnpe output hydrographs at the watershed outlet
j2 6580
$endprogram
```

Prior to the simulation of the urban stormwater process in Ballona Creek

Watershed, there are 18 site-specific unknowns per subcatchment/or channels to be

determined. These include unknowns from the subcatchment portion of INPUT.DAT: area, width, imperviousness (imp), slope (wslope), impervious Manning's Coefficient (I_n), pervious Manning's Coefficient (p_n), impervious depression storage coefficient (wstore1), pervious depression storage coefficient (wstore2), average capillary suction (suct), saturated hydraulic conductivity of soil (hydcon) and initial moisture deficit for soil (smdmax). And unknowns from the channels/pipes section: channel dimensions (4 unknowns depending on the type of conduit, dist, geom1, geom2, geom3), slope (pslope) and Manning's roughness coefficient (rough). Parameters that are more directly tied to the measurable quantities (wslope, imp, etc.) can be estimated from the SCAG land use and USGS DEM using the GIS process (see Appendixes). As for parameters that are not readily available in the Ballona Creek Watershed, their values are estimated based on the values cited from the literatures and hydrology handbooks under similar conditions.

5.1.2.1 Subcatchment Width

Among all the parameters, subcatchment width (width) is the most conceptual and tends to be difficult to measure, because it does not have a clear physical meaning in contrast to other parameters (subcatchment area, imperviousness, etc.). There are three possible methods to estimate the width depending on the location of

channels/pipes and the shape of subcatchment. These three estimations are listed as follows,

- The drainage channel/pipe locates in the middle of a rectangular shape subcatchment as shown in Figure 5.3, then the width is approximately twice the length of the main channel through the subcatchment.

$$W = 2l \qquad\qquad (5.1)$$
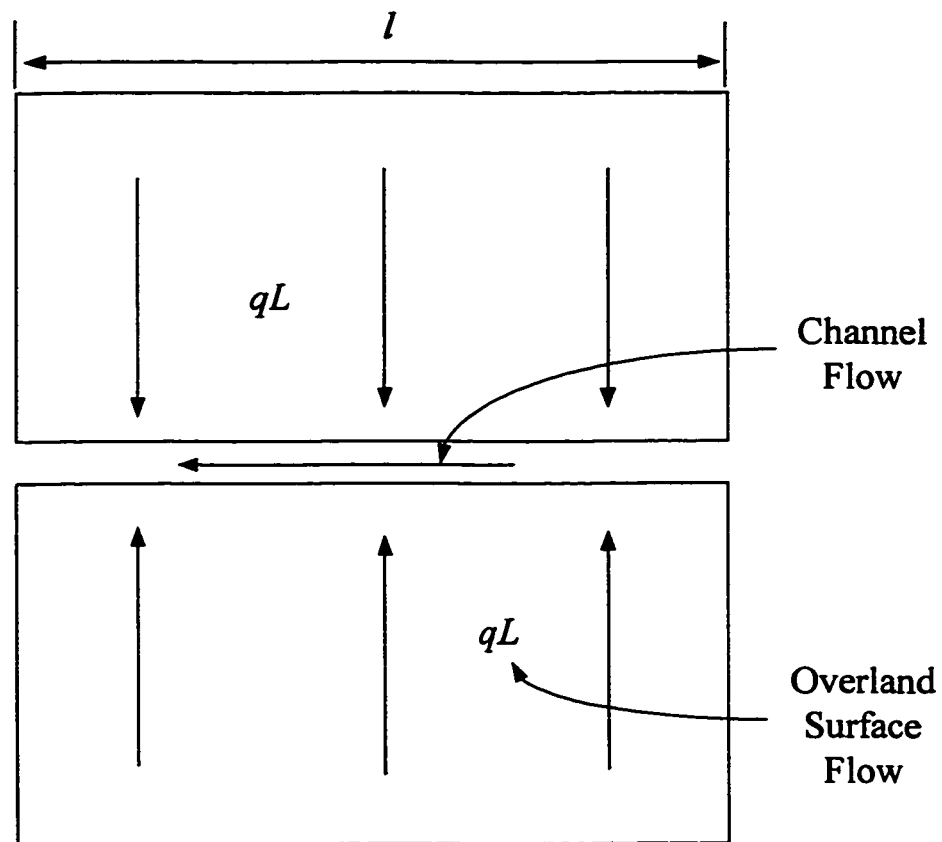
Figure 5.3 The First Method: Estimate the Subcatchment Width

- The drainage channel/pipe locates on the side of a rectangular shape subcatchment as shown in Figure 5.4, the width is equal to the length of the channel.

$$W = l \qquad (5.2)$$
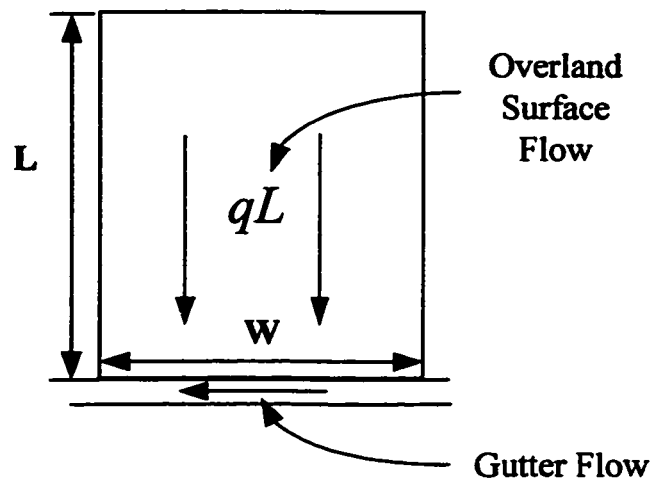
Figure 5.4 The Second Method: Estimate the Subcatchment Width

- The subcatchment has an irregular shape and its channel/pipe is off center as shown in Figure 5.5. A simple equation developed by DiGiano et al. (1977) can be used to estimate the width. A skew factor is first computed,

$$S_k = \frac{A_2 - A_1}{A} \qquad (5.3)$$

Where S_k = skew factor, $0 \leq S_k \leq 1$,

A_1 = area to one side of channel,

A_2 = area to other side of channel,

A = total area

The width is simply weighted between the two limits of l and $2l$ as

$$W = (2 - S_k)l \tag{5.4}$$

Where W   = subcatchment width,

l = length of main drainage channel

Figure 5.5 The Third Method: Estimate the Irregular Subcatchment Width

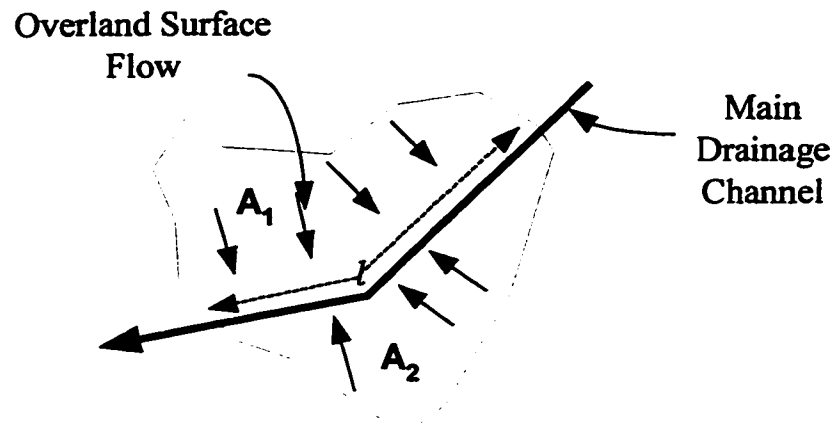In most cases, the third method is used to first estimate the width of subcatchment in Ballona Creek Watershed. It is important to start with reasonable initial guesses for the width because it may affect the final estimation during the calibration process.

5.1.2.2 Depression Storage Coefficient

The method to estimate the imprevious depression storage coefficient (WSTORE1) is based on works by Kidd (1978a) and Viessman et al. (1989). Their work show the WSTORE is related to the subcatchment slope (WSLOPE) and it can expressed as follows,

$$d_p = 0.0303 * WSLOPE^{-0.49} \tag{5.5}$$

The methods to estimate the subcatchment width, depression storage coefficient (Eq. 5.1 – 5.5), and other parameters are all implemented using the GIS process which are discussed in Appendixes.

5.2 Model Calibration

As with any modeling endeavors, the modified GIS/SWMM must go through a series of calibrations before it applies to the watershed. The calibration data should cover as wide a range of conditions as possible within the bounds of the study. In this manner, the model prediction might not perfectly matches the observation. But it will

respond to different conditions in a consistent manner. In this study, a selection of ten storm events with precipitation data and corresponding stream flow data are used to calibrate the GIS/SWMM. The data selected represent a wide range of conditions in the Los Angeles area in order to capture the watershed critical conditions.

5.2.1 Model Calibration Method

A calibration procedure is essentially an optimization problem. The goal of an optimization is to determine the values of the weights which minimize the cost function. The Complex Method developed in 1965 by Box (Box, 1965) was used in this research as the calibration algorithm. One powerful advantage of the Complex Method is that any cost function can be used in the optimization (Ramden, 1998). The Complex Method of Box was used by many researchers and was found to produce stable calibration results. Yuan (1994) applied this method on High-purity Oxygen Activated Sludge Process and found the algorithm to be very robust. He concluded that if the model has no random errors (no systematic errors), the algorithm is capable of estimating the parameter to an acceptable accuracy.

A subjective calibration process by using the trial and error "eyeballing" best-of-fit procedure has been done by many investigators in the past and probably is still widely used. This process is heavily dependent on the judgement and knowledge of the

modeler of the watershed. If this process is well performed, it could produce the same results as calibration based on the mathematical optimization technique. But the drawback of this approach is the ineffectiveness to handle a large number of data quickly and reliably. For the Ballona Creek Watershed, it is simply impossible using the manual calibration approach with the amount of data required. A mathematical calibration process has to be used for this study.
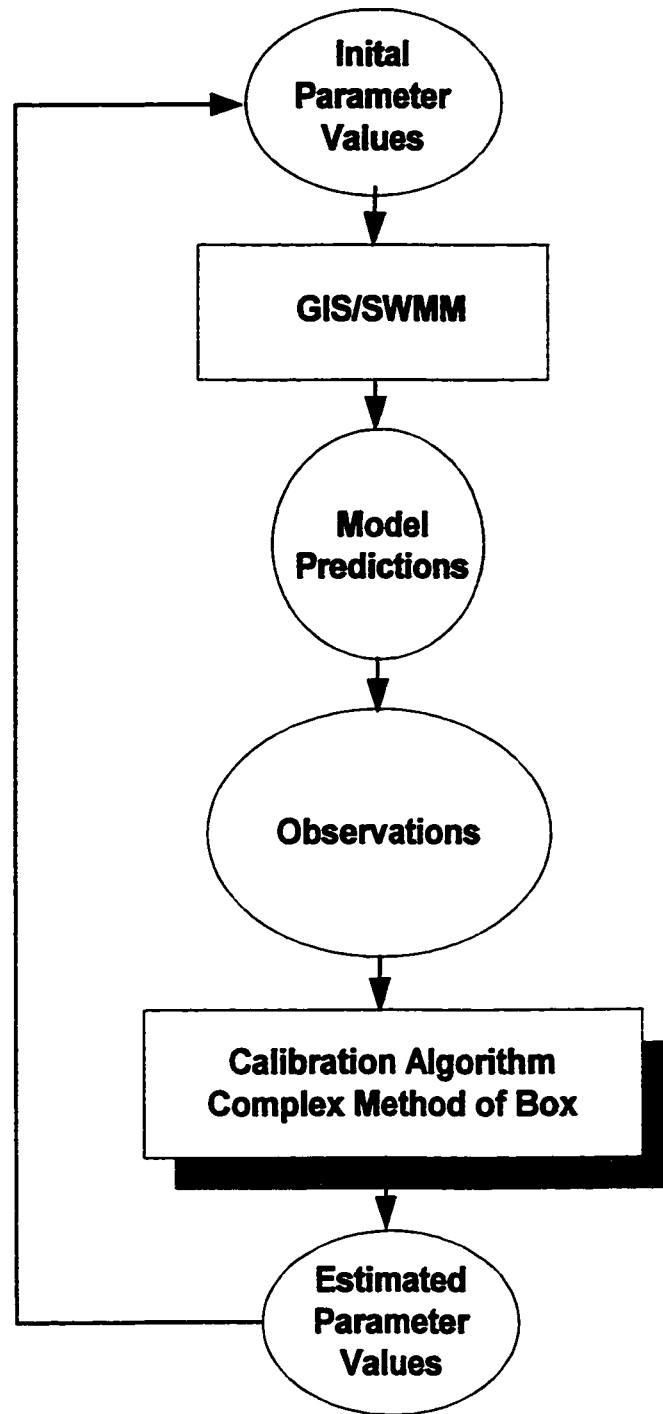
Figure 5.6 Procedure for Calibration Algorithm Evaluation

In this investigation, a calibration algorithm is incorporated into the modified GIS/SWMM as illustrated in Figure 4.2. and the procedure of calibration is depicted in Figure 5.6. A calibration algorithm generally begins by setting up an objective function. For the Complex Method, an objective function is designed to measures the agreement between the model predictions (outputs) and observations (stream flow gauge) with a set of parameter values. The objection function (cost function) is set up with a small values to represent close agreement between the prediction and the observation. The calibration algorithm is an iterative process. In each iteration, the parameters of the model are adjusted until a minimum in the objective function is achieved. This adjustment process is essentially a problem of minimizing a cost function (F).

5.2.1.1 Objective Function

One of the commonly used relative least-squares form is used as the objective function for the calibration algorithm. Eq. 5.6 represents the objective function used for this study.

$$\text{Minimize } F \quad = \left(\frac{Q^{*}-Q}{Q^{*}}\right)^{2} + \left(\frac{P^{*}-P}{P^{*}}\right)^{2} + \sum_{i=1}^{n}\left(\frac{f^{*}-f}{f^{*}}\right)^{2}_{i} \qquad (5.6)$$

Where Q = Total Flow Volume [cu ft]

P = Peak Flow Rate [cfs]

f = flow rate at the outlet hydrograph [cfs]

*   = as superscript, denotes predicted value

i = as subscript, denotes the ith observation of the outlet hydrograph

n = total number of observed variables of the outlet hydrograph

The relative least-squares objection function of Eq. 5.6 uses observations of total flow volume at the watershed outlet (Q), the peak flow rate (P) at the outlet hydrograph, and finally the flow rates (f) at the outlet hydrograph. Saez and Rittmann (1992) indicated in their study that the relative least-squares objective function is superior to other type of least-square criterion where observations (state variables) differ significantly in magnitude, such as in the urban stormwater process. In later sections, the total flow volume (Q) is shown to be at least tens to hundreds of magnitude larger then the peak flow rate (P).

5.2.1.2 Complex Method

Though the derivation of Complex Method is not rigorously based on mathematical theory, it has been proved to be a very robust optimization algorithm from many engineering problems with discontinuities and difficult-to-find or

nonexistent derivatives (Yuan, 1994). A figure adopted from Yuan is used to illustrate

the basic idea of Complex Method. For a 3 parameter system shown in Figure 5.7, at

least four sets of parameter are selected and distributed in a random fashion. The

randomly selected points are denoted as 1, 2, 3, and 4. This can also be expressed in

mathematical form in Eq. 5.7,

$$W_{i,j} = L_i + r_{i,j}(U_i - L_i) \tag{5.7}$$

Where $W_{i,j}$ = value of the ith parameter in the jth set of parameters

U_i = Upper bound of the ith parameter

L_i = Lower bound of the ith parameter

$r_{i,j}$ = a random real number ranging between 0 and 1

i = ith parameter

j = jth set of parameter
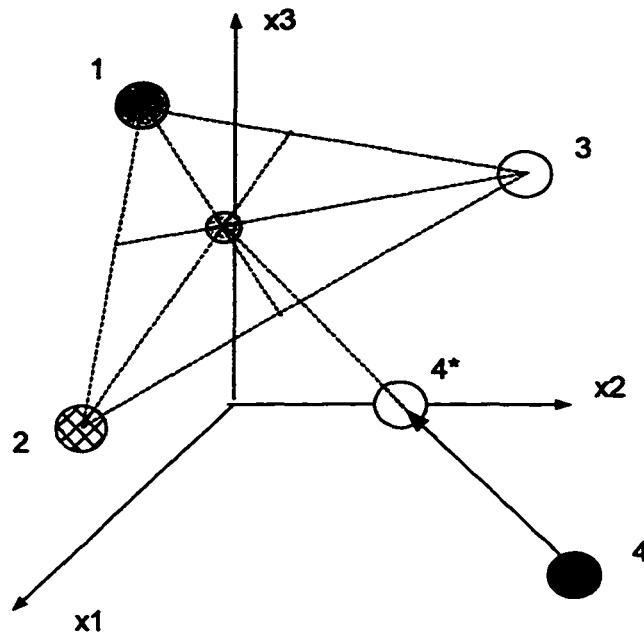
Figure 5.7 Illustration of the Complex Method (Adopted from Yuan, 1994)

Each point is used to make predictions and the objective function is evaluated from model predictions and observations. The point (set of parameters) that causes the largest error (or cost function) is identified. As illustrated in Figure 5.7, point 4 is identified as having the largest error then point 4 is moved half way to point 4* between the centroid of point 1, 2, 3, and point 4. Then the new set of parameters at point 4* are used to make predictions. A new cost function is evaluated and a comparison is made to other points (1, 2, and 3). Then the same procedure will repeat again until all set of parameters give the same function value (Yuan, 1994).

5.2.1.3 Parameter Constraints

By performing the sensitivity analysis (will be discussed in the later section), only four parameters are chosen for calibration process. The four parameters are subcatchment imperviousness (IMP), width (WIDTH), impervious depression storage coefficient (WSTORE1), and channel Manning's roughness coefficient (ROUGH). Since the flow data were collected only at the outlet of the watershed. All changes in model parameters are made uniformly throughout the watershed. For example, if imperviousness was increased to 110% of its original value it was changed by this percentage in all 1579 subcatchments. Four different calibration ratio factors are used to uniformly change the four parameters throughout the watershed. The four calibration ratio factors are listed in Table 5.5.

Table 5.5 Calibration Ratio Factors

Calibration Ratio Factor	Parameter	Description
CIMP	IMP	Catchment Imperviousness
CWIDTH	WIDTH	Catchment Width
CWSTORE1	WSTORE1	Catchment Imperviousness Depression Storage Coefficient
CROUGH	ROUGH	Channel/Pipe Manning's Roughness Coefficient

All four parameters are given a constraint in the upper and lower bounds to assure minimum number of iterations for the objective function to converge to a minimum value. The constraints of the four parameters are determined based on the following processes: 1) Physical meaning of the parameters; 2) Trial runs of the calibration algorithm. The constraints of the four parameter are listed as upper and lower bounds in Table 5.2. By performing the trial runs of the calibration process, a maximum number of iteration is increased from 2000 to 2500. Previous works by Yuan and others on the Activated Sludge Process, the maximum iteration number was 2000. This is reasonable since this study is more complex in turns of the number of calculation required in the urban stormwater model.

Table 5.6 Parameter Constraints

Parameter	Lower Constraint	Upper Constraint
CIMP	0.5	1.8
CWIDTH	0.8	1.8
CWSTORE1	0.5	1.88
CROUGH	0.5	2.28

5.3 Model Results and Discussion

Data (precipitation and the corresponding stream flow gauge data) from a selection of ten different storm events are used to calibrate the modified GIS/SWMM

model. For single-event simulation, data from ten events should be adequate to uncover the "derivative", i.e. the trend of the trend (Nix, 1994). The date of the selected storm events range from November, 1994 to December, 1996 and all were during the wet season part of the year in Los Angeles Basin (Stenstrom, 1993). Table 5.7 lists a break down of storm events selected in this study.

5.3.1 The Calibration Data

The precipitation data from the 1997 Edition of EarthInfo, Inc. NCDC Hourly Precipitation CDROM and the stream flow gauge hourly flow data at the Ballona Creek Watershed outlet (at the corner of Ballona Creek and Sawtelle Blvd.) is from the Los Angeles County of Public Works 1998 Edition.

Table 5.7 Description of 10 Storm Events Selected for the Calibration Process

Date of the Storm Event	Duration of the Precipitation (hours)
11/26/94	4
12/12/94	4
12/24/94	8
1/11/95	14
1/20/95	9
3/20/95	10
3/23/95	11
1/19/96	6
2/3/96	5
12/22/96	8

5.3.2 Calibration Results

The calibration results with a storm specific and overall calibrated parameters are shown in Table 5.8, 5.9, and 5.10. The overall calibrated parameters are computed from an average value of calibrated parameters from ten storm events. The model outputs (Total Flow Volume – Q and Peak Flow Rate – P) using the storm specific parameters and average parameters are shown from Figure 5.8 to 5.17. In Figure 5.8 to 5.17, the lines denoted with "Predicted" are outputs using the storm specific parameters, the lines denoted with "Predicted_All" are outputs using the average parameter values, and the lines denoted with "Observed" are observed outputs at the Ballona Creek Watershed outlet (Flow data from LADPW, 1998).

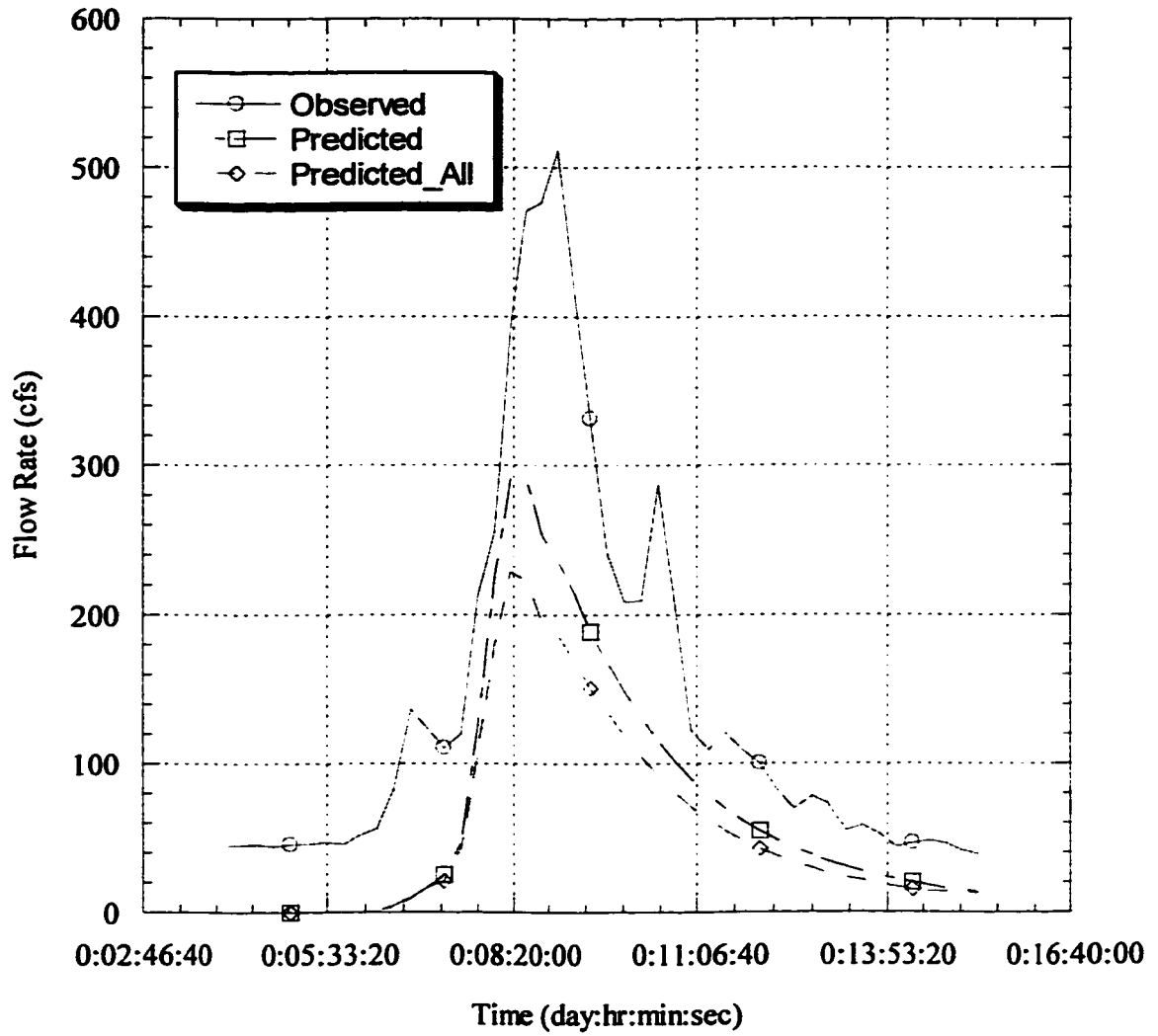## Storm Event on 11/26/1994

Figure 5.8 Outlet Hydrograph of the Storm Event occurred on 11/26/1994

Storm Event on 12/12/1994

Figure 5.9 Outlet Hydrograph of the Storm Event occurred on 12/12/1994

Figure 5.10 Outlet Hydrograph of the Storm Event occurred on 12/24/1994

Storm Event on 1/11/1995

Flow Rate (cfs)

2000

1500

1000

500

0

— Observed
— Predicted
— Predicted_All

0:22:13:20   1:01:00:00   1:03:46:40   1:06:33:20   1:09:20:00   1:12:06:40   1:14:53:20   1:17:40:00   1:20:26:40

Time (day:hr:min:sec)

Figure 5.11 Outlet Hydrograph of the Storm Event occurred on 1/11/1995
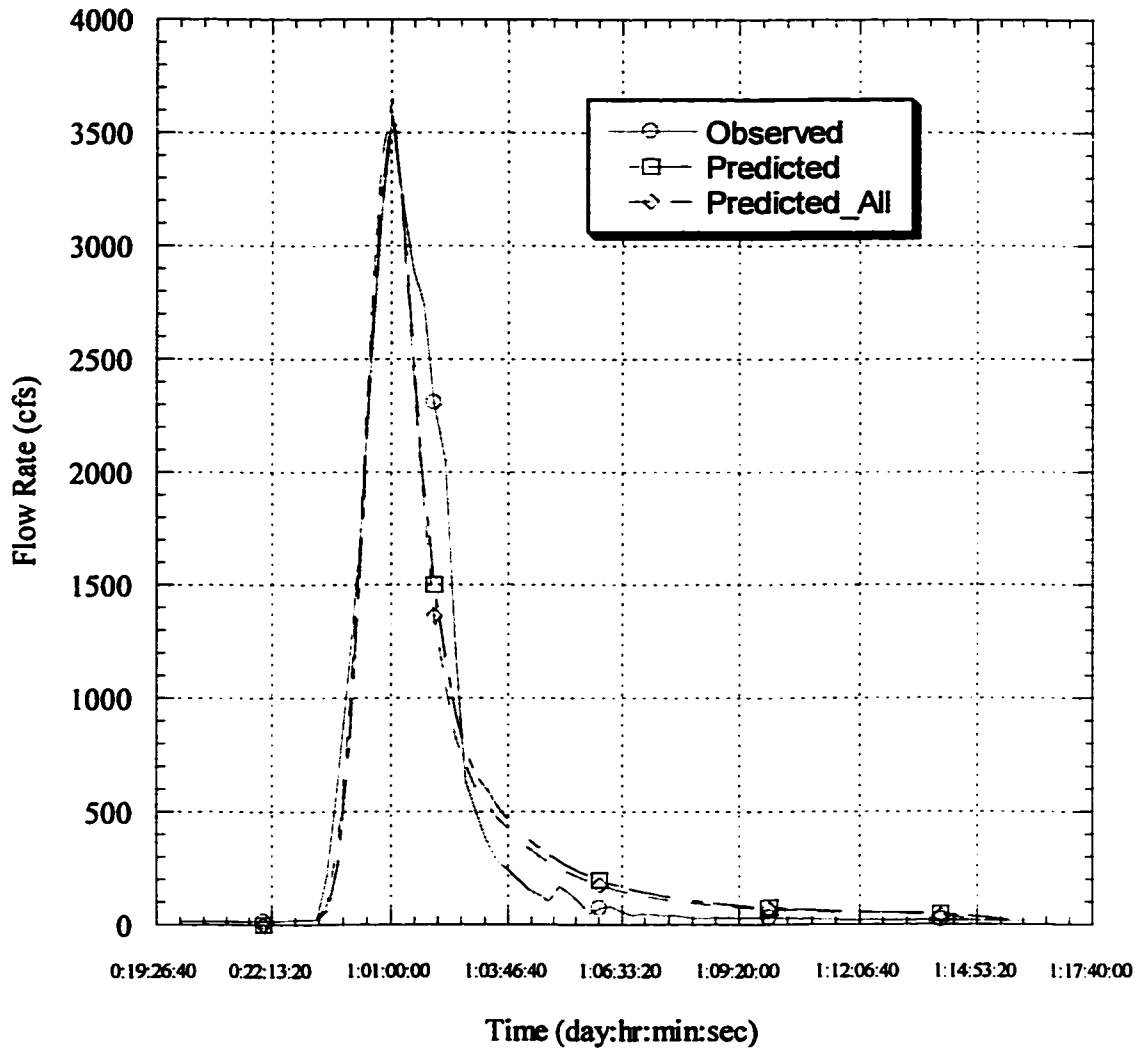
111

Storm Event on 1/20/1995

Figure 5.12 Outlet Hydrograph of the Storm Event occurred on 1/20/1995

Storm Event on 3/20/1995

Figure 5.13 Outlet Hydrograph of the Storm Event occurred on 3/20/1995

Storm Event on 3/23/1995
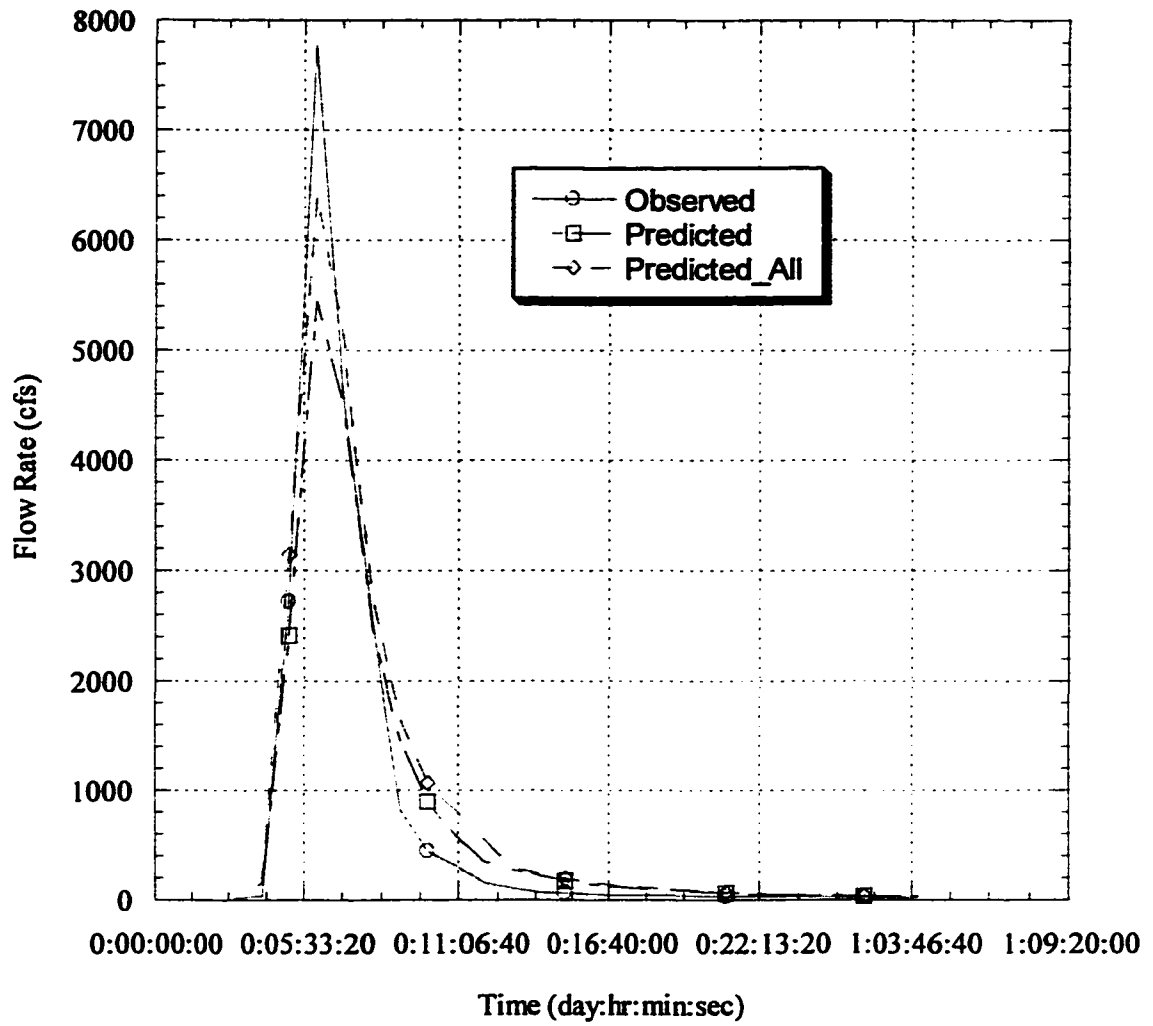
Figure 5.14 Outlet Hydrograph of the Storm Event occurred on 3/23/1995

Storm Event on 1/19/1996
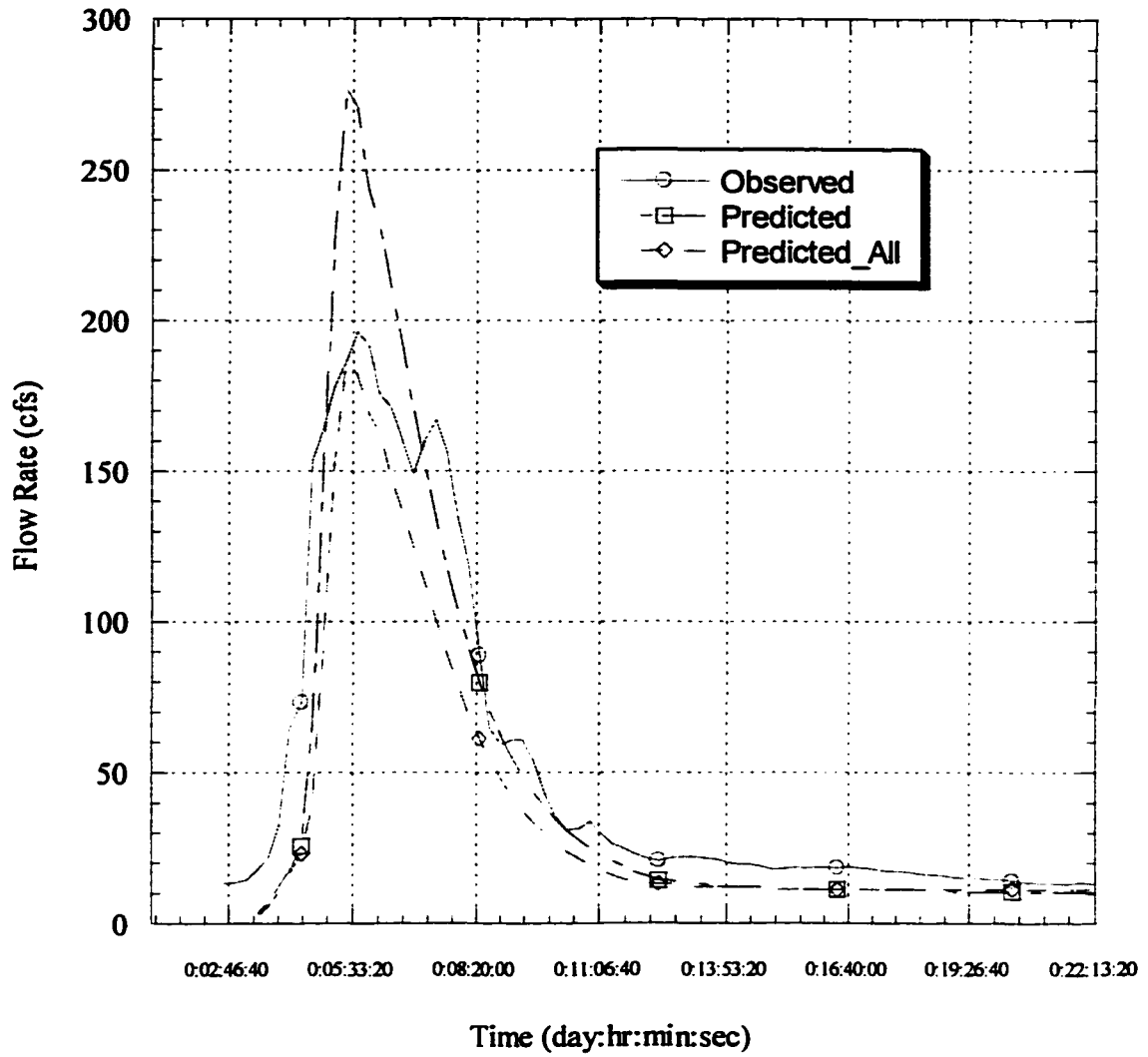
Figure 5.15 Outlet Hydrograph of the Storm Event occurred on 1/19/1996
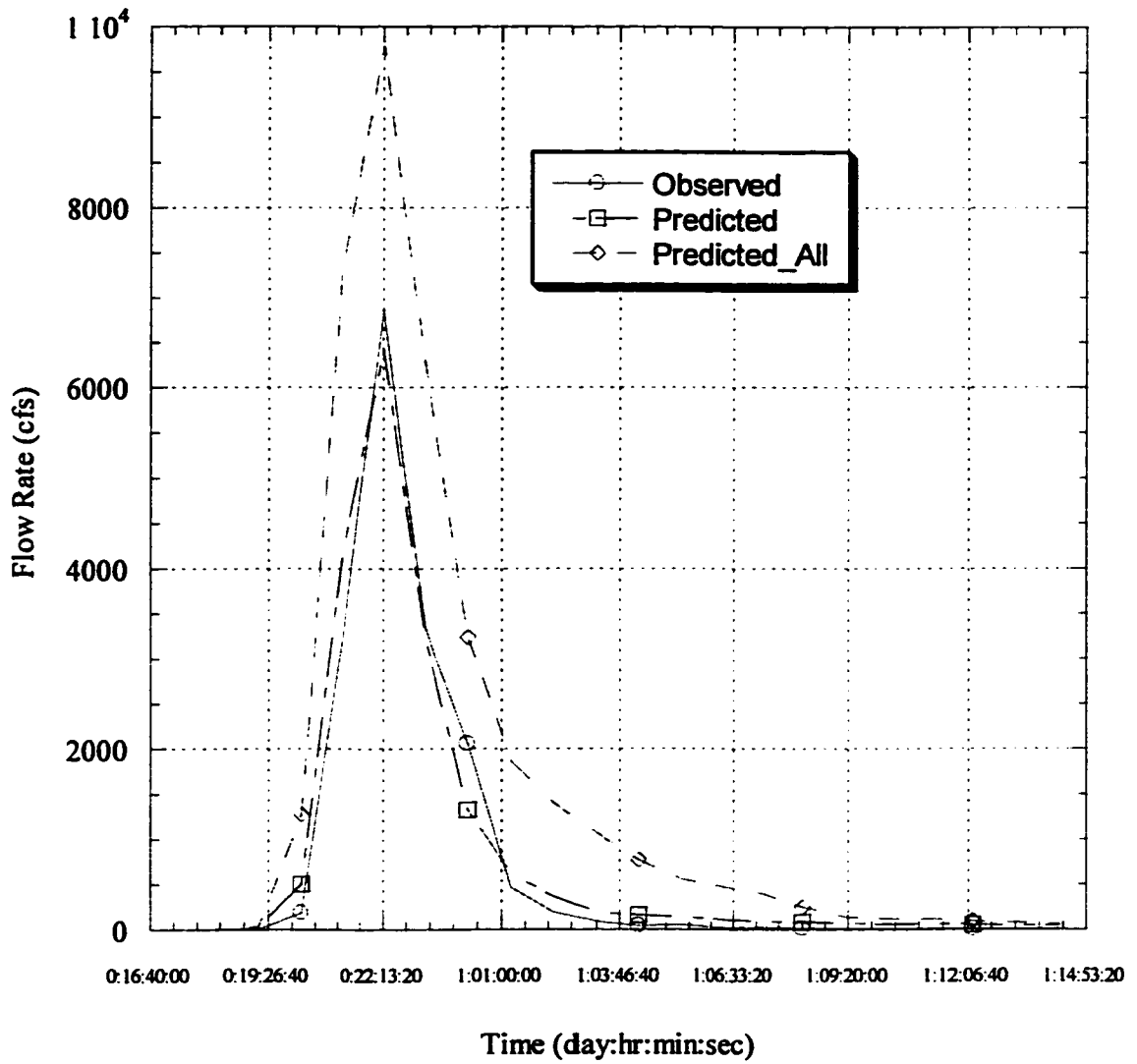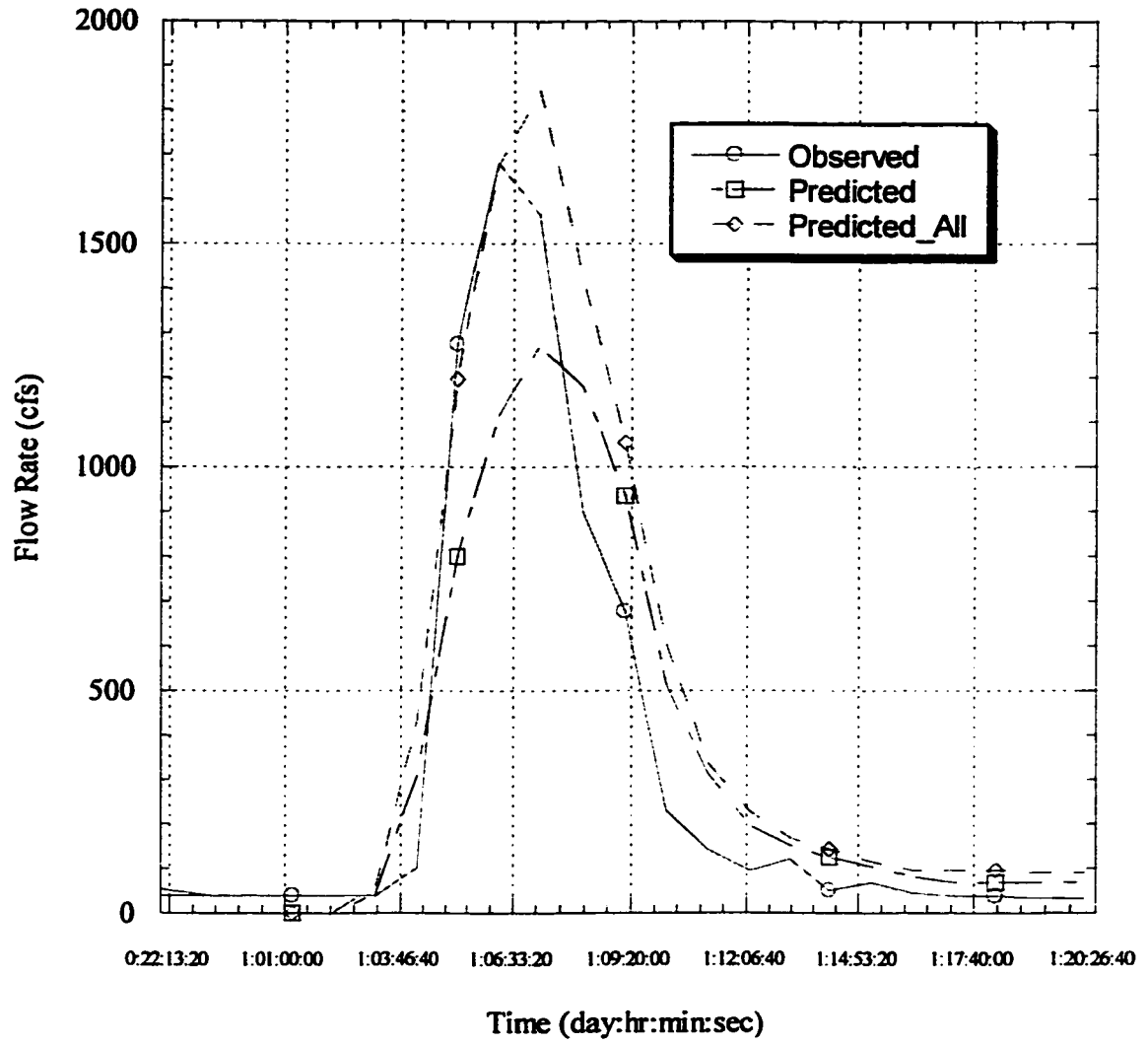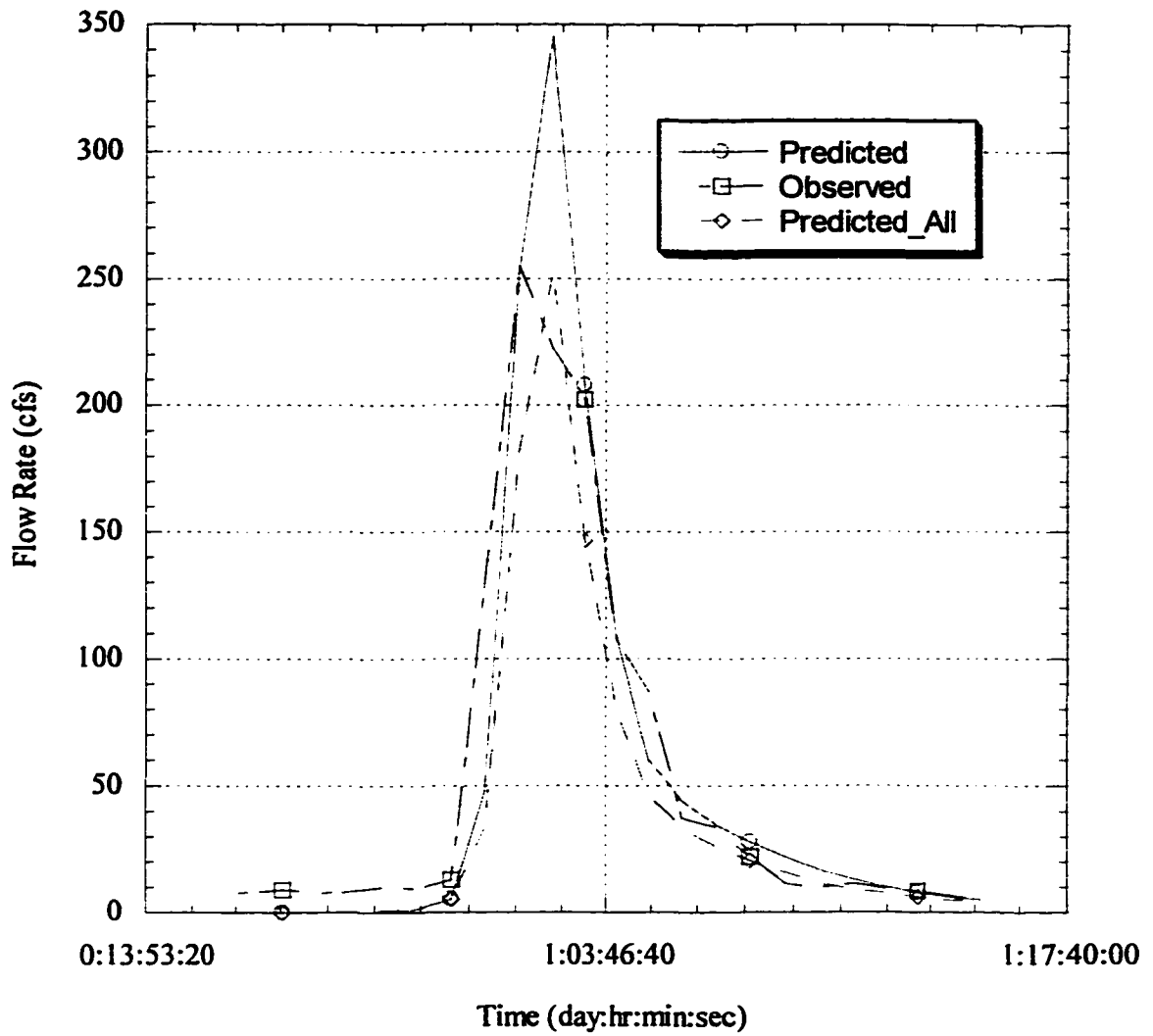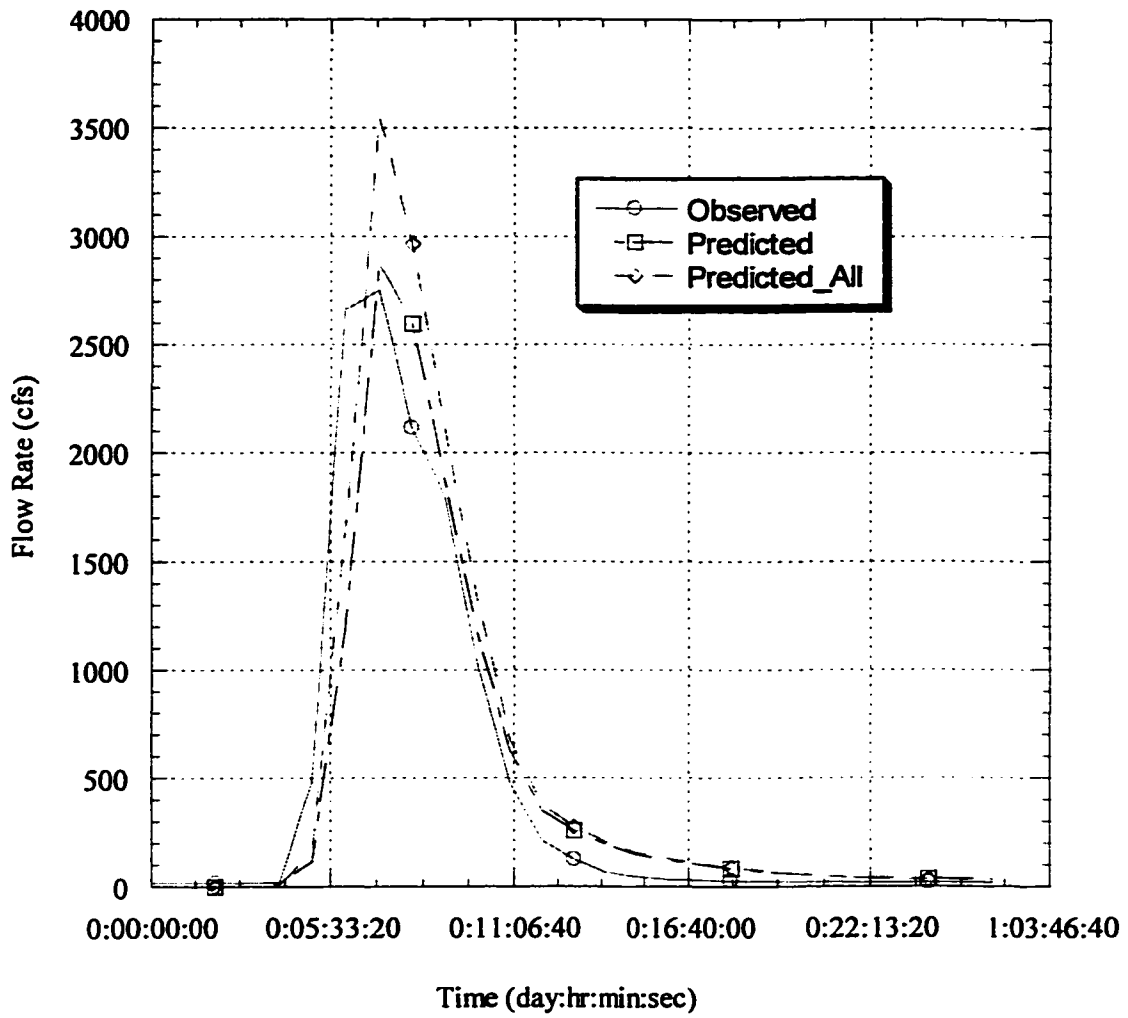
Storm Event on 2/3/1996
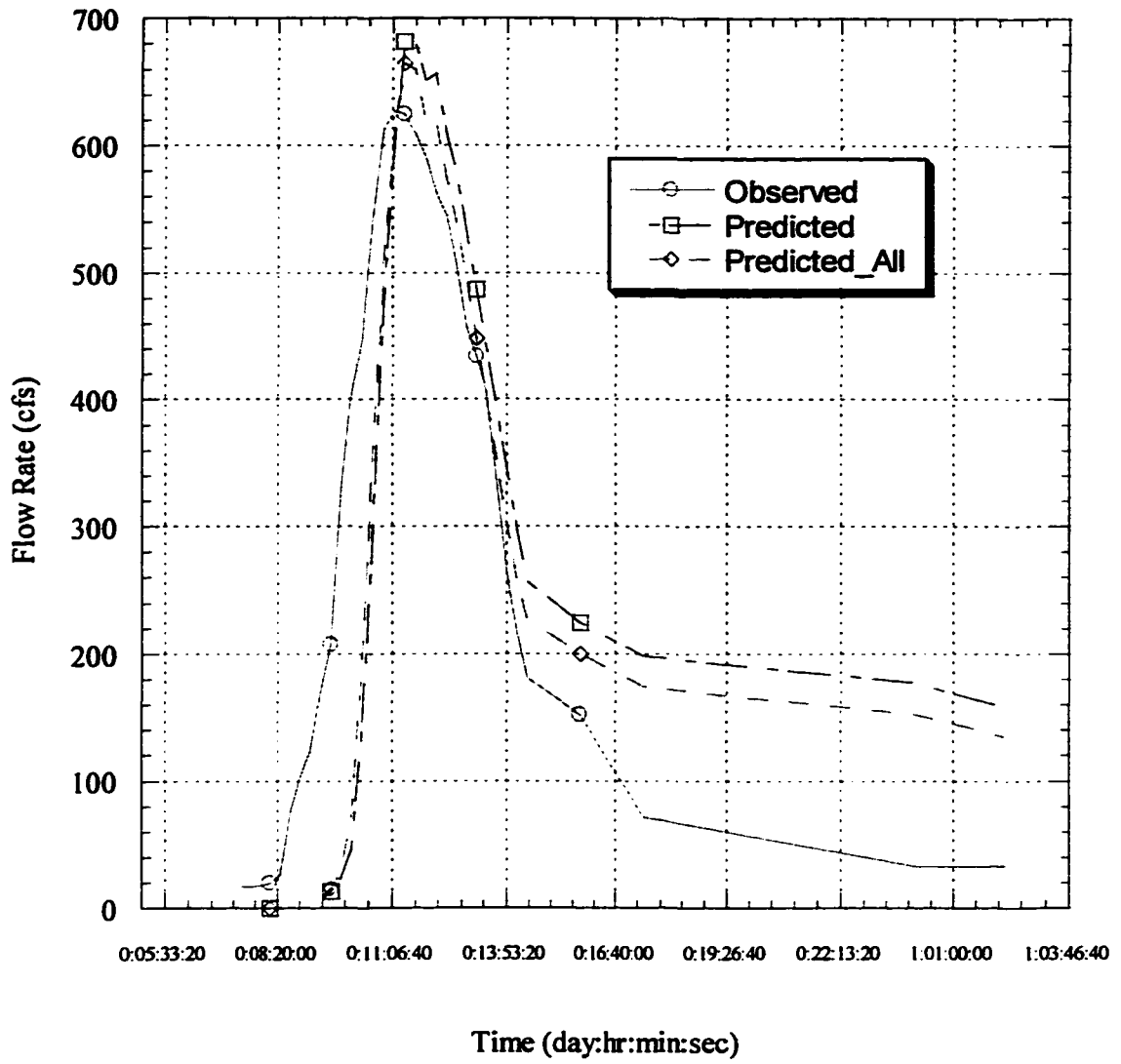
Figure 5.16 Outlet Hydrograph of the Storm Event occurred on 2/3/1996

Storm Event on 12/22/1996
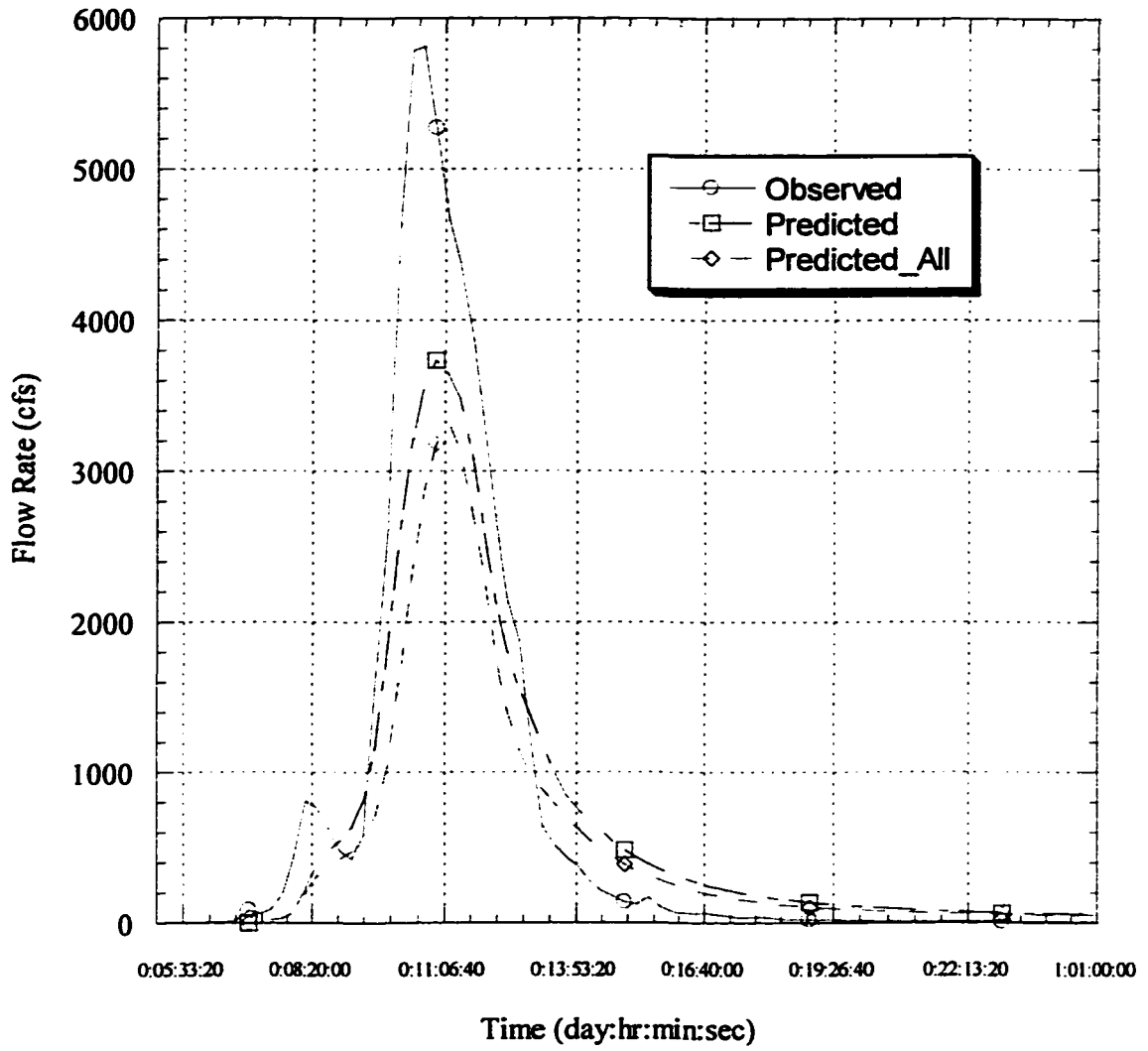
Figure 5.17 Outlet Hydrograph of the Storm Event occurred on 12/22/1996

Table 5.8 Calibrated Parameter Values for the Selected 10 Storm Events

	CIMP	CWIDTH	CWSTORE1	CROUGH
11/26/94	1.788	1.101	0.506	1.121
12/12/94	1.619	0.965	0.757	1.111
12/24/94	0.766	1.191	1.181	0.738
1/11/95	1.41	0.949	1.027	1.021
1/20/95	1.749	1.774	0.529	1.236
3/20/95	1.379	0.974	0.912	1.02
3/23/95	1.333	0.992	1.013	0.995
1/19/96	1.671	1.709	0.5	1.185
2/3/96	1.796	1.022	0.788	1.169
12/22/96	1.768	1.043	0.506	1.155
Average Parameter Values	1.528	1.172	0.772	1.075

Table 5.9 Model Outputs using the Specific Parameter Values and Average Parameter Values

	Observed		Specific Parameter Predicted (cu ft)		Average Parameter Predicted_All (cu ft)	
	Q (cu ft)	P (cfs)	Q* (cu ft)	P* (cfs)	Q* (cu ft)	P* (cfs)
11/26/94	5.87E+06	511.27	3.70E+06	294.78	2.38E+06	228.91
12/12/94	2.86E+07	3577.44	2.88E+07	3579.22	2.81E+07	3651.22
12/24/94	5.99E+07	6857.02	6.40E+07	6410.61	1.27E+08	9791.70
1/11/95	2.70E+07	1680.32	2.71E+07	1272.69	3.58E+07	1844.62
1/20/95	4.42E+06	254.77	4.40E+06	345.40	3.21E+06	252.52
3/20/95	4.36E+07	2754.18	4.36E+07	2875.87	5.10E+07	3553.15
3/23/95	7.24E+07	7778.92	7.18E+07	5447.23	8.45E+07	6412.91
1/19/96	3.79E+06	196.32	3.44E+06	270.69	2.61E+06	182.09
2/3/96	8.76E+06	627.10	8.21E+06	605.10	7.86E+06	614.38
12/22/96	5.29E+07	5815.11	4.69E+07	3732.86	3.75E+07	3319.26

Q = total flow volume

P = peak flow rate

* = superscript, denotes the model predictions

Table 5.10 Relative Errors Between the Observed and Predicted Values of Parameters

	Specific Parameter Predicted (cu ft)		Average Parameter Predicted_All (cu ft)	
	Q* [%]	P* [%]	Q* [%]	P* [%]
11/26/94	34.40	53.94	215.03	152.16
12/12/94	0.01	0.00	0.03	0.04
12/24/94	0.42	0.48	27.94	8.98
1/11/95	0.00	10.26	6.07	0.79
1/20/95	0.00	6.89	14.25	0.01
3/20/95	0.00	0.18	2.10	5.06
3/23/95	0.01	18.32	2.05	4.54
1/19/96	1.05	7.55	20.51	0.61
2/3/96	0.46	0.13	1.32	0.04
12/22/96	1.64	31.12	16.87	56.54

Based on the observation of model outputs illustrated in Figure 5.8 to 5.17,

both the specific parameters and average parameters calibrated model outputs

(Predicted and Predicted_All) are able to capture the shape of the observed outlet

hydrograph (Observed) and with reasonable accuracy. The only exception is the model

outputs from the storm event occurred on 11/26/1994. The relative errors of the storm

event on 11/26/1994 are several magnitude larger than the rest of the storms (Table 5.10). The reasonable guess for the source of error might be due to the inaccurate data collection occurred on 11/26/1994.

By comparing the relative errors and model outputs between the storm specific parameters and average parameter listed in Table 5.9 and 5.10, the following observation are noticed,

- The storm specific parameters produce smaller relative errors than the average parameters. This is quite reasonable because the specific parameters are calibrated from only one set of precipitation data and observed flow data of the particular storm event.

- The average parameters produce relatively small relative errors. It appears the compromise has been reached for the average parameter values. The range of the relative errors are reasonable due to the complexities of urban stormwater modeling.

- The relative errors of the storm specific calibrated total flow volume (Q) are generally less than the peak flow's (P). And the relative errors of the average parameter calibrated peak flow (P) are generally less than Q's

- Both the storm specific and average parameters of the storm event occurred on 12/12/1994, 3/20/1995, and 2/3/1996 produce surprisingly small relative errors.

Based on the above observation, the calibrated GIS/SWMM generally produces outputs with reasonable accuracy (Total Flow Volume, Peak Flow, and the shape of the outlet hydrograph).

5.3.3 Sensitivity Analysis

Sensitivity analysis is very important as a part of the modeling process. Because it is very effective for assessing uncertainty of the model outputs and gives the model results a proper perspective. In this section, we will look at how errors in various model parameters might affect the output of the calibrated model.

Sensitivity analysis basically changes one model parameter while holding all others constant and observes the changes in model input. Figure 5.18 shows the sensitivity of runoff volume to percent changes from the calibrated ratio factors of imperviousness (CIMP), width (CWIDTH), impervious depression storage (WSTORE1), channels Manning's roughness coefficient (CROUGH), pervious depression storage (WSTORE2), subcatchment impervious Manning's coefficient (CIMP_N), and subcatchment pervious Manning's coefficient (PER_N). The percent changes in runoff volume is most from changes in CIMP and WSTORE1. Changes in all other parameters caused insignificant changes. One thing needs to point out in Figure 5.18 is the percent change in runoff volume in the region of negative percent

change in CWIDTH. The reason of the dramatic decrease in runoff volume with small percent decrease in CWIDTH is the assumption made in the deviation of Eq. 4.22 and 4.23 in Chapter 4. The assumption made was the depth of flow of the overland surface flow is very small comparing with the width of the subcatchment. In this way, the wetted perimeter can be approximated by the width of the subcatchment. If the width of subcatchment is decreased to a point that it is no longer very large comparing with the depth of flow. Then the assumption made can no longer hold true and so is Eq. 4.22 and 4.23. Therefore, this model can not be used when the depth of flow is large comparing with the subcatchment width. In reality, the fact that the depth of flow is comparable in length with the subcatchment width is very rare or if impossible. Therefore, the assumption made in the deviation of Eq. 4.22 and 4.23 is reasonable and accurate for the urban stormwater modeling.

In Figure 5.19 shows a similar trend with percent changes in runoff peak flow versus changes in model parameters. CWIDTH and CIMP_N also play a minor role in turns of its effect on percent changes in runoff peak flow with CWIDTH causes more percent changes than CIMP_N. Overall, CIMP and WSTORE1 cause more percent changes in runoff peak.
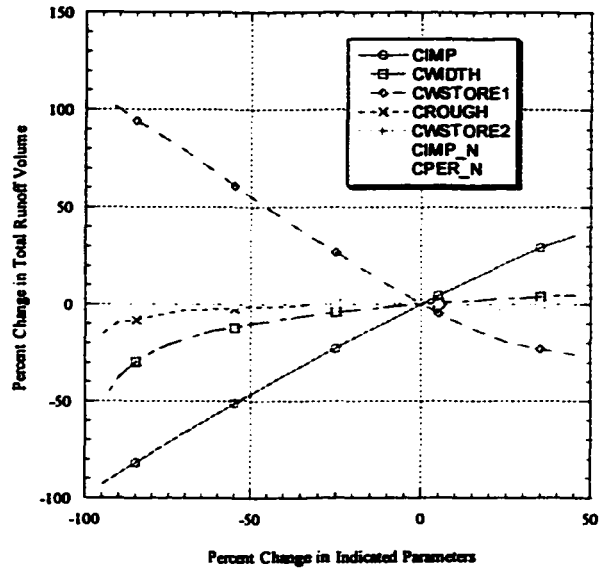
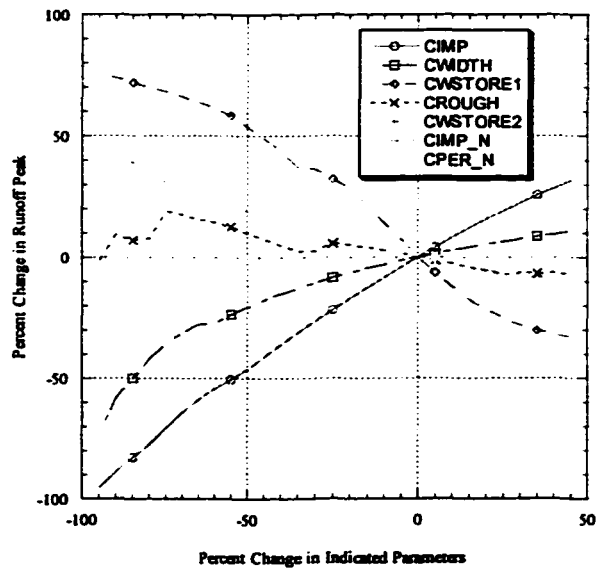Figure 5.18 Sensitivity Analysis of Ballona Creek Watershd, Total Runoff Volume

Figure 5.19 Sensitivity Analysis of Ballona Creek Watershed, Peak Runoff Flow

124

5.4 Quality Simulation

Normally, an urban stormwater model must be able to produce reasonably accurate quantity simulations before it can be applied on quality simulation. This is also true for the calibration process. Before pollutant parameters can be calibrated, the hydrologic and hydraulic parameters must be thoroughly calibrated first. Unfortunately, at the time of this writing, only one set of observed storm event quality data (3/14/1998) collected from the watershed outlet is available but the corresponding precipitation data has not been published. Without adequate observed storm event water quality data, it is virtually impossible to perform a detail calibration study. Though with only one set of storm event water quality data, we still can use the calibrated GIS/SWMM model to demonstrate the feasibility of predicting the pollutant loadings during a single storm event. The precipitation data from the storm event occurred on 12/12/1994 are used. Table 5.11 lists some of water quality data collected on 3/13/1998 at the watershed outlet.

Table 5.11 A Selected Set of Water Quality Data Collected on 3/13/1998

Date Time	3/13/98 11:30pm	3/14/98 3:30pm	3/14/98 8:30am	Event Mean Conc
TSS (mg/L)	6.16	3.74	3.91	5.20
COD (mg/L)	31.91	17.78	22.22	26.69
Cl- (mg/L)	7.31	6.78	21.17	8.79
NO3- (mg/L as NO3-N)	0.86	0.88	1.52	0.94
SO42- (mg/L)	19.54	21.24	58.12	24.59

Assuming the Event Mean Concentration (EMC) of pollutants collected on 3/13/1998 are valid during the storm event occurred on 12/12/1994. A select set of pollutant data and runoff volume of 12/12/1994 storm event are used to calculate the total mass loadings. Table 5.12 lists the mass loadings of the selected pollutants from Table 5.11.

Table 5.12 Mass Loadings of the Selected Pollutants for Storm Events on 12/12/1994

	Event Mean Conc	Mass Loadings (kg)
TSS (mg/L)	5.20	4.14E+03
COD (mg/L)	26.69	2.12E+04
Cl- (mg/L)	8.79	7.00E+03
NO3- (mg/L as NO3-N)	0.94	7.49E+02
SO42- (mg/L)	24.59	1.96E+04

6. SUMMARY AND CONCLUSION

The main objective of this research was to develop an integrated stormwater management model with GIS for the urban stormwater process. The integrated GIS/Model can be used to help decision makers or planners in stormwater abatement strategies. GIS was shown to be feasible to process and handle large amount of data for the urban stormwater modeling.

An integrated GIS and empirical urban runoff model was developed to estimate the annual pollutant loadings in the Santa Monica Bay Watershed. The runoff equation derived from the rational method was successfully embedded in the GIS. Within the GIS, all the physical characteristics (data coverages) of the watershed were successfully linked and related with the runoff model. Based on the results obtained from the overall integrated system, the following conclusions are drawn:

1. A GIS provides a stable and an efficient platform to store and manipulate an substantial amount of data required by stormwater modeling. Since a GIS stores the data in reference to the spatial features of the physical world, it can be used to identify the spatial relationships between map features.

2. The model's prediction of the annual pollutant loadings in the watershed can easily

   be identified in a GIS from the largest unit of the whole watershed to the smallest

   unit of land use polygons. This feature provides an efficient way to pinpoint the

   heavily polluting areas in a watershed.

3. A combination of a GIS and an empirical urban runoff model can be used as a tool

   to test the potential nonpoint source control strategies.

An integrated form of GIS and a deterministic stormwater model was

developed. The original SWMM was modified and adapted to the Ballona Creek

Watershed. A GIS was integrated with the modified SWMM to process the data

management part of GIS/SWMM model. A procedure to generate mean areal

precipitation data using the raster-based GIS was developed. The method was able to

estimate mean areal precipitation data in a watershed that has limited number of rain

gauges. Most of the model inputs are stored and managed by GIS. The required data

inputs to the modified SWMM can be programmed and written as a text file.

A model calibration algorithm was developed and evaluated for the urban

stormwater process. A total of ten storm events data were used to calibrate the data.

The calibrated parameters were able to predict the model outputs with reasonable

accuracy. The relative errors for the runoff volume between the observed and predicted

data range from 0.03% to 27.94%. And the relative errors for the runoff peak between the observed and predicted data range from 0.01% to 56.54%.

A sensitivity analysis was used to quantify the uncertainty of the model parameters. The subcatchment imperviousness (IMP) and impervious depression storage (WSTORE1) are found to be the most significant parameters and cause the most percent changes in the model outputs (runoff volume and runoff peak). The next significant parameter is the abstract subcatchment parameter – subcatchment width (WIDTH). The pervious depression storage (WSTORE2) and pervious Manning's coefficient (PER_N) were found to have virtually no effects on the model outputs.

The results of this investigation show that a stormwater process model integrated with GIS is superior to a conventional approach in stormwater modeling. Because using GIS as the data management system, it can effectively manage large quantity of data that are typical for stormwater modeling. The methodology of integrating GIS and stormwater model presented in this investigation can easily be applied and scaled up on larger watershed.

7. FUTURE RESEARCH

As stated in the last chapter, the work documented in this dissertation is the completion of the hydrologic and hydraulic parts of GIS/SWMM system. Much research needs to be conducted with the quality simulation and its calibration. The following are the proposed further research on urban stormwater modeling.

1. Develop a procedure to better estimate the rainfall data using radar data. Land-based weather radar generally provides better capability to measure precipitation and covers wider area.

2. Develop a fuzzy logic /or neural network algorithm to calibrate the quality part of GIS/SWMM system. Due to the limited availability and extreme variability of the pollutant data, fuzzy set logic or/and neural network algorithm will help to improve the model estimation.

3. Develop a postprocessor for the modified GIS/SWMM. The interface will be used to retrieve the model output and be displayed in numerical form or converted to graphical form using the built-in GIS functions.

4. Incorporate a cost and benefit algorithm in an integrated system described in the last task. This is to be used to develop the Best Management Practices (BMPs) for the target watershed.

5. Integrate a receiving surface water model to route flows and pollutant loads

   through receiving waters.

REFERENCES

Anderson, J.R., Hardy, E.T., Roach, J.T., and Witmer, R.E. (1976). "A land use and land cover classification system for use with remote sensor data: U.S. Geological Survey Professional Paper 964.

ARC/INFO User Guide. (1992). Environmental Systems Research Institute, Inc. Ver. 6.1.1.

ASCE Manuals and Reports of Engineering Practice No. 77 (1992). Design and Construction of Urban Stormwater Management Systems. ASCE, New York.

Barbe, D.E., Cruise, J.F., and Mo, X. (1996). "Modeling the Buildup and Washoff of Pollutants on Urban Watersheds", *Water Resources Bulletin*. Vol. 32, No. 3, pp. 511-519.

Bedient, P.B., and Huber, W.C. (1992). Hydrology and Floodplain Analysis. Addison-Wesley Publishing Company.

Brebbia, C.A. (1975). Mathematical Models for Environmental Problems. Pentech Press, London.

Carriere, P., Mohaghegh, S., and Gaskari, R. (1996). "Performance of a Virtual Runoff Hydrograph System", Journal of Water Resources Planning and Management. Vol. , No., pp. 421-427.

Cline, T.J., Molinas, A., and Julien, P.Y. (1989). "An Auto-Cad-Based Watershed Information System for the Hydrologic Model HEC-1", *Water Resources Bulletin*. Vol. 25, No. 3, pp. 641-652.

Corbitt, R.A. (1990). Standard Handbook of Environmental Engineering. McGraw Hill, Inc.

Creutin, J.D., Delrieu, G., and Lebel, T. (1988). "Rain Measurement by Rainage – Radar Combination: A Geostatistical Approach", *Journal of Atmosphere and Oceanic Technology*. Vol. 5, pp. 102-115.

Driscoll, E.D., Shelley, P.E., and E.W. Strecker (1990). *Pollutant Loadings and Impacts from Stormwater Runoff, Volume III*: Analytical Investigation and Research Report. FHWA-RD-88-008, Federal Highway Administration.

Driver, N.E., and Tasker, G.D. (1990). Techniques for Estimation of Storm-Runoff Loads, Volumes, and Selected Constituent Concentrations in Urban Watersheds in the United States. U.S. Geological Survey Water-supply Paper 2363.

Duckson, Jr., D.W. (1989). "Land-Use and Water-Quality Relationships in the Georges Creek Basin, Maryland", *Water Resources Bulletin*. Vol. 25, No. 4, pp. 801-807.

Elmasri, R., and Navathe, S.B. (1989). Fundamentals of Database Systems. The Benjamin/Cummings Publishing Company, Inc.

Engel, B.A., Srinivasan, R., Arnold, J., and Rewerts, C. (1993). "Nonpoint Source (NPS) Pollution Modeling Using Models Integrated with Geographic Information Systems (GIS)", *Wat. Sci. Tech.* Vol 28, No. 3-5, pp. 685-690.

Fam, S., Stenstrom, M.K., and Silverman, G. (1987). "Hydrocarbons in Urban Runoff", *Journal of Environmental Engineering*, ASCE. Vol. 113, No. 5, pp. 1032-1046.

Franchini, M., and Galeati, G. (1997). "Comparing Several Genetic Algorithm Schemes for the Calibration of Conceptual Rainfall-Runoff Models", *Hydrological Sciences-Journal-des Sciences Hydrologiques*, Vol. 42, No. 3, pp.357-379.

Gilliland, M.W., and Baxter-Potter, W. (1987). "A Geographic Information System to Predict Non-Point Source Pollution Potential", *Water Resources Bulletin*. Vol. 23, No. 2, pp. 281-291.

Hay, L.E., and Knapp, L.K. (1996). "Integrating a Geographic Information System, A Scientific Visualization System, and a Precipitation Model", *Water Resources Bulletin*. Vol. 32, No. 2, pp. 357-369.

He, C, Riggs,J.F, and Kang, Y.T. (1993). "Integration of Geographic Information Systems and a Computer Model to Evaluate Impacts of Agriculture Runoff on Water Quality", Water Resources Bulletin. Vol. 29, No. 6, pp. 891-900.

Heidtke, T.M., and Auer, M.T. (1993). "Application of a GIS-Based Nonpoint Source Nutrient Loading Model for Assessment of Land Development Scenerios and

Water Quality in Owasco Lake, New York", *Wat. Sci. Tech.* Vol. 28, No. 28, pp. 595-604.

Hoggan, D.H. (1989). Computer-Assisted Floodplain Hydrology & Hydraulics. McGraw-Hill, Inc.

Jeton, A.E., and Smith, J.L. (1993). "Development of Watershed Models for Two Sierra Nevada Basins Using a Geographic Information System", *Water Resources Bulletin.* Vol. 29, No. 6, pp. 923-932.

Joint Water Pollution Control Plant Annual Monitoring Report (1993). County Sanitation Districts of Los Angeles County. NPDES No. CA0053813. RWQCB Order No. 91-112. Monitoring and Reporting Program No. 1758.

Kidd, C.H.R. (1978). *"A Calibrated Model for the Simulation of the Inlet Hydrograph for Fully Sewered Catchments"*, Proceedings International Conference on Urban Storm Drainage, University of Southampton, April 1978, Helliwell, P.R., ed., Pentech Press, London, 1978, pp. 172-186.

Kim, K. (1993). *Feature-Oriented Urban Classification Using Remote Sensing and a Geographical Informaton System.* Ph.D. Diss., The University of Wisconsin, Madison. Madison, WI.

Krajewski, W.F. (1987). "Cokriging Radar-Rainfall and Rain Gage Data". *Journal of Geophysical Research.* Vol. 92, No. D8, pp. 9571-9580.

Krug, W. R. (1996). "Simulation of Temporal Changes in Rainfall-Runoff Characteristics, Coon Creek Basin, Wisconsin", Water Resources Bulletin. Vol. 32, No. 4, pp. 745-752.

Lau, S.L., Bay, S., and Stenstrom, M.K. (1993). "Contaminants in Urban Runoff and their Impact on Receiving Waters", Presented at: Asian WaterQual '93: Fourth IAWQ Asian Regional Conference on Water Conservation and Pollution Control, Oct. 5-9, 1993, Jakarta, Indonesia.

Maidment, D.R. (1993). Handbook of Hydrology. McGraw-Hill, New York.

Marsalek, J. (1991). "Pollutant Loads in Urban Stormwater: Review of Methods for Planning-Level Estimates". *Water Resources Bulletin.* Vol. 27, No. 2, pp. 283-291.

Mattson, M.D., and Godfrey, P.J. (1994). "Identification of Road Salt Contamination Using Multiple Regression and GIS", *Environmental Management*. Vol. 18, No. 5, pp. 767-773.

National Oceanic and Atmospheric Administration (1991). *Contaminant Trends in the Southern California Bight: Inventory and Assessment.* NOAA Technical Memorandum NOS ORCA 62.

National Research Council (1990). Monitoring Southern California's Coastal Waters. National Academy Press.

Nix, S.J. (1994). Urban Stormwater Modeling and Simulation. Lewis Publishers.

Overton, D.E., and Meadows, M.E. (1976). Stormwater Modeling. Academic Press, New York.

Robinson, K.J., and Ragan, R.M. (1993). "Geographic Information System Based Nonpoint Pollution Modeling", *Water Resources Bulletin*. Vol. 29, No. 6, pp. 1003-1008.

Sabins, Jr., F. F. (1987). Remote Sensing, Principles and Interpretation. 2nd Edition. Freeman.

Saez, P.B., and Rittmann, B.E. (1992). "Model Parameter estimation using least squares", *Water Resources Bulletin*. Vol. 26, No. 6, pp. 789-796.

Shamsi, U.M. (1996). "Storm-Water Management Implementation Through Modeling and GIS", Journal of Water Resources Planning and Management, pp. 114-127.

Singh, V.P., and Chowdhury, P.K. (1986). "Comparing Some Methods of Estimating Mean Areal Rainfall", Water Resources Bulletin, Vol. 22, No. 2, pp. 275-282.

Silverman, G.S., Stenstrom, M.K., and Fam, S. (1988). "Land Use Considerations in Reducing Oil and Grease in Urban Stormwater Runoff", *Journal of Environmental Systems*. Vol. 18, No. 1, pp. 31-47.

Stenstrom, M.K., and Strecker, E.W. (1993). *Annual Pollutants Loadings to Santa Monica Bay from Stormwater Runoff.* Assessment of Storm Drain Sources of Contaminants to Santa Monica Bay, Vol. 1.

Stenstrom, M.K., Silverman, G.S., and Burszty, T.A. (1984). "Oil and Grease in Urban Stormwaters", *Journal of Environmental Engineering*, ASCE. Vol. 110, No. 1, pp. 58-72.

State Of The Bay. (1993). "Characterization Study of the Santa Monica Bay Restoration Plan", Santa Monica Bay Restoration.

Schultz, G.A. (1994). "Meso-Scale Modelling of Runoff and Water Balances using Remote Sensing and other GIS data", *Hydrological Sciences –Journal- des Sciences Hydrologiques*. Vol. 39. No. 2, pp. 121-142.

Tim, U.S., Mostaghimi, S., and Shanholtz, V.O. (1992). "Identification of Critical Nonpoint Pollution Source Areas Using Geographic Information Systems and Water Quality Modeling", *Water Resources Bulletin*. Vol. 28, No. 5, pp. 877-887.

Tzeng, C.J. (1992). *Advanced Dynamic Modeling of the High Purity Oxygen Activated Sludge Process*. Ph.D. Diss., The University of California, Los Angeles. Los Angeles, CA.

Ventura, S.J., and Kim, K. (1993). "Modeling Urban Nonpoint Source Pollution with a Geographic Information System", *Water Resources Bulletin*. Vol. 29, No. 2, pp. 189-198.

Viessman, Jr., Lewis, G.L., and Knapp, J.W. (1989). Introduction to Hydrology. Harper & Row, Publishers, New York.

Walker, J.F., Pickard, S.A., and Sonzogni, W.C. (1989). "Spreadsheet Watershed Modeling for Nonpoint-Source Pollution Management in a Wisconsin Basin", *Water Resources Bulletin*. Vol. 25, No.1, pp. 139-147.

Wanielista, M.P., and Yousef, Y.A. (1993). Stormwater Management. John Wiley & Son, Inc.

Whipple, W., Randall, C.W., Grigg, N.S., Shubinski, R.P., Grizzard, T., and Tucker, L.S.(1983). Stormwater Management in Urbanizing Areas. Prentice-Hall, Inc. Englewood Cliffs, New York.

Xu, F., Prato, T., and Fulcher, C. (1993). "Broiler Litter Application to Land in an Agricultural Watershed: A GIS Approach", *Wat. Sci. Tech.* Vol. 28, No. 3-5, pp. 111-118.

Yuan, W. (1994). *Dynamic Models and Expert Systems for the Activated Sludge Process*. Ph.D. Diss., The University of California, Los Angeles. Los Angeles, CA.

Yin, T.Y. (1995). *Developing a Decision Support System for Operation and Control of the High Purity Oxygen Activated Sludge Process*. Ph.D. Diss., The University of California, Los Angeles. Los Angeles, CA.

APPENDIX A. GIS - Implementation of IDSM

In Eq. 4.11, d_{ij} represents the distance from rain gauge i (located in the center of grid box i) to the center of grid box j. Its representation in raster GIS (GRID module of ARC/INFO GIS) can be written as follows,


```
EUC_DISTANCE_I = EUCDISTANCE (SELECT(RAINGAUGE, 'GAUGE_I'), #, #, #,
#)
```


Where EUC_DISTANCE_I is $d_{i,j}$, RAINGAUGE is GIS database (Coverage) which contains spatial and attribute information of rain gauges in watershed, GAUGE_I is rain gauge i, SELECT (...) is a selection function which selects cell values (GAUGE_I) from the input grid (RAINGAUGE) on a cell-by-cell basis within the analysis window, #'s is optional flags that are unused for this study, and EUCDISTANCE is a euclidean distance function which calculates for each cell the Euclidean distance to the closest source (GAUGE_I).

Euclidean distance is calculated from the center of the source cells to the center of each of the surrounding cells. True Euclidean distance is calculated to each cell in the distance functions. Conceptually, the Euclidean algorithm can be described as follows. For each cell, the distance is calculated to each source cell by calculating the hypotenuse with the x-max and y-max as the other two legs of the triangle. This

calculation derives the true Euclidean distance. The shortest distance to a source is determined and if it is less than the specified maximum distance, the value is assigned to the cell location on the output grid.

Figure A.1 Euclidean Distance Calculation of d_{ij}

The output values for the Euclidean distance grid are floating-point distance values. If the cell is at an equal distance to two or more sources, the cell is assigned to the source that is first encountered in the scanning process.

The actual algorithm computes the information using a two-scan process, therefore, the speed of the function is independent of the number of source cells, the distribution of the source cells, and the maximum distance specified. The only factor that does influence the speed with which the function executes is the size of the grid. The computation time is linearly proportional to the number of cells in the analysis window.

APPENDIX B.   GIS – Development Work of Drainage Database

- Populating slope value of each subcatchment in the subcatchment GIS database

  (CATCHMENT)

  - Convert vector based subcatchment GIS coverage (CATCHMENT) to its raster

    based counterpart by using the POLYGRID command to create

    GRID_CATCH.

  - Create the elevation grid (raster) coverage by clipping GRID_CATCH from the

    USGS DEM coverage – LA_ELEV:

    SUBCAT_ELEV = CON (GRID_CATCH, LA_ELEV, 0)

  - Use the SLOPE function to generate a grid based slope coverage

    (SUBCAT_SLOPE) of SUBCAT_ELEV.

  - Resample SUBCAT_SLOPE to match the original GRID_CATCH coverage by

    using the RESAMPLE function

  - Use the low pass filter to reduce the of number of polygons in the output

    coverage by using the FILTER COMMAND

    If subcatchment j (C_j) contains N number of basins, then the percent slope of

    C_j can be expressed as follows,

    $$PC_j = \frac{\sum_{i=1}^{N} PB_i * AB_i}{\sum_{i=1}^{N} AB_i}$$ (A.1)

Where PB_i = percent slope of basin i

    AB = area of basin i

    i = denotes the ith basin

    j = denotes the jth subcatchment

    PC_j = percent slope of subcatchment j

    Area of C_j = denominator of Eq. A.1

- Use LATTICEPOLY to convert the grid based SUBCAT_SLOPE to vector based coverage (CSLOPEP)

- Under ARC, use the IDENTITY command to generate a new coverage using the vector-based subcatchment coverage (CATCHMNT) as input and CATCH_SLOPE as identity coverage

Using the following relates illustrated in Figure B-1 to populate percent_slope in vector-based CATSLOPE table.

Figure B.1 The Multiple Relates Between the Slope-Related Subcatchment Databases

Catslope.pat   cslope.pat   slope_cat.pat
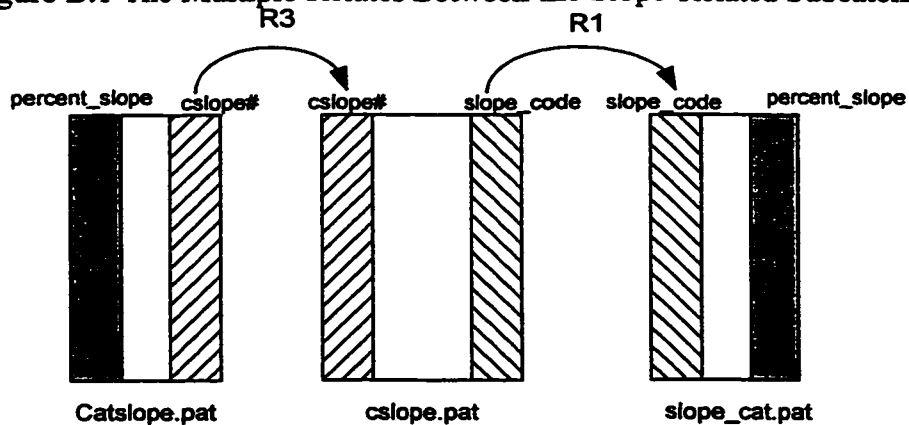
It can be implemented as the following command in ARC/INFO:

```
PERCENT_SLOPE in CATSLOPE table =
R3//R1//PERCENT_SLOPE
```

- Populating the following parameters to the CATCHMENT.PAT,

IMP	=	subcatchment imperviousness
IMP_N	=	subcatchment imperviousness Manning's coefficient
P_N	=	subcatchment pervious Manning's coefficient

By using the following multiple relates illustrated in Figure B.2.
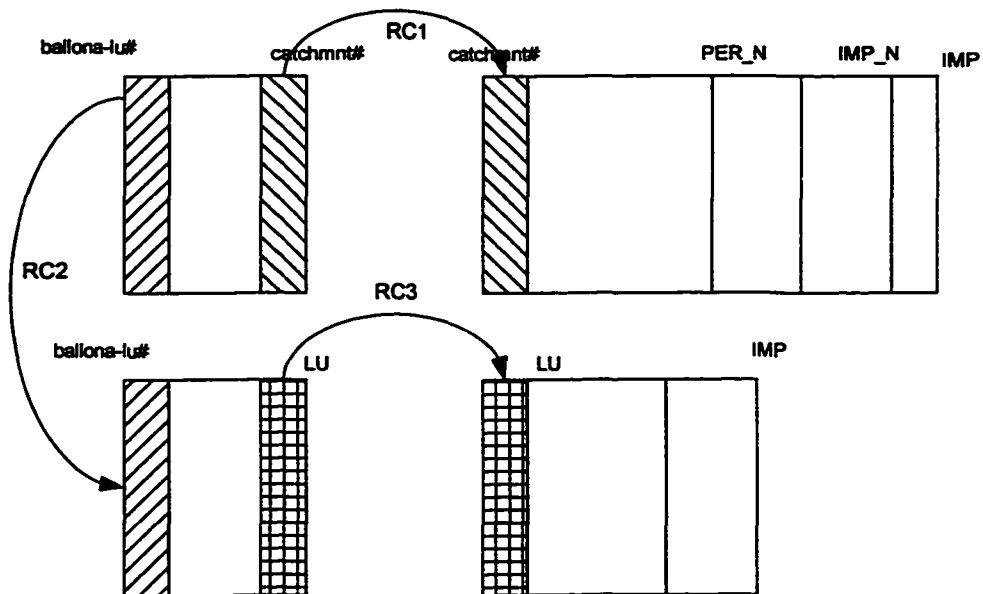
Figure B.2 The Multiple Relates Between the Land Use Related Subcatchment Databases

Percent Slope

☐	0 - 2.485
■	2.485 - 5.46
■	5.46 - 9.671
■	9.671 - 15.235
■	15.235 - 27.555

400   0   400   800 Feet
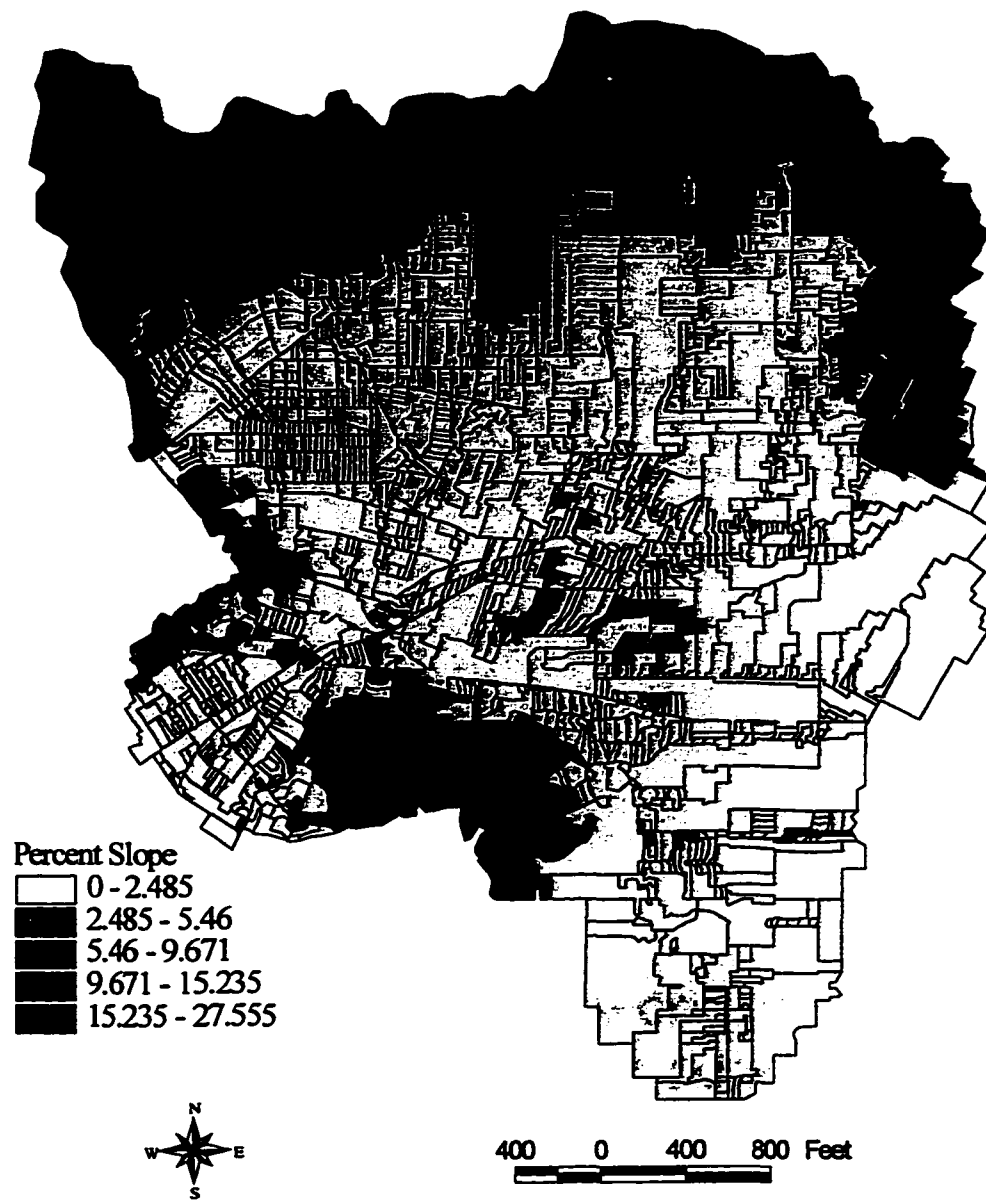
Figure B.3 Percent Slope Coverage of Subcatchment Coverage

Imperviousness of Subcatchment

- 0 - 30.466
- 30.466 - 48.996
- 48.996 - 62.313
- 62.313 - 76.907
- 76.907 - 92

400　0　400　800　Feet
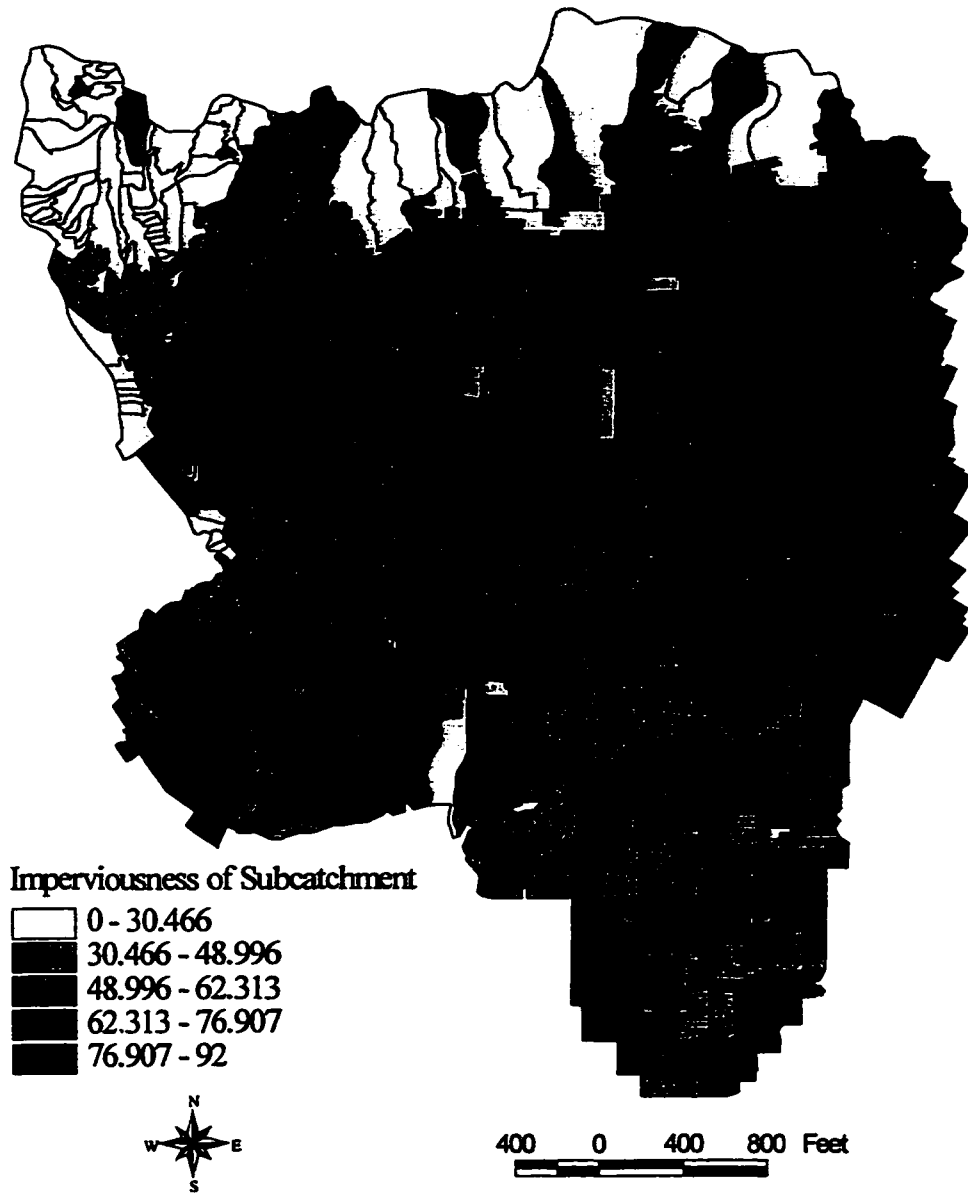
Figure B.4　Imperviousness of Subcatchment Coverage

144

Impervious Depression Storage
- 0 - 0.18
- 0.18 - 0.294
- 0.294 - 0.67
- 0.67 - 2.018
- 2.018 - 4.985

400   0   400   800 Feet
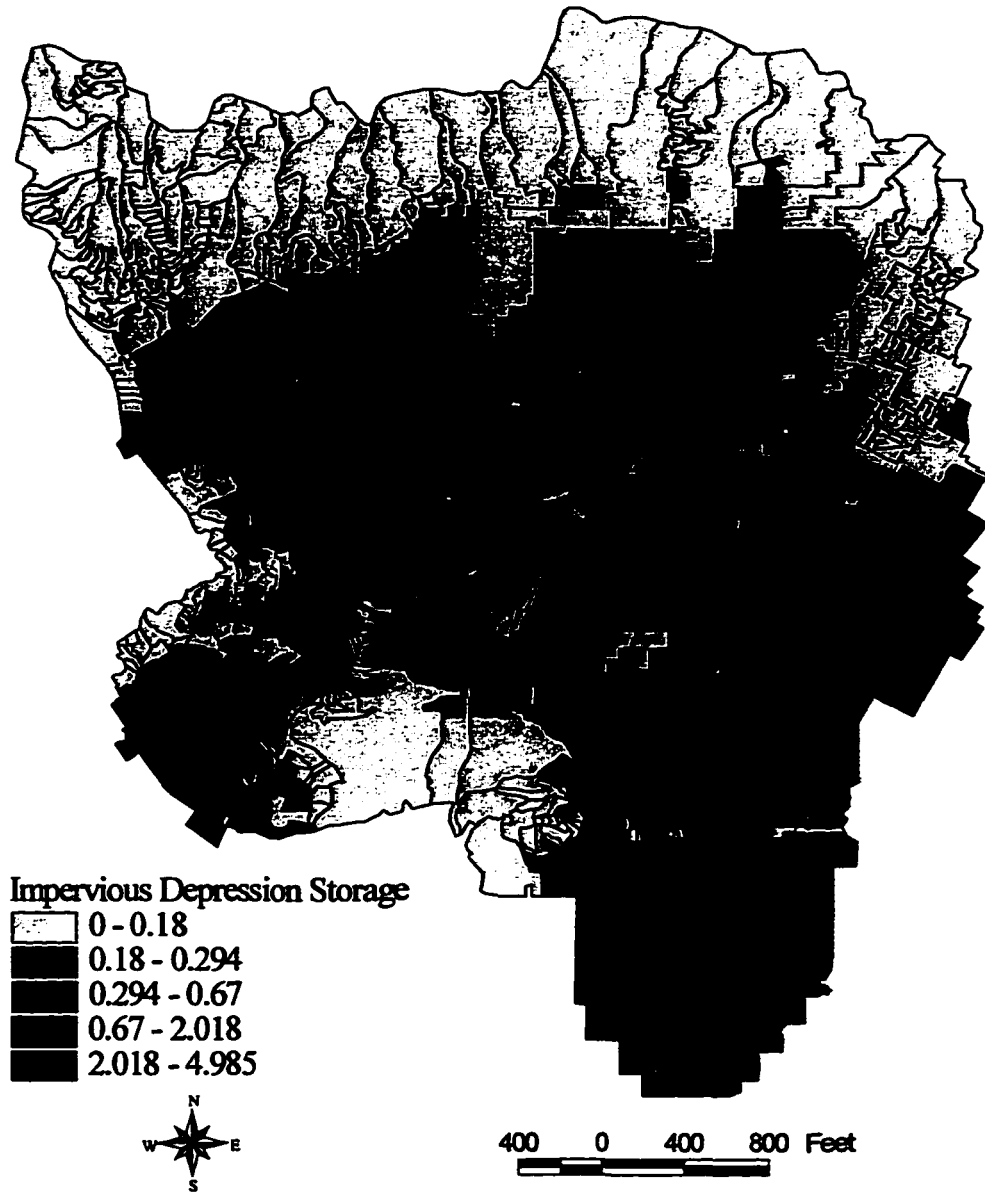
Figure B.5 Impervious Depression Storage of Subcatchment Coverage

Subcatchment Width
- 31.394 - 499.429
- 499.429 - 957.625
- 957.625 - 1534.923
- 1534.923 - 2832.917
- 2832.917 - 7309.821

400   0   400   800 Feet
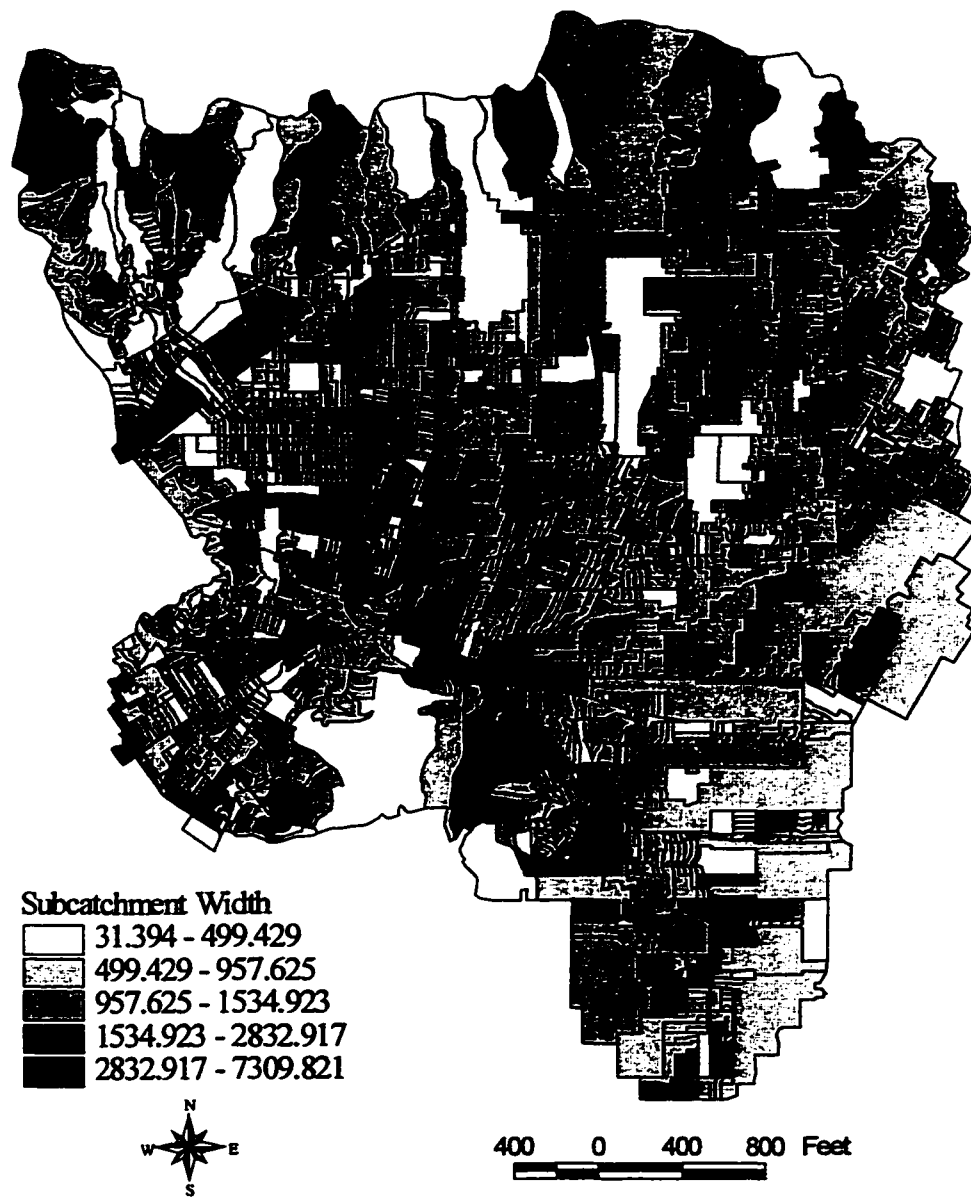
Figure B.6 Catchment Width of Subcatchment Coverage

APPENDIX C.   GIS – Development Work of Channels/Pipes Database

- Populating slope value of each channels/pipes in the channels/pipes GIS database (DRNSIZE)

    - Convert vector based channels/pipes GIS coverage (DRNSIZE) to its raster based counterpart by using the LINEGRID command to create GRID_DRNSIZE

    - Create the elevation grid (raster) coverage by clipping GRID_DRNSIZE from the USGS DEM coverage – LA_ELEV:

        DRN_ELEV = CON (GRID_DRNSIZE, LA_ELEV, 0)

    - Use the SLOPE function to generate a grid based slope coverage (DRN_SLOPE) of DRN_ELEV.

    - Resample DRN_SLOPE to match the original GRID_DRNSIZE coverage by using the RESAMPLE function

    - Use the low pass filter to reduce the of number of polygons in the output coverage by using the FILTER COMMAND

    - Use LATTICEPOLY to convert the grid based SUBCAT_SLOPE to vector based coverage (CSLOPEP)

    - Use RECLASS to convert DRNSLOPE (grid) to integer grid coverage with SLOPE in integer form

- Use GRIDLINE to convert it to vector-base line coverage. The following can be use:

```
GRIDLINE drn_slope drnslope DATA THINFILTER SHARP ~
SLOPE_CODE
```

Using the following relates illustrated in Figure C-1 to populate percent_slope in vector-based DRNSLOPE table.
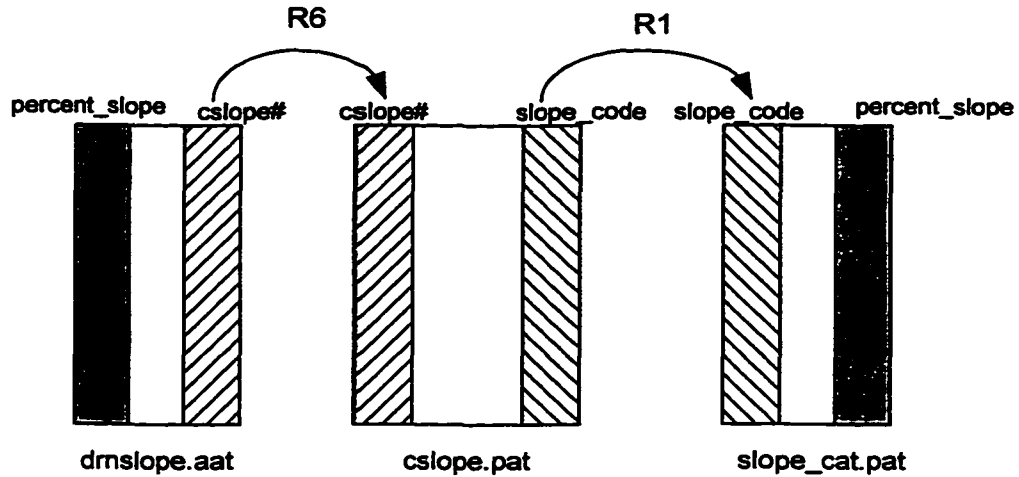

Figure C.1 The Multiple Relates Between the Slope-Related Channels/Pipes Databases

It can be implemented as the following command in ARC/INFO:
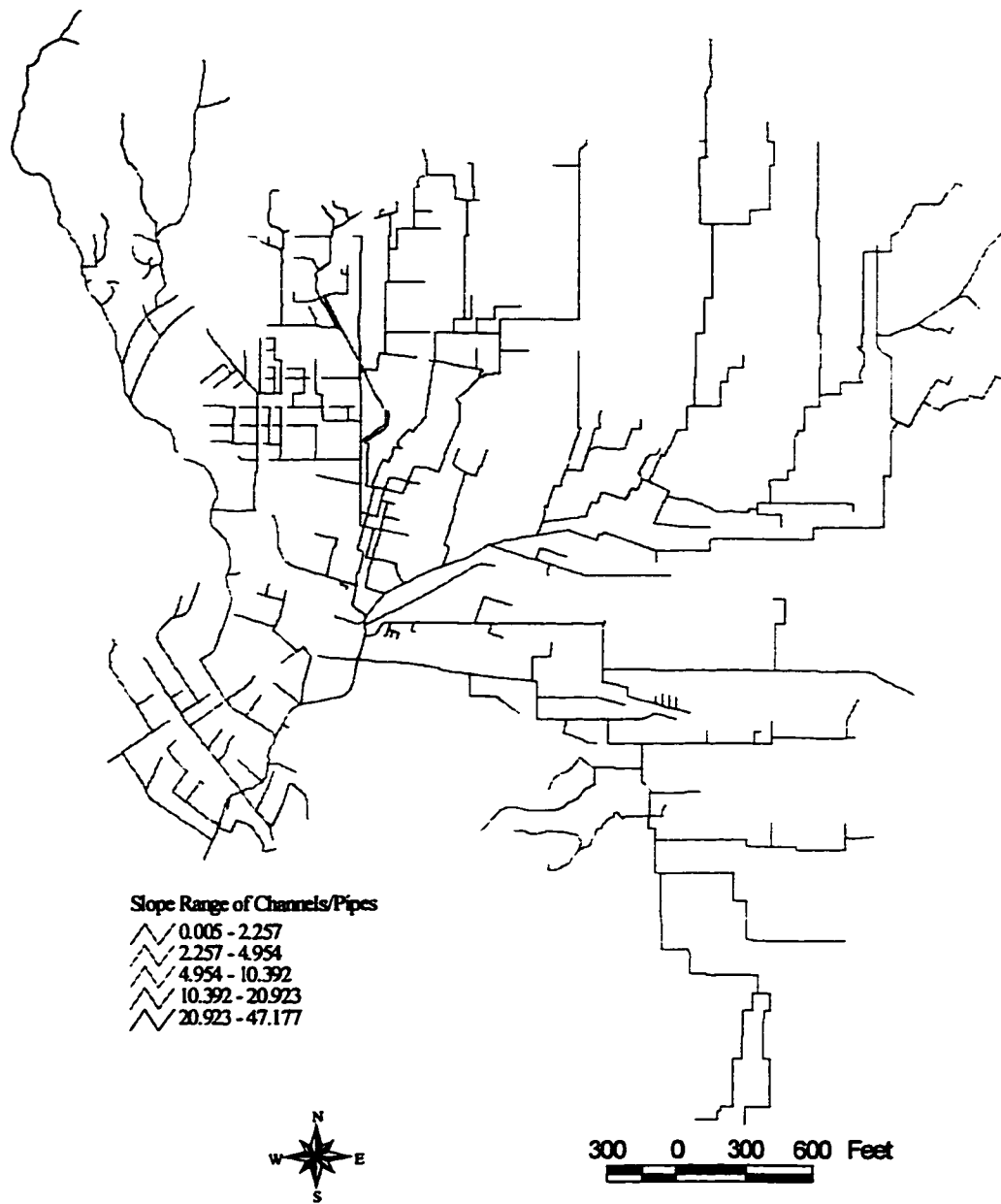
```
PERCENT_SLOPE in DRNSLOPE table =
R6//R1//PERCENT_SLOPE
```

Slope Range of Channels/Pipes

- $\diagup\!\!\diagup$ 0.005 - 2.257
- $\diagup\!\!\diagup$ 2.257 - 4.954
- $\diagup\!\!\diagup$ 4.954 - 10.392
- $\diagup\!\!\diagup$ 10.392 - 20.923
- $\diagup\!\!\diagup$ 20.923 - 47.177

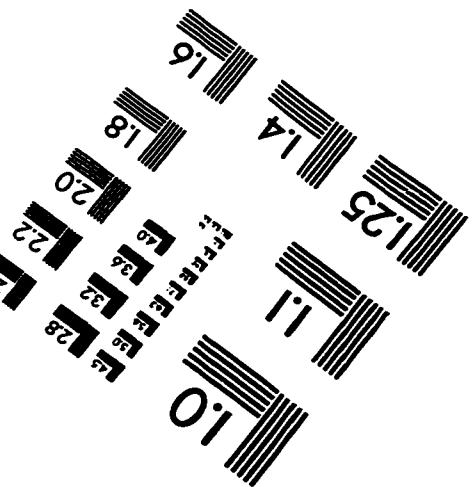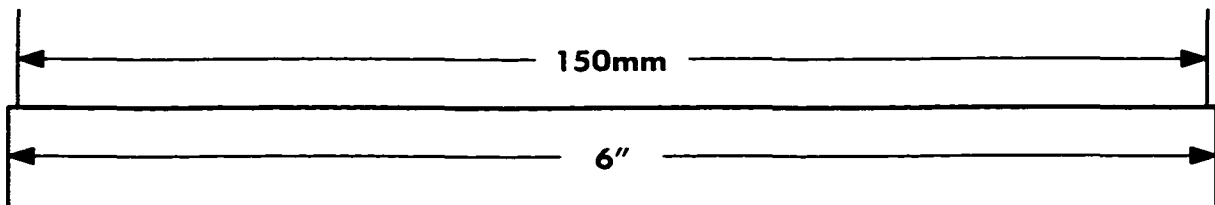300   0   300   600   Feet

Figure C.2 Slope Ranges of Channels/Pipes Coverage

Channels/Pipes Types

/\\/ Reinforced Concrete Pipe
Reinforced Concrete Box
Trapezoidal Open Channel
Arch Conduit

N
W   E
S

300   0   300   600 Feet
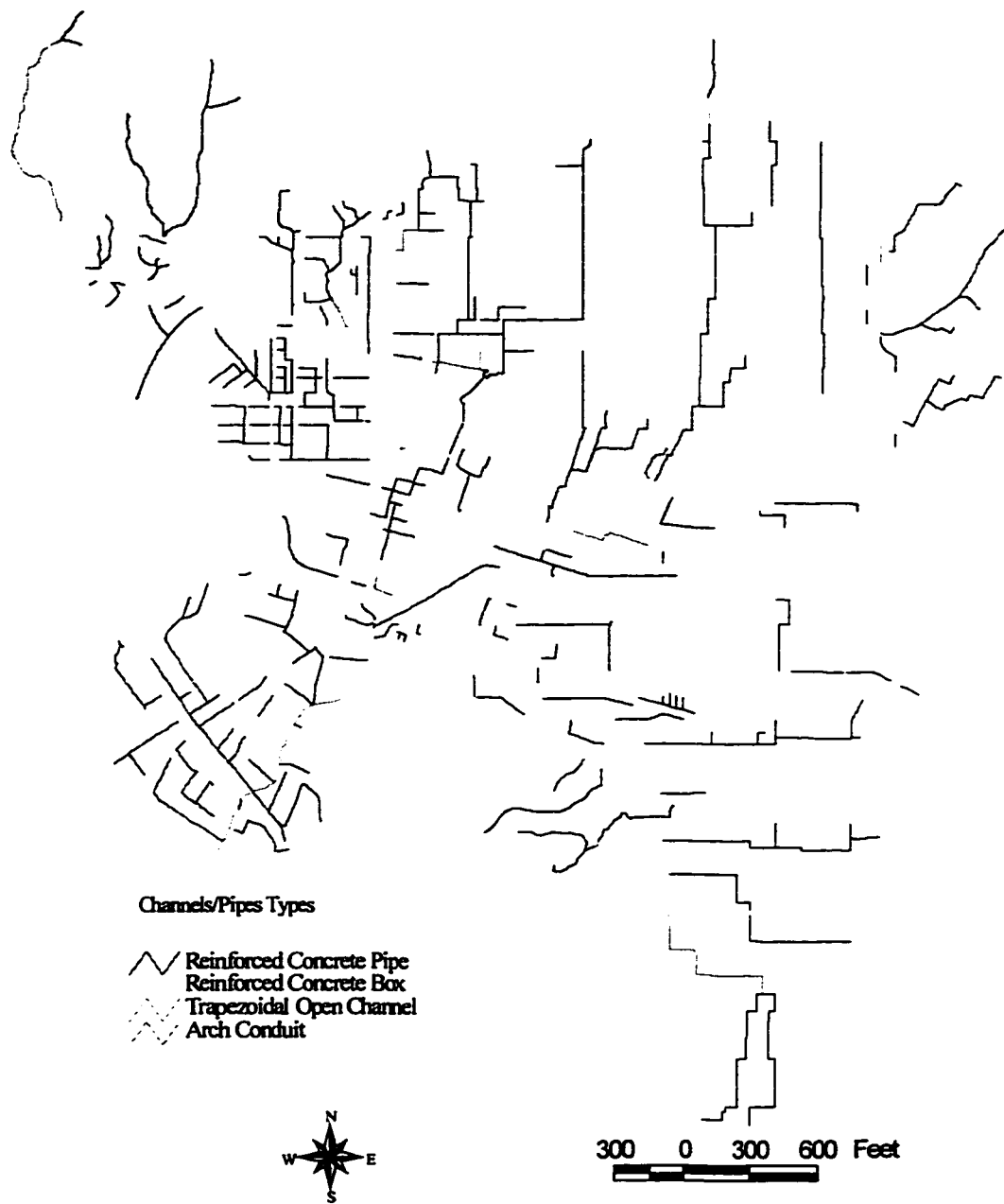
Figure C.3 Channel Types of Channels/Pipes Coverage

150

IMAGE EVALUATION
TEST TARGET (QA–3)

150mm

6"